

¹H MAGNETIC RESONANCE SPECTROSCOPY IN THE INVESTIGATION OF MULTIPLE SCLEROSIS AND OTHER DISORDERS OF WHITE MATTER.

by

Charles Anthony Davie MB ChB. MRCP.

A thesis submitted for the degree of Doctor of
Medicine in the Faculty of Clinical Medicine
of the University of Glasgow.

March 1997

N.M.R. Research Group
Institute of Neurology, Queen Square,
London, WC 1N 3BG.

This work was carried out at the Institute of Neurology,
Queen Square, London.

Head of Department Professor W.I. McDonald

Research Supervisor Professor D.H. Miller

ProQuest Number: 13815498

All rights reserved

INFORMATION TO ALL USERS

The quality of this reproduction is dependent upon the quality of the copy submitted.

In the unlikely event that the author did not send a complete manuscript and there are missing pages, these will be noted. Also, if material had to be removed, a note will indicate the deletion.



ProQuest 13815498

Published by ProQuest LLC (2018). Copyright of the Dissertation is held by the Author.

All rights reserved.

This work is protected against unauthorized copying under Title 17, United States Code
Microform Edition © ProQuest LLC.

ProQuest LLC.
789 East Eisenhower Parkway
P.O. Box 1346
Ann Arbor, MI 48106 – 1346

Thesis
10870
Copy 1



**This thesis is dedicated to my wife, Bernadette
and to my parents Maureen and John Davie.**

Abstract

¹H magnetic resonance spectroscopy (MRS) is a technique that allows the in vivo and non-invasive quantification of metabolites from the human brain. MRS was used in the study of patients with multiple sclerosis (MS) to determine the metabolic profile of acute MS lesions and areas of normal appearing white matter (NAWM). Abnormally elevated metabolite peaks attributable to mobile lipids and cytosolic proteins indicative of myelin breakdown were found in all acute lesions studied. A study of chronic MS lesions and NAWM was performed in patients in the four clinical subgroups of MS - benign, relapsing/remitting, primary and secondary progressive disease to evaluate mechanisms of disability in MS. This study showed a correlation between reduction of NAA - a neuronal marker and disability in the different clinical subgroups of MS.

To test the hypothesis that a reduction in NAA may occur as a consequence of axonal loss, a group of patients were studied with hereditary autosomal dominant cerebellar ataxia (ADCA) a condition in which axonal loss is known to be a striking pathological feature. This study supported the relationship between axonal loss and reduction of NAA by showing a significant reduction in the concentration of NAA from cerebellar white matter. To provide a more rigorous test of the hypothesis that axonal loss is an important determinant in the development of disability, an MRS study was performed in two groups of MS patients - a group with severe cerebellar deficit and a group with no clinical evidence of cerebellar

involvement in these two conditions. Again, this study showed a strong correlation between the presence of persistent functional deficit and axonal loss as evidenced by a reduction of N acetyl aspartate only in the group of MS patients with severe cerebellar deficit.

MRS was also performed in a group of patients with neuropsychiatric manifestations of systemic lupus erythematosus (SLE) to determine whether MRS is useful in differentiating this condition from MS. The pattern of abnormality did not allow differentiation of SLE lesions from the chronic plaques occurring in MS. Finally, MRS was carried out in a group of adult patients with phenylketonuria (PKU) who had abnormalities visible with magnetic resonance imaging (MRI) to show that MRS is able to differentiate between the pathological processes that produce MRI abnormalities in MS and those occurring in PKU. Patients with PKU showed a normal metabolite profile from MRI visible lesions and NAWM indicating axonal preservation from lesions which on conventional MRI resemble lesions seen in MS.

These studies have shown that ^1H MRS is a useful non-invasive technique which can help, not only in understanding the pathophysiology of MS, but may also help in differential diagnosis.

CONTENTS

TITLE	1
DEDICATION	2
ABSTRACT	3
CONTENTS	6
LIST OF FIGURES	11
LIST OF TABLES	13
LIST OF APPENDICES	14
ABBREVIATIONS	15
ACKNOWLEDGEMENTS	17
PUBLICATIONS ARISING FROM THESIS	18

<u>CHAPTER 1.</u>	<u>INTRODUCTION</u>	page 20
1.1	History	20
1.2	Nuclei and metabolites visible with MRS	20
1.3	^{31}P MRS studies	21
1.4	Recent advances in the study of the ^1H nucleus	21
1.5	Metabolites visible with ^1H MRS	22
	1.5.1 N- acetyl containing compounds	23
	1.5.2 Choline containing compounds	26
	1.5.3 Creatine and Phosphocreatine	26
	1.5.4 Lactate	27
	1.5.5 Neurotransmitters	28
	1.5.6 Myo-Inositol	29
	1.5.7 Lipids and cytosolic proteins	30
1.6	Magnetic resonance and multiple sclerosis	30
	1.6.1 The role of MRI in understanding MS	
	1.6.2 MRS studies in MS	31
1.7	The use of MR in the differential diagnosis of MS	35
1.8	Unresolved issues regarding the pathophysiology and differential diagnosis of MS	36
	illustrations	38
<u>CHAPTER 2.</u>	<u>GENERAL METHODS</u>	44
2.1	The NMR experiment	
	2.1.1 Precession	44
	2.1.2 Chemical shift	45
	2.1.3. Relaxation within tissues	46
	2.1.4 Relaxation properties and echo-time	46
2.2	Volume localisation	
	2.2.1 Surface coil methods	47
	2.2.2 Volume selection by frequency selective RF pulses	48
	2.2.3 Single-shot methods of volume selection (PRESS and STEAM)	48
2.3.	Shimming	50
2.4	Water suppression	52
2.5	Post-processing	
	2.5.1 Fourier Transformation	53
	2.5.2 Apodisation	53

2.5.3	Phase correction	53
2.5.4	Baseline correction	54
2.6	Peak assignments	54
2.6.1	Extract identification	54
2.6.2	Editing techniques (J modulation)	55
2.7	Metabolite quantitation	55
2.7.1	Determination of peak areas	55
2.7.2	Relative quantitation	56
2.7.2	Absolute quantitation	56
	illustrations	58
CHAPTER 3.	<u>¹H MAGNETIC RESONANCE SPECTROSCOPY IN ACUTE MULTIPLE SCLEROSIS LESIONS</u>	6 6
3.1	Summary	66
3.2	Introduction	67
3.3	Materials and methods	68
3.3.1	Subjects	68
3.3.2	Magnetic resonance imaging and spectroscopy	69
3.4	Results	
3.4.1	Controls	70
3.4.2	Short echo time spectra: patients	71
3.4.3	Long echo time spectra: patients	72
3.5	Discussion	73
3.5.1	Increased lipid resonances and the course of demyelination	73
3.5.2	Reversible reduction in NAA/creatine ratio	76
3.5.3	Other observations	77
3.5.4	Implications for monitoring therapy	78
	legends and illustrations	79
CHAPTER 4	<u>PERSISTENT FUNCTIONAL DEFICIT IN MULTIPLE SCLEROSIS AND AUTOSOMAL DOMINANT ATAXIA IS ASSOCIATED WITH AXON LOSS</u>	9 1
4.1	Summary	91
4.2	Introduction	92
4.3	Materials and methods	93
4.3.1	Patients	94

4.3.2	Magnetic resonance imaging and spectroscopy	95
4.4	Results	
4.4.1	MRS	98
4.4.2	MRI	99
4.5	Discussion	
4.5.1	Decreased [NAA] and cerebellar atrophy in the MS group with cerebellar deficit	101
4.5.2	Other findings	103
	legends and illustrations	106
CHAPTER 5	<u>1H MAGNETIC RESONANCE SPECTROSCOPY OF CHRONIC CEREBRAL WHITE MATTER LESIONS AND NORMAL APPEARING WHITE MATTER IN MULTIPLE SCLEROSIS</u>	118
5.1	Summary	118
5.2	Introduction	119
5.3	Materials and methods	120
	5.3.1 Patients	120
	5.3.2 Magnetic resonance imaging and spectroscopy	121
5.4	Results	123
	5.4.1 MRS lesions	
	5.4.2 MRS normal appearing white matter	125
5.5	Discussion	
	5.5.1 [NA] in MS lesions	126
	5.5.2 Correlation between the reduction of [NA] from an MS lesion and the degree of disability measured on the kurtzke score	128
	5.5.3 Reduction of [NA] from normal appearing white matter in patients with primary progressive disease	128
	5.5.4 Other findings	129
	legends and illustrations	130

<u>CHAPTER 6</u>	<u>¹H MAGNETIC RESONANCE SPECTROSCOPY OF SYSTEMIC LUPUS ERYTHEMATOSUS INVOLVING THE CENTRAL NERVOUS SYSTEM</u>	1 4 2
6.1	Summary	142
6.2	Introduction	142
6.3	Patients and methods	
	6.3.1 Patients	144
	6.3.2 Magnetic resonance imaging and spectroscopy	145
	6.3.3 Psychiatric assessment	146
	6.3.4 Neuropsychological assessment	146
6.4	Results	147
	6.4.1 MRI	
	6.4.2 MRS	147
	6.4.3 Psychiatric assessment	148
	6.4.4 Neuropsychological assessment	149
6.5	Discussion	150
	6.5.1 Spectroscopy findings in SLE	150
	6.5.2 Lack of correlation between spectroscopic, neuropsychological and neuropsychiatric features	151
	legends and illustrations	153
<u>CHAPTER 7</u>	<u>¹H MAGNETIC RESONANCE SPECTROSCOPY AND MAGNETISATION TRANSFER IN ADULT CASES OF PHENYLKETONURIA</u>	1 6 1
7.1	Summary	161
7.2	Introduction	161
7.3	Patients and methods	
	7.3.1 Patients	163
	7.3.2 NMR techniques	163
7.4	Results	
	7.4.1 MRI	165
	7.4.2 MRS	165
	7.4.3 Magnetisation transfer (MT)	166
7.5	Discussion	
	7.5.1 Normal [NAA]	167
	7.5.2 Moderate reduction of MT in PKU	167

	10	
7.5.3 Other findings	167	
legends and illustrations	169	
<u>CHAPTER 8</u>	<u>CONCLUSIONS AND IMPLICATIONS</u>	172
	<u>FOR FUTURE RESEARCH</u>	
	legend and illustration	178
REFERENCES		179
APPENDIX		206

LIST OF FIGURES

- 1.1 long echo ^1H spectrum from white matter of healthy control
- 1.2 Short echo ^1H spectrum from white matter of healthy control
- 1.3a,b Chemical structure of some metabolites visible with ^1H MRS
- 2.1 ^1H NMR spectrum of ethanol
- 2.2 STEAM sequence
- 2.3 T_2 weighted coronal MRI showing a volume of interest localised to the lentiform nucleus
- 2.4 Comparison of control spectra from the cerebral hemisphere and the basal ganglia.
- 2.5
- a,b ^1H NMR spectrum before and after water suppression
- 2.6, The effect of line broadening on the ^1H NMR spectrum
- 2.7 The effect of line broadening on the ^1H NMR spectrum
- 2.8 The effect of phasing on the ^1H NMR spectrum
- 2.9 J modulation effect on the lactate signal
- 3.1A Control ^1H spectrum from healthy control. TE 10ms and 135ms
- 3.1B MRI of lipoma in the quadrigeminal plate
- 3.1C ^1H spectrum of lipoma
- 3.2 Short echo spectrum from acute enhancing MS lesion
- 3.3 Images A-D MRI of acute enhancing MS lesion
- 3.4 Spectra A-C Spectra from same acute enhancing MS lesion
- 3.5 Serial short echo spectra of MS lesion showing resolution of lipid/cytosolic protein resonances
- 3.6 Short echo spectrum from MS lesion at various echo times
- 3.7 Serial Long echo spectra from MS lesion showing partial resolution in the NAA/creatine ratio
- 3.8 Mean NAA/creatine ratio in the patient group over time
- 3.9 Spectrum from acute MS lesion showing the presence of lactate
- 4.1 Voxel localised to the cerebellar white matter
- 4.2 Spectrum from cerebellar white matter in an MS patient with severe ataxia (upper spectrum) versus healthy control (lower spectrum)
- 4.3 Spectrum from cerebellar white matter in an MS patient with no ataxia (upper spectrum) versus healthy control (lower spectrum)
- 4.4 Spectrum from cerebellar white matter in an ADCA patient with ataxia (upper spectrum) versus healthy control (lower spectrum)
- 4.5 Plot of [NA] in all patients and controls
- 4.6 Scattergraph of [NA] versus Kurtzke expanded disability status

- score (EDSS) in all MS patients
- 4.7 Scattergraph of [NA] versus Kurtzke cerebellar functional score in all MS patients
- 5.1 Spectrum from an area of parietal white matter in a healthy control
- 5.2 Spectrum from a chronic white matter lesion in an MS patient with relapsing remitting disease
- 5.3 Spectrum from a chronic white matter lesion in an MS patient with secondary progressive disease
- 5.4 Spectrum from a chronic white matter lesion in an MS patient with primary progressive disease
- 5.5 Spectrum from a chronic white matter lesion in an MS patient with benign disease
- 5.6 Spectrum from an area of normal appearing white matter (NAWM) in an MS patient with primary progressive disease
- 5.7 Scattergraph of [NA] versus Kurtzke EDSS in the MS patients with relapsing remitting disease
- 5.8 Scattergraph of [NA] versus Kurtzke EDSS in the MS patients in all subgroups
- 6.1 High signal lesions on T₂ weighted MRI in patient with SLE
- 6.2 Gadolinium enhancement on T₁ weighted MRI in patient with active SLE
- 6.3 Short echo spectra from a frontal lesion in an SLE patient (upper spectrum, from an area of NAWM (middle spectrum) and from a healthy control (lower spectrum))
- 6.4 Long echo spectra from a frontal lesion in an SLE patient (lower spectrum, from an area of NAWM (middle spectrum) and from a healthy control (upper spectrum))
- 7.1 T₂ weighted MRI in patient with phenylketonuria showing high signal lesions in the posterior trigones
- 7.2 Spectrum from lesion in patient with PKU (upper spectrum) compared to healthy control (lower spectrum)
- 8.1 ¹H MRS of cervical spinal cord from a healthy control

LIST OF TABLES

Table 1.1	Metabolites visible with magnetic resonance spectroscopy
Table 1.2	Chemical shift frequencies for ^1H spectrum
Table 2.1	T_1 and T_2 relaxation times of the major metabolites in the ^1H NMR spectrum
Table 4.1	Clinical and MR data in MS patients with cerebellar deficit
Table 4.2	Clinical and MR data in MS patients without cerebellar deficit
Table 4.3	Clinical and MR data in patients with autosomal dominant cerebellar ataxia
Table 5.1	Clinical data and [NA] in the MS lesion subgroups
Table 6.1	Clinical, MR and psychiatric data of patients with systemic lupus erythematosus (SLE)
Table 6.2	Commonest occurring psychiatric symptomatology in SLE patients
Table 6.3	Neuropsychological deficit in SLE patients
Table 7.1	Clinical details and phenylalanine levels at time of study in patients with phenylketonuria (PKU)

LIST OF APPENDICES

- A Further methods regarding absolute quantitation of metabolites**

ABBREVIATIONS

ADCA	Autosomal dominant cerebellar ataxia
AIDS	Acquired immunodeficiency syndrome
ATP	adenosine triphosphate
ADP	adenosine diphosphate
β_{eff}	effective magnetic field
β_0	static magnetic field generated by the magnet
β_{∞}	field generated by electronic environment
CH	chronic hepatic encephalopathy
CHESS	Chemical Shift Selective Method
Cho	choline containing compounds
CNS	central nervous system
Cr	creatine
CSI	chemical shift imaging
EAE	experimental allergic encephalomyelitis
EDSS	extended disability status score
FID	free induction decay
FT	Fourier transformation
GABA	gamma-amino-butyric acid
Gd	gadolinium
Gd-DTPA	gadolinium
glu	glutamate
gln	glutamine
glx	glutamate and glutamine
^1H	hydrogen
HD	Huntington's disease
Hz	Hertz
In	myo-inositol
ISIS	Image Selected In vivo Spectroscopy
lac	lactate
M	Molar
mM	millimolar
mm ³	cubic millimetre
mmol/kg	millimoles per kilogram
MRI	magnetic resonance imaging
MRS	magnetic resonance spectroscopy
MS	multiple sclerosis

MT	magnetisation transfer
MTR	magnetisation transfer ratio
NA	N -acetyl groups
NAA	N -acetylaspartate
NAAG	N -acetyl-aspartyl glutamate
NAWM	normal appearing white matter
NMR	nuclear magnetic resonance
O2A	oligodendrocyte -type2 astrocyte
p	level of significance
³¹ P	phosphorus
PCr	phosphocreatine
PET	positron emission tomography
PD	proton density
phe	phenylalanine
PI	proton index
PKU	phenylketonuria
ppm	parts per million
PRESS	Point REsolved Spectroscopy
PSE	present state examination
r	correlation value
RF	radio-frequency
SLE	systemic lupus erythematosus
SNR	signal to noise ratio
STEAM	Stimulated Echo Acquisition mode
T	Tesla
T ₁	spin-lattice relaxation time
T ₂	spin-spin relaxation time
TE	echo-time
TE _f	fast spin echo
TM	mixing time
TR	relaxation time

Acknowledgements

There are many friends and colleagues who I wish to acknowledge in the preparation of this thesis. I am greatly indebted to Professor David Miller who has closely supervised my research at all stages, contributing at every level from the fundamental ideas on which the studies were based to the proof reading of the final thesis prior to submission. Similarly Professor Ian McDonald has acted as a mentor throughout. His vision in identifying the important unresolved questions in multiple sclerosis research has not only provided a vital structure to this work but his clearness of thought has provided direction in the formulation of this thesis.

Many colleagues have been of vital assistance in implementing the physics sequences (while patiently explaining to me what they meant) and providing technical backup necessary for this study. These include Gareth Barker, David MacManus, Paul Tofts, Amanda Brennan, Stephanie Webb.

There are many other people who have been of great help in different ways and who I would like to thank. Dr. Alan Thompson provided invaluable assistance in the PKU study and kindly allowed me to study many MS patients under his care. Professor Maria Ron, Dr. Anthony Feinstein and Dr. Luke Kartsounis who were closely involved in psychiatric and cognitive assessment of patients in the SLE study. I have learnt in the last three years that an important part of research involves "informal" discussions with colleagues often on apparently unrelated topics. I am therefore very grateful to Bob Brenner, John Thorpe, Achim Gass, Nick Lossef and Ming Li all of whom were of invaluable help in this respect.

I am also grateful to the large number of technical staff from GE Electric who would attempt to iron out any problems that developed with the NMR machine or spectroscopy software and who provided the NMR unit with physiological phantoms.

I would like to thank the computing staff, statisticians and library staff at the National Hospital for Neurology and Neurosurgery for their help. I am also particularly grateful to the large number of patients and volunteers who gave up often large amounts of time participating in the various studies.

Finally I would like to thank my wife for her patience and understanding during the last three years.

Publications arising from this thesis

Davie CA, Hawkins CP, Barker GJ, Brennan A, Tofts PS, Miller DH, et al. Detection of lipid in the brain of healthy subjects by proton NMR spectroscopy [abstract]. In: Proceedings of the eleventh meeting of the Society of Magnetic Resonance in Medicine 1992; Works in Progress:1724.

Davie CA, Hawkins CP, Barker GJ, Brennan A, Tofts PS, Miller DH, et al. Detection of myelin breakdown products by proton magnetic resonance spectroscopy. Lancet 1993;341:630-631.

Davie CA, Barker GJ, Tofts PS, Quinn N, Miller DH. Proton MRS in Huntington's disease. Lancet 1994; 343: 1580.

Davie CA, Hawkins CP, Barker GJ, Brennan A, Tofts PS, Miller DH, et al. Serial proton magnetic resonance spectroscopy in acute multiple sclerosis lesions. Brain 1994; 117: 49-58.

Davie CA, Barker GJ, Brenton D, Miller DH, Thompson AJ. Proton magnetic resonance spectroscopy in adult cases of phenylketonuria [abstract]. J Neurol Neurosurg Psychiatry 1994; 57: 1292.

Davie CA, Wenning GK, Barker GJ, Tofts PS, Quinn N, Marsden CD et al. Differentiation of multiple system atrophy from idiopathic Parkinson's disease using proton magnetic resonance spectroscopy. Ann Neurol 1995; 37: 204-210.

Davie CA, Feinstein A, LD. Kartsounis, GJ. Barker, NJ. McHugh, MJ. Walport, MA. Ron, IF. Moseley, WI. McDonald, DH. Miller. Proton Magnetic resonance spectroscopy of Systemic Lupus Erythematosus involving the central nervous system. The Journal of Neurology 1995;242:522-528.

Davie CA, Barker GJ, Webb S, Tofts PS, Thompson AJ, Harding AE, McDonald WI, D.H. Miller DH. Persistent functional deficit in multiple sclerosis and autosomal dominant cerebellar ataxia is associated with axon loss. Brain 1995; 118: 1583-1592.

Submitted for publication

Davie CA, Barker GJ, Webb S, Tofts PS, Thompson AJ, McDonald WI, Miller DH. ¹H magnetic resonance spectroscopy of chronic cerebral white matter lesions and normal appearing white matter in multiple sclerosis. Submitted to Journal of Neurology, Neurosurgery and Psychiatry

CHAPTER 1

Introduction

1.1 HISTORY

Magnetic Resonance Imaging (MRI) is a technique that has shown itself to be particularly valuable in the study of the multiple sclerosis (MS) lesion. Although the principles of nuclear magnetic resonance (NMR) were established as early as 1946, it was only with the first demonstration of the MS lesion by Young et al (1981), that MRI began to realise its potential as an important tool in the diagnosis of MS (Ormerod et al.,1987; Paty et al.,1988; Fazekas et al.,1988; Offenbacher et al.,1993) and as a non-invasive means in studying the evolution of the MS plaque (Lukes et al.,1983; Miller et al.,1988a; Kermode et al., 1990; Kidd et al., 1993; Katz et al., 1993). Prior to this time NMR had been used almost exclusively as a spectroscopic technique for chemical analysis. Initially the role of magnetic resonance spectroscopy (MRS) was restricted to in-vitro analysis. Later, the technique was applied to in-vivo experiments in animals (Ackerman et al., 1980) and studies of plant systems (Schaeffer et al., 1975). Since then MRS has become an established means of non-invasively investigating cellular metabolism within the healthy human brain (Cady et al., 1980; Frahm et al.,1989a; Van Rijen et al 1989; Beckman et al., 1991) and in several disease states (Arnold et al., 1990a, b; Matthews et al., 1991b; Gideon et al., 1992; Shino et al., 1993; Davie et al., 1995)(Vion-Dury et al., 1994).

1.2 NUCLEI AND METABOLITES VISIBLE WITH MRS

In contrast to conventional MRI which exploits the NMR properties of the Hydrogen nucleus, MRS is able to use other nuclei which possess a property known as spin. These include phosphorus, Lithium, Carbon,

Fluorine, Sodium and Nitrogen. The potential value of these various nuclei with MRS is dependent on their natural abundance and NMR sensitivity. A wide range of metabolites can be identified using these various nuclei (table 1.1). Hydrogen (^1H) and Phosphorus (^{31}P) have been the two main nuclei used for clinical studies in humans and MRS is now routinely used to provide information from localised areas within the human brain concerning metabolite concentrations, the mobility (or relaxation properties) of various substances as well as the metabolic exchange rates occurring between metabolites.

1.3 ^{31}P MRS studies

Studies using ^{31}P MRS have been particularly useful in the investigation of oxidative metabolism in cells (Moon and Richards, 1973), animals (Ackerman et al., 1980) and humans (Chance et al., 1980; Arnold et al., 1984; Hayes et al., 1985). ^{31}P MRS is able to detect signals from the molecules containing high energy-phosphate bonds which include the three phosphates of adenosine triphosphate (ATP), phosphocreatine (PCr), inorganic phosphate and phosphomonoesters. Changes in the signal from these metabolites allows evaluation of the energy balance occurring in a wide range of physiological and non-physiological conditions. In addition, ^{31}P MRS can provide information about intracellular pH and, indirectly from changes in the three ATP resonances, allow measurement of free and bound magnesium concentration in the brain thus giving some insight into glycolytic pathways.

1.4 RECENT ADVANCES IN THE STUDY OF THE ^1H NUCLEUS

MRS studies using the hydrogen nucleus were slower to develop, mainly for reasons of greater technical difficulty. The hydrogen

nucleus has a concentration in the human brain of approximately 91 Molar in grey matter and 80 Molar in white matter (Norton et al., 1966) which is predominantly in the form of water. Although such a concentration makes water ideal for imaging of the brain by NMR, other mobile metabolites containing hydrogen are present in the human brain in millimolar concentrations. The majority of these metabolites resonate at frequencies close to that of water and therefore the signals they produce are swamped by the water signal in conventional imaging. An important advancement in proton MRS has been the development of techniques which allow adequate suppression of the water signal and as a result, identification and quantitation of other compounds which contain hydrogen. Other important advances have gone hand in hand with this, including the introduction of more effective sequences for localisation, improved resolution allowing the study of smaller volumes in vivo and, more recently, methods which allow absolute metabolite quantitation. These developments will be discussed in the methods section. With such technical progress, it is now possible using proton MRS to identify and quantify, non-invasively, a large number of metabolites in the human brain from volumes as small as 1ml (Frahm et al., 1990). Table 1.1 shows some of the metabolites that have been assigned in the proton spectrum. The ability to identify a particular metabolite is dependent on a number of factors. These include its concentration, the proximity to the remaining suppressed water peak, the presence of other metabolites that produce signal at similar frequencies within the spectrum and, its mobility within different tissues which influences the amount of signal produced in any given MRS experiment. For these reasons, it is a rather small number of metabolites which are particularly well visualised by proton MRS.

1.5 METABOLITES VISIBLE WITH ^1H MRS

Until recently the four main peaks visible with proton MRS were N-acetyl containing compounds (NA) - the largest contribution coming from N-acetyl aspartate (NAA), choline containing compounds (Cho), creatine / phosphocreatine and lactate (lac) (Figure 1.1). Again with technical advances, which allow the collection of short echo-time spectra, it is possible to visualise routinely, signal from other substances including glutamate and glutamine, GABA, myo-inositol, and broad resonances from lipids and macromolecules (Figure 1.2). In order to use proton MRS to evaluate the metabolic changes occurring in the healthy and diseased brain, it is important to have a clear understanding about what is known regarding the chemical function and properties of some of these substances and whether any of them may be used as markers for particular cell types. The chemical structure (Figure 1.3a,b) and chemical shift frequencies for the ^1H spectrum are given in table form (Table 1.2).

1.5.1 N-acetyl containing compounds

NAA is an amino-acid which was first described by Tallan et al (1956) (Figure 1.3a). It is the second most abundant amino-acid in the human brain, second only to glutamate. Despite this, the precise role of NAA in the central nervous system is unknown. Studies by Patel and Clark (1979) and later reproduced by Brenner et al (1993b) showed that NAA was synthesised within mitochondria from aspartate and acetyl-coenzyme A and is then exported to the cytosol. NAA also arises as a breakdown product of N-acetyl-aspartyl-glutamate (NAAG) (Blakely et al., 1988). NAAG is present in mammalian brain at about one tenth of the concentration of NAA and contributes to the NA resonance on MRS seen at 2.02 parts per million (ppm) (Birken and Oldendorf, 1989). More

recently Urenjak et al (1992, 1993) have shown in cultured neural cells from rats that NAA is specifically expressed in neurones, oligodendrocyte -type2 astrocyte (O2A) progenitors and immature oligodendrocytes. It is undetectable in cortical astrocytes, meningeal cells and mature oligodendrocytes. The presence of NAA within O2A progenitor cells is of interest. These cells act as precursors in the development of oligodendrocytes and type 2 astrocytes. Although O2A progenitor cells have recently been demonstrated within adult brain (Scolding et al., 1994), they are present in very small numbers (approximately 1% of oligodendroglial lineage cells) and therefore, in adults at least, are unlikely to contribute significantly to the total concentration of NAA. Similarly, immature oligodendrocytes are infrequent within the mature adult brain. These observations then, indicate that in the adult brain at least the vast majority of NAA is contained within neurones. Thus analysis of NAA concentration within different regions of the brain may provide specific information concerning neuronal dysfunction and loss. The neuronal localisation of NAA has also been shown with immunocytochemical techniques. Simmons et al.(1991) have shown that NAA is present not only within the cell body but distributed throughout the axon and proximal dendrites. The predominant localisation of NAA to neurones is also supported by clinical MRS studies of disease processes in which neuronal loss is a prominent pathological feature. Examples of these include stroke (Gideon et al., 1992), HIV (Chong et al., 1993) and degenerative disorders (Van der Knaap et al., 1992) in which a reduction of NAA has been demonstrated. Additionally, MRS studies from non-neuronal tumours of human brain such as meningiomas and astrocytomas (Demaerel et al., 1991b; Frahm et al., 1992) show marked reduction or complete loss of NAA.

Several theories have been advanced to explain the function of NAA. A number of lines of evidence have suggested that NAA acts as a donor of acetyl groups for lipid synthesis, particularly in myelination (D'Adamo et al., 1966; Burri et al., 1991) since the acetyl group of NAA is incorporated into brain lipids far more effectively than acetate alone. It has been proposed by Patel and Clark (1980) that NAA acts as a carrier for carbon moieties from the mitochondria to lipogenic enzymes in the cytosol. If this theory is correct, it may perhaps explain why O2A progenitor cells express NAA, since these precursor cells are important in the process of myelination occurring during development. NAA is found in very small concentrations outside the central nervous system being present in other organs in quantities less than 1% of that seen in brain. Furthermore, NAA shows regional variation in concentration within the brain with a number of biochemical studies showing that its concentration increases rostrally in the central nervous system (CNS) (Tallan, 1957; Curatola et al., 1965). MRS studies have shown an approximately 25% higher concentration of NAA in grey matter than white matter with Michaelis et al (1993) finding a concentration of 8.8 and 11.7mmol/kg for cerebral white and grey matter respectively in healthy young adults. NAAG on the other hand increases caudally in concentration and is undetectable in grey matter with MRS (Michaelis et al., 1993).

There is some disparity between *in vitro* measurements of NAA and those calculated from *in vivo* MRS studies. Post mortem biochemical studies suggest an NAA concentration of approximately 6mM (Tallan, 1956; Petroff et al 1988) in mammalian brain. Lower *in vitro* values may be the result of autolysis of NAA after death and higher MRS values may arise because of overlap of the aspartyl resonances at 2.02 ppm with other compounds such as macromolecules (Rothman et al 1994).

1.5.2 Choline containing compounds (Cho)

The resonance observed at 3.2 ppm in the spectrum In MRS is not one compound but the combination of signal from a number of metabolites. These include free choline, phosphocholine, glycerophosphocholine, acetylcholine, phosphatidylcholine and sphingomyelin (Miller BL, 1991). Other metabolites including carnitine containing compounds (Miller BL, 1991) and betaine (Brenner et al., 1993a) have also been shown to be present in this resonance. The contribution to this peak from free choline (which is present in human brain at a concentration of less than 0.08mM) is small and it has been suggested that the Cho resonance is more likely to reflect total brain choline stores (Miller BL, 1991). In contrast to NAA, the concentration of Cho as detected by MRS is greater in white matter than grey matter with approximate concentrations of 1.8mM and 1.4mM respectively (Michaelis et al., 1993). There is quite marked regional variation of concentration within the brain of Cho with particularly high levels seen in the pons (Michaelis et al., 1993). An elevation of Cho has been observed in a number of conditions producing inflammation and it seems likely from experimental studies carried out on animals with acute experimental allergic encephalomyelitis (EAE) that this is the result of increased membrane turnover during the inflammatory response (Brenner et al., 1993a).

1.5.3 Creatine and Phosphocreatine

Whereas ^{31}P MRS produces a signal specifically from creatine phosphate, the creatine signals at 3.02 and 3.9 ppm in the proton spectrum is a combination of creatine (Cr) and phosphocreatine (PCr). These metabolites are present in high concentration in the brain acting as a reserve for high energy phosphates in the processes of oxidative metabolism. Creatine kinase converts creatine to phosphocreatine by

utilising ATP. These chemicals are in equilibrium with each other by the following equation,



Since they are in equilibrium, the total concentration of the two should accordingly remain constant in the brain. For this reason the Cr peak is often used as an internal standard of reference with the relative concentration of the other metabolites being expressed as a ratio to creatine. Using absolute quantitation, the estimated concentration of Cr from recently published studies has been estimated at 6.7mM and 8.4mM in cerebral grey and white matter respectively (Kreiss et al., 1994). These metabolites also show regional variation in the brain, with in one study, concentrations being as high as 9.1mM in the cerebellum and as low as 6.0 mM in the pons (Michaelis et al., 1993).

1.5.4 Lactate (lac)

Lactate, when present, produces a double resonance or doublet at 1.33 ppm in the proton spectrum. Under normal physiological circumstances a small signal from lac, can occasionally be detected in the human brain during rest. For example, lac has been observed in the visual cortex during the resting state at a concentration of 0.5-1.0mM (Merboldt et al., 1992). Furthermore, an increase in lactate concentration has been detected from the visual cortex (Prichard et al., 1991) and basal ganglia (Kuwabara et al., 1994) after functional activation studies in healthy controls. Such observations are in keeping with a study using positron emission tomography (PET) which showed that normal neuronal activity may produce a temporary, localised, anaerobic environment (Fox et al., 1988).

An increased concentration of cerebral lactate has been reported in several disease states which produce an increase in glycolytic activity. These include stroke (Bruhn et al., 1989), glial tumours (Demaerel et

al., 1991b), mitochondrial disease (Matthews et al., 1991b, 1993) and acute MS lesions (Miller et al., 1991). It has been proposed that persistent lactate production in stroke is the result of macrophage activation (Petroff et al., 1992).

1.5.5 Glutamate, glutamine and gamma-amino-butyric acid (GABA)

Glutamate, glutamine and gamma-amino-butyric acid (GABA) are all detectable by ^1H MRS in the human brain. Unlike the well defined resonances produced by the metabolites discussed above, glutamate produces a more complex signal which is present in the in the NMR spectrum between 2.1-2.5 ppm and 3.5-3.9ppm. Glutamate acts as an excitatory neurotransmitter in the brain and, as a component of the Krebs's cycle, plays an important role in oxidative metabolism. The concentration of glutamate estimated by ^1H MRS is 8.1mmol/kg in cerebral white matter and 12.5mmol/kg in cerebral grey matter (Michaelis et al., 1993). These values are 20-35% less than the values for glutamate which have been assayed biochemically (Kauppinen RA and Williams SR, 1991) and it has been suggested that a proportion of glutamate is located in a non-cytoplasmic intracellular compartment which is not visible with NMR (Kauppinen et al., 1993). It has been postulated that many of the degenerative neurological disorders are, at least in part, caused by an excitotoxic effect of increased glutamate release and recently there have been reports of an observed increase in glutamate and glutamine in patients with Huntington's disease (HD) studied by ^1H MRS (Taylor-Robinson et al., 1994; Davie et al., 1994a). Glutamine is detectable in far smaller concentrations in the brain by MRS, being present at approximately 20% of the concentration of glutamate in grey matter (Michaelis et al., 1993). Glutamine plays an important role in the metabolism of ammonia and it is therefore not

surprising that the concentration of glutamine is markedly elevated in patients with chronic hepatic encephalopathy (CHE) secondary to increased levels of ammonia (Kreiss et al., 1992). Elevated levels of glutamine have also been observed in MRS studies at an echo time of 135ms in children with ornithine transcarbamylase deficiency (Gadian et al., 1991).

The resonances of GABA, an inhibitory neurotransmitter, overlap with those of glutamate and glutamine in the NMR spectrum. It is possible however, with specialised editing techniques, to identify specifically the signal from GABA under physiological conditions (Rothman et al., 1993) and to observe an increase in concentration after anticonvulsant administration (Preece et al., 1991).

1.5.6 Myo-Inositol

Myo-Inositol (In) is an osmolyte that produces a resonance in the proton spectrum at 3.54 ppm. It has an approximate concentration of 6.0mmol/kg and 6.6mmol/kg from cerebral white and grey matter respectively (Kreiss, 1994). There is likely to be a minor contribution to this signal from glycine which resonates at 3.55ppm and has an approximate brain concentration of less than 0.7mmol/kg (Perry et al 1971). It has been suggested that In may act as a marker for astrocytes. This seems unlikely since experimental studies in cultured cells from rats has shown expression of In from both neurones as well as cortical astrocytes (Urenjak et al., 1993). In has been shown to be elevated after prolonged cocaine and polysubstance abuse (Chang et al., 1994) and in patients with Alzheimer's disease (Miller BL et al., 1993). Kreiss et al (1992) have reported decreased levels of In, in patients with CHE. The significance of alterations of In in these various disease states remains unclear.

1.5.7 Lipids and macromolecules

It has become apparent with the use of short echo-time MRS, that broad resonances occur in the human spectrum of healthy controls between 0.9 and 1.3 ppm (Davie et al., 1992) and that these signals are not the result of contamination from subcutaneous scalp fat. Studies by Behar et al (1994) have shown similar resonances arising from macromolecules in the cytosol in rat and human brain. Kauppinen et al (1992) have shown that thymosin β 4, a macromolecule, produces a resonance at 1.4ppm in a cerebral cortex preparation from the guinea pig. Further experimental studies by Callies et al (1993) have shown the appearance of resonances at 0.9 and 1.3 ppm after the induced formation of lipid droplets in myeloma cells. These studies, then, provide evidence that the resonances between 0 and 2 ppm in the NMR spectrum represent signal from lipids and cytosolic proteins.

1.6 **MAGNETIC RESONANCE AND MULTIPLE SCLEROSIS**

1.6.1 The role of MRI in understanding MS

MRI studies have demonstrated important differences between the four main subpopulations of MS patients (Thompson et al., 1990a; 1991; 1992; Kidd et al., 1994) in relation to lesion size, the frequency at which new lesions appear and enhance after Gadolinium (Gd-DTPA) administration and lesion volume. In patients with primary progressive MS (patients in whom the disease course has been progressive from onset) , MRI tends to show fewer and smaller cerebral lesions than patients with secondary progressive MS in whom the illness initially has a relapsing remitting pattern and then becomes progressive (Thompson et al.,1991). Additionally, in the patients with primary progressive disease, new lesions tend to develop less often and rarely exhibit Gd-DTPA enhancement. In patients with the relapsing/remitting

form of MS, conventional MRI studies tend to show a high incidence of lesion development (Thompson et al., 1992). However, only a weak relationship has emerged between MRI lesion load and clinical disability (Li et al., 1984; Filippi et al., 1994). There is a number of factors contributing to this. First, the site of lesions may be important; many lesions occur in areas of the brain which are clinically 'silent' (Phadke and Best 1983) and would not be expected to greatly influence disability which, on current grading systems (Kurtzke, 1983), is heavily weighted towards locomotor function. Secondly, the degree of disability may be influenced by the extent of spinal cord involvement as suggested by a modest though significant correlation between clinical disability and cord atrophy (Kidd et al., 1994). And finally, there is considerable pathological heterogeneity between lesions (Dawson, 1916; Allen, 1991; Barnes et al 1991): some MS plaques may show very marked axonal loss (Allen, 1991; Lassmann et al 1994) which may contribute to functional impairment while in others there may simply be demyelination which may be compatible with normal function (Halliday et al., 1972). Conventional MRI cannot identify myelin breakdown products and is not able to differentiate between the various pathological processes occurring within an MS lesion which include inflammation, oedema, demyelination, remyelination and axonal loss (Allen, 1991; Prineas, 1993). By virtue of its ability to identify myelin breakdown products and measure levels of NAA, a neuronal marker, MRS has the potential to differentiate some of the pathological events occurring within the MS lesion and thus help to understand the mechanisms that produce disability.

1.6.2 MRS studies in MS

MRS provides a non-invasive means of monitoring metabolic changes within the MS plaque and from areas of normal appearing white matter (NAWM). Technical advances in MRS now permit the study of volumes as small as 1ml (Frahm et al., 1990), the size of many MS lesions. The first studies of MRS in MS were carried out at long-echo times (TE) and were able to provide information concerning NAA, Cho, Cr and lac. In these studies, Cr was used as an internal standard of reference. Arnold et al (1990b) carried out MRS from the cerebral hemispheres in seven MS patients using, in six of them, large volumes of between 120 and 160 mls. In four of the patients they observed a reduction of the NAA/Cr ratio compared to controls. They also studied one acute lesion which was clinically symptomatic. This lesion showed no abnormality of the metabolite ratios compared to controls. Although this study was carried out on large volumes of interest and performed on a small number of patients, the finding of a reduced NAA/creatine ratio from chronic plaques was of interest since it suggested that MRS may be able to differentiate between old and new lesions. Furthermore, given that NAA is predominantly found within neurones, the authors speculated that a reduction of NAA within plaques could be used as an index of axonal damage.

In a larger study of 16 MS patients, Wolinsky et al (1990) were able to carry out short echo-time MRS at a TE of 30ms on 25 plaque containing volumes of interest. The advantage of using a short TE was the ability to visualise lipid and protein signal in the region of the spectrum between 0 and 2 ppm. In this study, eight of the spectra showed changes consistent with the presence of free lipids. The increased lipid signal in some patients (though not all) correlated with recent clinical activity. The authors felt that these lipid peaks represented myelin

breakdown products and that MRS may be useful in determining whether recent demyelination had occurred within an MS lesion. Gadolinium (Gd) was not used in this study and it was not possible therefore to date accurately the lesions though in a subsequent report by the same group, there was a greater tendency for lipid peaks to be seen from lesions that demonstrated Gd enhancement (Narayana et al., 1992) indicating that demyelination may occur early in the development of the MS lesion. Other groups have also observed increased lipid peaks in MS lesions. Larsson et al. (1991) performed MRS at an echo-time of 30ms in 15 patients with MS. They observed resonances corresponding to free lipids in six lesions. These signals were visible as early as 10 days in lesions which were clinically symptomatic and were present in one lesion judged on clinical grounds to be eight months old. The authors were able to carry out repeat studies in four patients and in one of these, the intensity of signal in the lipid region of the spectrum increased from the first study at day 10 to the follow up at day 70. However there was no systematic follow up of the patient group and Gd was not given. It was therefore not possible to characterise the temporal course of the elevated lipid peaks or their relationship to blood brain barrier impairment. A study by Koopmans et al (1993) has also found elevated resonances at 0.9 and 1.3ppm in MS lesions. This group also observed an increase in the In/Cr ratio in lesions. The significance of this latter finding is uncertain though it was speculated by the authors that an increase in In may also act as a marker for demyelination.

The finding of increased lipid and protein signals in MS lesions has however not been universal. A number of investigators have been unable to confirm this finding. Bruhn et al (Bruhn et al., 1992) in an MRS study of eight children with established MS failed to observe elevated lipid

peaks either within chronic lesions or from two enhancing plaques using a TE of 20ms. It is of course possible that the pathophysiology of MS lesions in childhood differs from that of adults. This to some extent is supported by neurophysiological studies of optic neuritis in childhood (Kriss et al., 1988) where recovery is far more complete than in adults. It is also notable that the two acute lesions (as evidenced by Gd enhancement) that were looked at in this study were rather small and did not fill the volume of interest. It is possible therefore that failure to detect elevated signal in the lipid/protein region of the spectrum may have been the result of a partial volume effect. The same group (Poser et al., 1992) have also reported short-echo time MRS in one patient from a large, acute demyelinating lesion detecting only small resonances at 0.9 and 1.3 ppm which they attributed to mobile aliphatic hydrocarbons such as cholesterol esters and lac respectively. Grossman and co-workers (1992) studied 16 patients with clinically definite MS. They performed MRS at a TE of 19ms in 21 lesions, seven of which enhanced after Gd. They did not detect lipid signals at 0.9 and 1.3 ppm from any of the lesions studied. They did however detect elevated peaks between 2.1 and 2.6ppm in five of the seven enhancing lesions and five of the 14 lesions which showed no enhancement. The authors felt that these elevated peaks were possible markers for demyelination. As with other groups, this study also reported decreased levels of NAA with a reduction seen in 17 of 21 lesions. There was no correlation between decreased NAA and the presence of Gd enhancement.

There has been, therefore, some conflict in the published literature about the presence of elevated lipid/protein resonances in MS lesions and, if present, whether they represent markers of myelin breakdown. It has been argued that these peaks may represent contamination of the

spectroscopic volume of interest from subcutaneous scalp fat. To date there have been no serial MRS studies which would help to resolve this issue. It is known from post-mortem studies of MS brains that myelin breakdown products in the form of cholesterol ester are present for over six months in lesions which had been symptomatic. If lipid resonances occur in the acute lesion it should be possible to follow them serially and document their gradual resolution. Such a study would also provide serial information regarding changes in the other spectroscopically visible metabolites. In particular, this may be of particular interest in the case of NAA. Arnold (1992) has reported reversibility of the NAA/Cr ratio from an acute MS lesion raising the possibility that at least in some cases, NAA may act as a marker of neuronal dysfunction rather than loss. This hypothesis is supported by the work of Brenner et al (1993b) who have shown a reduction of the NAA/Cr ratio despite structurally intact neurones in the brains of guinea pigs with chronic EAE. A serial study of acute MS lesions may therefore provide confirmation of this finding by Arnold and if so, give a clearer time-scale of how long such recovery takes.

MRS may also be a useful means of observing metabolic changes within areas of NAWM (Husted et al., 1994). It is known from pathological studies that small foci of myelin breakdown products or cuffs of inflammatory cells may be seen in NAWM and this is consistent with MR studies which have shown changes in the relaxation values of water from such areas (Miller et al., 1989). It is conceivable that subtle histological changes within NAWM are at least in part responsible for the development of disability in MS.

1.7 THE USE OF MR IN THE DIFFERENTIAL DIAGNOSIS OF MS

The diagnosis of MS remains a clinical one, it being necessary to demonstrate a dissemination of lesions in the central nervous system within time and space (Poser et al., 1983). In this regard, conventional MRI may be invaluable in providing support for diagnosis with new lesions developing on MRI more frequently than the occurrence of clinical relapse (Thompson et al., 1991, 1992). MRI of the brain is abnormal in over 95% of patients with clinically definite MS (Ormerod et al., 1987) and this figure increases if taken in conjunction with imaging of the spinal cord (Kidd et al., 1993). However, high signal lesions seen with MRI are by no means specific to MS. Similar changes can be observed in healthy controls, being particularly common in individuals over the age of 50 (Gerard and Weisberg, 1986; Fazekas, 1989). Furthermore, a wide variety of other neurological conditions may also cause white matter abnormalities detectable on brain MRI. These include among others systemic lupus erythematosus (SLE) (Miller et al., 1992a), sarcoidosis (Miller et al., 1988b), Behçet's disease (Morrissey et al 1993), acute disseminated encephalomyelitis (Kesselring et al 1990), phenylketonuria (PKU) (Thompson et al, 1993), the leukodystrophies (Demaerel et al., 1991a) and the acquired immunodeficiency syndrome (AIDS) (Olsen et al 1988). The differential diagnosis of neurological disorders producing white matter abnormalities on MRI is extensively covered by Thorpe and Miller (1994). Of these conditions, neurosarcoidosis and SLE are particularly important since, they may also produce a clinical picture which is indistinguishable from that of MS. In other conditions such as PKU, it is unclear whether the signal change that may occur on brain MRI arises from the same pathological processes that contribute to the lesions in MS. MRS has the potential to improve diagnostic specificity in these

conditions and furthermore provide information regarding metabolic heterogeneity between them.

1.8 UNRESOLVED ISSUES

There is then, a number of unresolved questions, regarding the pathophysiology and differential diagnosis of MS. The aim of this thesis is to determine whether the application of MRS is useful in addressing such issues. They include:

- (1) The mechanisms that produce disability in MS.
- (2) The time course of demyelination in the acute MS lesion.
- (3) The time course of changes in NAA in the acute MS lesion.
- (4) The identification of pathological and metabolic heterogeneity in MS lesions and NAWM.
- (5) The role of MRS in evaluating other neurological conditions which may radiologically and/or clinically mimic MS?

Table 1.1
Some examples of metabolites identified
by MRS in human and animal tissues

Nucleus	Metabolites				
¹ H	alanine	aspartate	glutamate	glutamine	
	glycine	taurine	phenylalanine		
	choline	lactate	phosphorylcholine		
	GABA	glucose	myo-inositol	lipids	
	acetate	creatine	phosphocreatine	glucose	
	scylloinositol		N-acetylaspartate		
³¹ P	adenosine triphosphate		phosphomonoesters		
	phosphodiester		inorganic phosphate		
	phosphocreatine		glucose-6-phosphate		
¹³ C	glucose	lactate	glutamate	glycogen	citrate
¹⁵ N	urea	glutamine	glutamate	citrulline	GABA
	aspartate	ammonia	alanine	N-acetylaspartate	
¹⁹ F	halothane	5 Fluoro-uracil and its metabolites			

Figure 1.1

Proton MRS from healthy control
periventricular white matter TE 135ms TR 2.2secs

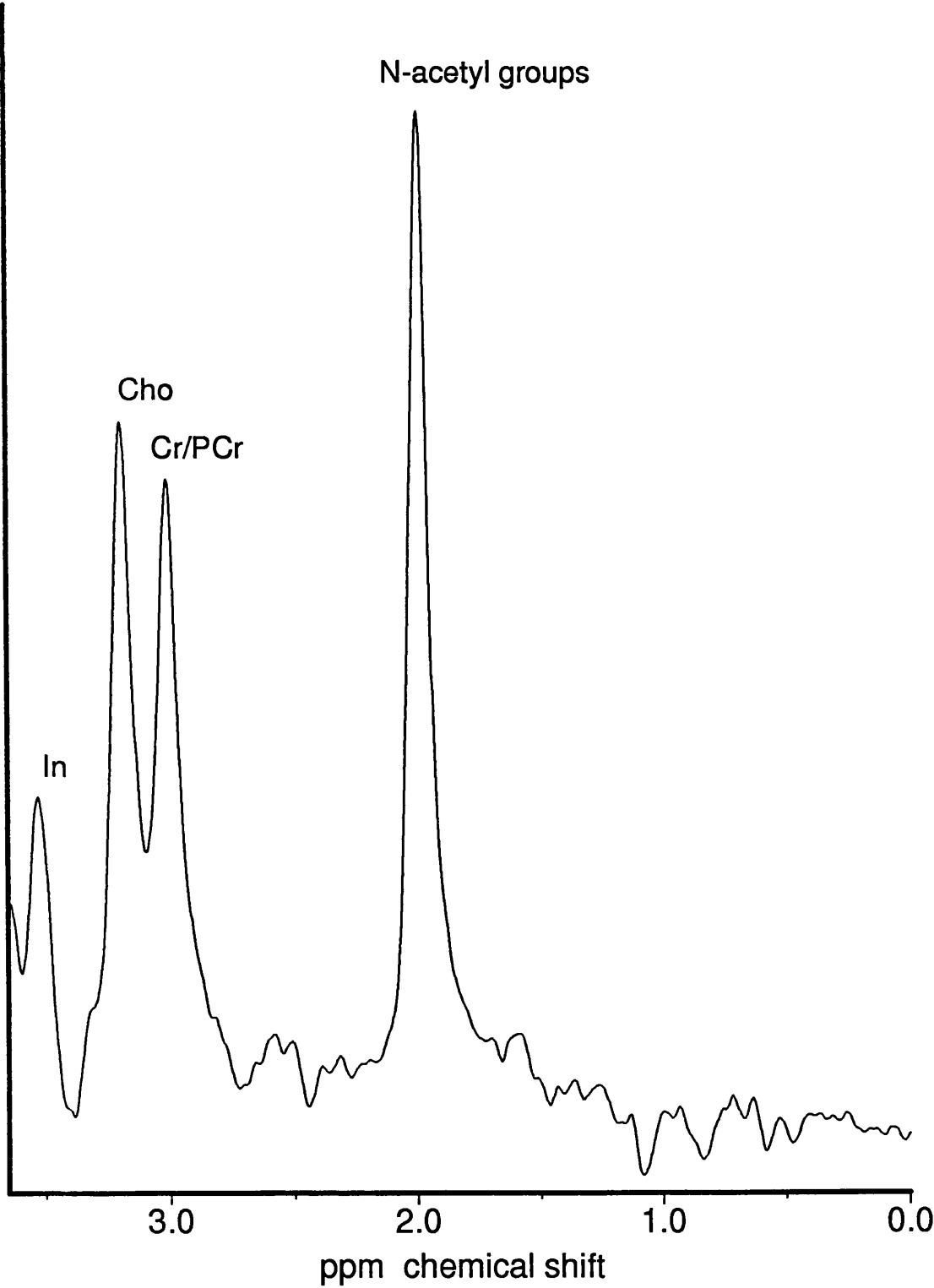


Figure 1.2

Proton MRS from healthy control
Periventricular white matter TE 10ms TR 2 secs

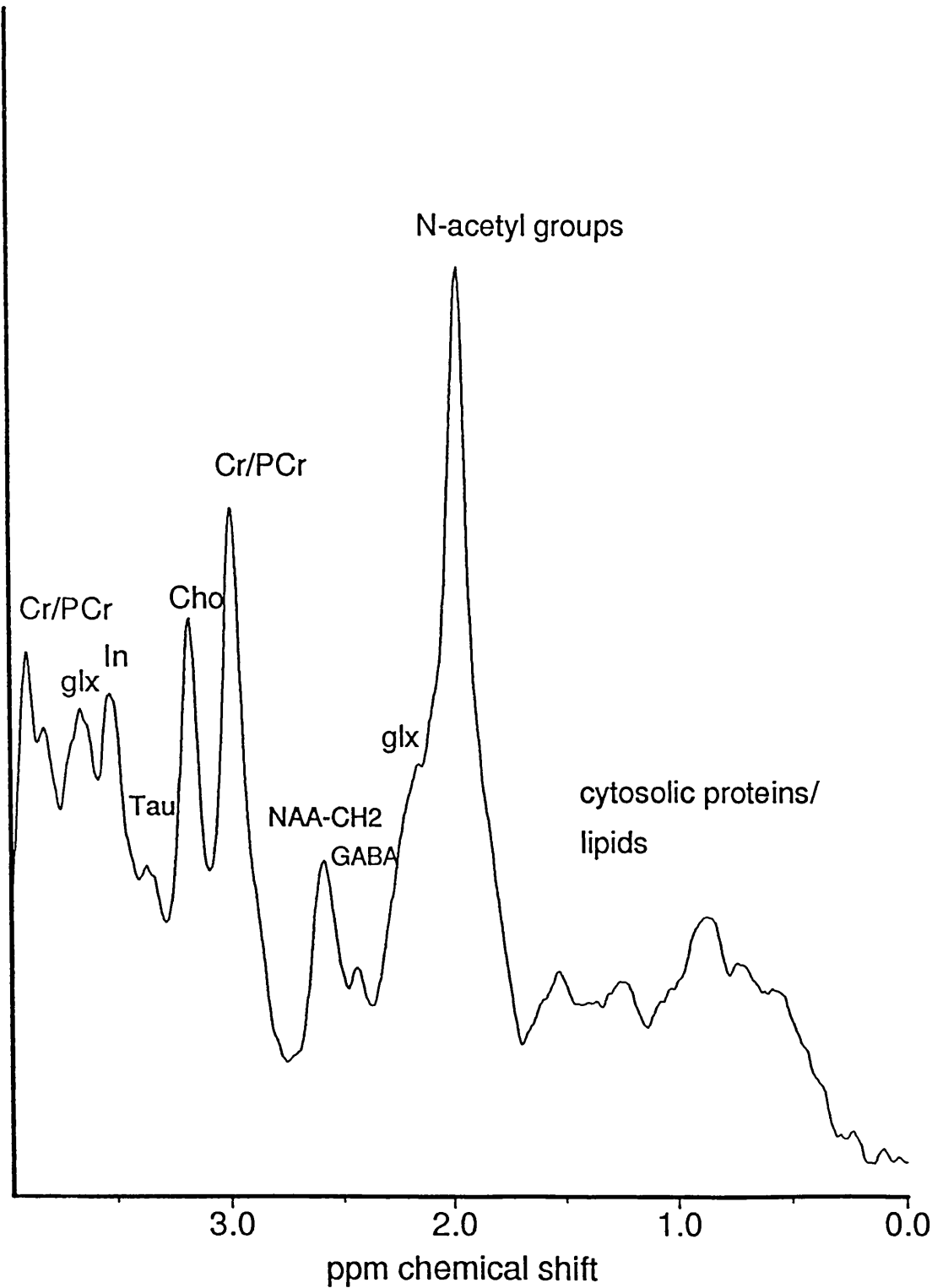


Figure 1.3a Chemical structures of some metabolites visible with Proton MRS

Compound	Structure
N-acetylaspartate	$ \begin{array}{c} \text{O}^- \\ \diagdown \\ \text{C} \\ \diagup \\ \text{O} \end{array} - \text{CH}_2 - \text{CH} - \text{C} \begin{array}{c} \diagup \text{O}^- \\ \diagdown \text{O} \end{array} $ $ \begin{array}{c} \\ \text{NH} \\ \\ \text{C} = \text{O} \\ \\ \text{CH}_3 \end{array} $
Creatine / Phosphocreatine	$ \begin{array}{c} \text{O}^- \\ \diagdown \\ \text{C} \\ \diagup \\ \text{O} \end{array} - \text{CH}_2 - \text{N} \begin{array}{c} \parallel \\ \text{CH}_3 \end{array} - \text{C} \begin{array}{c} \parallel \\ \text{NH} \end{array} \text{NH}_3^+ $
Choline	$ \text{HO} - \text{CH}_2 - \text{CH}_2 - \text{N}^+ \begin{array}{c} \text{CH}_3 \\ \text{CH}_3 \end{array} $

Figure 1.3b Chemical structures of some metabolites visible with Proton MRS

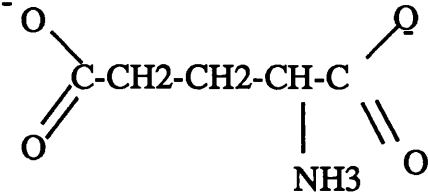
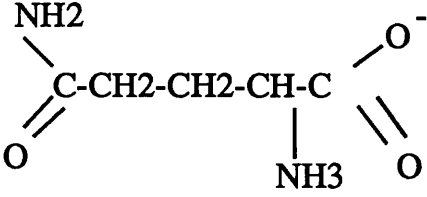
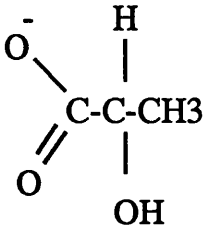
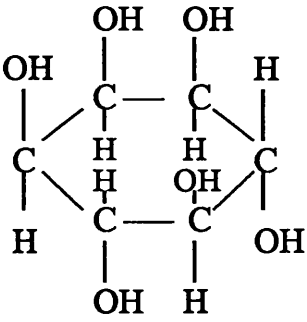
Compound	Structure
Glutamate	
Glutamine	
Lactate	
Myo-inositol	

Table 1.2

CHEMICAL SHIFTS OF METABOLITES IN 1H SPECTRUM

COMPOUND CHEMICAL SHIFT (PPM)			COMPOUND CHEMICAL SHIFT (PPM)		

Lactate	CH	4.12	Inositol	CH	3.54
	CH3	1.33			
Creatine	CH2	3.93	Glutamine	CH	3.76
	CH3	3.04		gamma	CH2
NAA	β CH2	2.70	Glutamate	βCH	2.06
	CH3	2.02		gamma	CH2
alpha	CH	4.40		β CH	2.10
GABA	βCH2	1.91	Taurine	SCH2	3.44
alpha	CH2	2.31		NCH2	3.27
gamma	CH2	2.36			
Aspartate	βCH	2.69	Alanine	CH	3.78
	β CH	2.82		βCH3	1.48

CHAPTER 2

Methods

2.1 THE NMR EXPERIMENT

2.1.1 Precession

NMR is dependent on the observation that the nuclei of atoms with odd atomic numbers possess a property known as spin or precession. This can be visualised as a spinning motion of the nucleus about its axis. In keeping with the theories of classical electromagnetism this spin endows such nuclei with a magnetic charge or “moment”. Only those nuclei that possess spin give rise to NMR signals. Each species of nucleus possessing an odd atomic number has a nuclear magnetic moment which is specific to that particular nucleus. When an appropriate nucleus is placed in a magnetic field, it will absorb energy at a specific frequency. The possible orientations of the nucleus within the magnetic field are dependent on the type of spin they possess. ^1H has a spin quantum number of $I=1/2$ and can have one of two possible orientations within the magnetic field. These two orientations have slightly different energy levels-the energy difference between them being proportional to the magnitude of the magnetic field. In a spectroscopy experiment it is possible to ‘tune’ in to different nuclei by applying a short-wave radiofrequency pulse which will specifically excite one type of nucleus and not the others. A particular advantage of this type of stimulation compared to other spectroscopic techniques (such as infrared for example) is that radiofrequency penetration into tissue is very effective and therefore all material within a volume is examined. Following the radiofrequency pulse, the nuclei absorb energy and ‘resonate’ for a fraction of a second. This resonance induces an oscillating voltage in the NMR coil which is detectable by the

spectrometer. Another name for this oscillating voltage is the free induction decay (FID). The FID then undergoes Fourier transformation (FT). This is a mathematical procedure performed by a computer which separates out the frequency components of a signal from its amplitudes as a function of time. This converts the FID to a spectrum.

The resonance frequency for a particular nucleus, for example ^1H , is directly proportional to the local magnetic field experienced by the nucleus. If this field were simply the applied magnetic field which was perfectly uniform over the entire sample, all protons would absorb energy at the same frequency and thus one could not differentiate between protons in different chemical environments. In imaging, this problem is overcome by applying gradients to the magnetic field. This modifies the resonant frequency in such a way that the precise frequency is dependent on the spatial position of a nucleus within the gradient. In spectroscopy this is not necessary because of an intrinsic property known as chemical shift.

2.1.2 Chemical shift

When a nucleus is placed in an external field, the actual magnetic field experienced by each individual nucleus is very slightly different from the applied field. This is because the external field induces electronic currents in atoms and molecules which produces a further small field at the nucleus. The size of this small field (known as B_{∞}) is dependent not only on the size of the external field (B_0), but also on the degree of shielding produced by surrounding electrons. Since the electron environment of each nucleus will depend on its chemical environment, the effective magnetic field (B_{eff}) is slightly different and therefore nuclei in different environments give rise to signals at different frequencies. The separation of resonance frequencies from an arbitrarily chosen reference frequency is known as chemical shift.

Chemical shift is expressed in dimensionless units known as parts per million (ppm).

The different protons within a chemical give rise to separate signals or resonances. The intensities of the signals as measured by their areas are proportional to the number of nuclei that contribute to them. To illustrate this, the spectrum of ethanol ($\text{CH}_3\text{-CH}_2\text{-OH}$) is shown in Figure 2.1. Three different resonant frequencies are shown which from left to right represent the H in the OH group, the H_2 in the CH_2 group and the H_3 in the CH_3 group. Some of the resonances in Figure 2.1 split into multiple lines or multiplets. This splitting is a manifestation of J-coupling which is discussed more fully in section 2.6.1 of this chapter. In theory the ratios of the three peak areas from ethanol should be 1:2:3, reflecting the different number of protons in each environment. The amount of signal however is also dependent on other factors including the relaxation times which are now discussed.

2.1.3 Relaxation within tissues

When a nucleus is exposed to an appropriate radio-frequency (RF) pulse it gains energy along the direction of the applied magnetic field. When the RF pulse is removed, the nucleus subsequently returns to its initial state of equilibrium. It does this via two relaxation processes: longitudinal or spin-lattice relaxation (T_1) and transverse or spin-spin relaxation (T_2). T_1 describes the return to equilibrium along the direction of the magnetic field whereas T_2 represents the return of magnetisation in the plane perpendicular to the field. In most instances the T_1 times are much longer than those of T_2 . For instance NAA in the occipital white matter of healthy controls has a T_1 of approximately 1.5 secs and a T_2 of 450ms (Table 2.1).

2.1.4 Relaxation properties and echo-time.

The various metabolites discussed in Chapter 1 all exhibit different relaxation times. The values for these are dependent on magnetic field strength. Approximate values (Frahm et al., 1989b) for the relaxation times of the main metabolites are shown in Table 2.1. The T_1 and T_2 values for other metabolites including proteins and lipids are far shorter. These substances only produce a visible signal in the proton spectrum when a short T_2 weighting is used (e.g. 10-50ms). The effect of increased T_2 weighting on protein and lipid signal in the human brain is shown in Figure 3.6. As the TE is increased, the signal from the lipid and protein moieties to the right of NAA gradually disappear so that by a TE of 135ms no signal is seen in this region. If one is specifically interested in lactate, NAA, creatine or Cho all of which have a relatively long T_2 value (Table 2.1), a long T_2 weighting such as 135 or 270ms is often employed since this will improve water and fat suppression.

2.2 VOLUME LOCALISATION

Perhaps one of the most important advances in MRS in the last few years has been the development of NMR sequences which allow accurate localisation of a volume of interest (voxel) within the human brain. Ideally a sequence should allow collection of an undistorted spectrum from a well defined volume without contamination from signal outside the voxel. For a localisation sequence to be useful in a clinical setting it must be easy to use as well as providing reliable and consistent results.

2.2.1 Surface Coil Methods

This was the earliest localisation method suggested (Haase et al.,

1983) and relies on a flat circular coil to excite a limited volume. The coil transmits radio-frequency pulses and receives the NMR signal. Although this system has the advantages of being easy and providing very good signal to noise ratio (SNR), the volume is neither well defined nor restricted (Haase et al., 1983)

2.2.2 Volume selection by frequency selective RF pulses

Most spectroscopic localisation methods currently employed select planes in an object by applying frequency selective pulses in the presence of linear gradients. These can be split into two groups; those involving a combination of several acquisitions known as multishot and those achieving localisation of a volume in a single shot.

The most frequently used multishot method is the so called ISIS or Image Selected In vivo Spectroscopy technique devised by Ordidge et al (1986). This technique selects a cube by the combination of a minimum of eight acquisitions. As with the singleshot sequences, this method has the advantage of being able to define a freely selectable volume in terms of size and position. The ISIS technique however also has the advantage of very small T_1 relaxation losses and no T_2 losses. This has made it particularly useful in ^{31}P NMR where the T_2 values are very short in vivo. A major disadvantage of this sequence is the limited ability to suppress signal from outside the voxel. This has limited its use in ^1H MRS where extra-voxel contamination from subcutaneous lipid may be a problem.

2.2.3. Single-shot methods of volume selection.

PRESS

The PRESS method (Point REsolved Spectroscopy) (Ordidge et al., 1985)

excites only those magnetisations that contain the desired voxel as part of an excited slice. The three slices required stem from a 90° excitation pulse and two 180° refocussing pulses. The voxel is defined by the intersection of the three planes. For use in proton spectroscopy, the sequence is preceded by one or more chemical-shift selective water suppression pulses. Although PRESS has the advantages of good SNR and being easy to use it has the drawback of requiring 180° refocussing pulses which means that it is not possible to optimise the SNR with short repetition times. PRESS also has greater T_2 relaxation losses than the Stimulated Echo Acquisition Mode (STEAM) sequence and therefore may be less useful in studying highly bound metabolites with short spin-spin relaxation times (T_2)

STEAM

The STEAM sequence (Granot et al., 1986; Frahm et al., 1987) is the method used in the clinical MRS studies described in this thesis. It is similar to the PRESS technique but instead defines the voxel by the intersection of three slices selectively excited by three successive 90° pulses. The STEAM sequence can be written in the abbreviated form as

$$90^\circ - TE/2 - 90^\circ - TM - 90^\circ - TE/2 - Acq$$

This is illustrated diagrammatically in Figure 2.2

The STEAM sequence has a number of advantages over other singleshot localisation methods such as PRESS. Although the STEAM sequence does produce some T_2 relaxation loss this can be reduced to a minimum since there is no T_2 loss between the the second and third RF pulse -the so called mixing time (TM). This has allowed, when appropriate, the collection of spectra at an echo time as short as 10ms. The implementation of such a short echo-time is particularly useful when trying to visualise highly bound metabolites such as lipids and

macromolecules which have very short T_2 relaxation times. The STEAM sequence also provides a better resolution of signal from glutamine and glutamate in the 2.0-2.5 region of the spectrum compared to PRESS. This sequence is easy to use thus allowing the author to acquire spectra from patients and controls in the various clinical studies described in the following chapters. This sequence has become established as a reliable means of volume localisation in proton MRS (Frahm et al., 1987, 1989a, 1990) and one that is now routinely used in clinical MRS studies of the brain (Arnold et al., 1990; Gideon and Henriksen, 1992; Chong et al., 1993). As with nearly all spectroscopy sequences, several acquisitions have to be collected to produce a good signal to noise ratio (SNR). SNR is dependent on several factors including the size of the volume of interest and echo-time collected. In the current studies, volumes ranging from 3-12ml have been collected with echo-times of 10ms, 135ms and 270 ms. It has therefore proved necessary to acquire between 128 and 512 averages to collect one spectrum for each volume of interest.

Before collection of the spectroscopic data there are two further procedures that must be carried out. These are shimming and water suppression.

2.3 SHIMMING

Following on from the earlier description of the NMR experiment as applied to spectroscopy, it is important that the magnetic field over the volume of interest is as uniform as possible to allow maximum advantage of the chemical shift that results from nuclei being in different chemical environments. Improving the homogeneity of the magnetic field results in the protons within a particular chemical group resonating at the same frequency and therefore producing a narrower line-width in the spectrum. This is important for two

reasons. First, it allows differentiation of signals from different chemical groups that resonate at similar frequencies in the spectrum. Conversely, with poor field homogeneity, the peaks from different chemicals merge making quantitation less accurate. This can be a particular problem with the resonances from creatine at 3.02 ppm and choline containing substances at 3.2ppm. The homogeneity of the magnetic field is also important in allowing optimal water suppression. By producing narrow line-widths it is possible to suppress most of the signal from the water resonance without distorting the resonances from the remaining chemical groups.

Correction of the magnetic field is carried out with the use of supplemental coils- known as shim coils. By adjusting the current in the three shim coils x,y and z, one is able to correct for inhomogeneities in the magnetic field. Although magnetic field inhomogeneity may result from external factors such as pieces of ferromagnetic material becoming inadvertently attached to the magnet, the uniformity of the field may also be altered by particular susceptibility effects from the area of the brain being studied. For example it is more difficult to produce narrow line-widths from spectra acquired in the basal ganglia. Figure 2.3 is a T₂ weighted spin-echo sequence (TR 2000ms TE 80ms) showing the basal ganglia from a healthy control. The low signal visible in the basal ganglia is the result of iron deposition within the globus pallidus. This is a normal finding in healthy individuals, though more extensive iron deposition extending laterally into the putamen may be of pathological significance. Iron deposition within the basal ganglia produces susceptibility effects (hence the signal loss on imaging) which are reflected by broadening of the line-widths in spectra collected from the basal ganglia compared to areas of the brain where iron deposition is not a feature (Figure 2.4.)

such as the cerebral hemispheres.

2.4 WATER SUPPRESSION

The concentration of water in the healthy human brain is approximately 79.5molar (M) in white matter and 91M in grey matter (Norton et al., 1966) making it an ideal molecule to use when imaging the brain. In contrast, the metabolites which are visible with MRS have concentrations within the millimolar range. One of the major difficulties with proton MRS has been the accurate detection of signal from these substances in the presence of a water concentration which is approximately 10,000 times greater. There have been great advances in methods that allow selective suppression of the water signal from the spectrum. The most widely used technique and the one adopted in the following studies is the use of presaturation pulses. With this method, one applies a pulse sequence over a particular frequency range to selectively excite and then dephase the signal from that part of the spectrum. This occurs prior to the STEAM sequence. In the case of water, this produces a 1000 fold reduction in signal. The presaturation method that has been adopted is the CHEmical Shift Selective method (CHESS) (Haase et al., 1985; Doddrell et al., 1986). This is a sequence of three RF pulses each followed by a spoiler gradient. The first two RF pulses are 90° . The third pulse which tends to range between 110° and 140° depending on factors such as the echo-time, can be modified by the operator to optimise water suppression. The saturation pulses are specifically designed to excite only a 50 Hz range of frequencies centred around the water signal which resonates at 4.7ppm. The effect of water suppression on the resulting spectrum is shown in Figure 2.5.

2.5 POST PROCESSING

2.5.1 Fourier Transformation

The spectroscopic data is acquired as an oscillating signal - known as the FID which represents an amalgamation of signal from all the resonating nuclei of the various metabolites. To resolve out the different frequencies and characteristics of individual metabolites the data undergoes FT. This mathematical procedure is, as mentioned earlier, a means of separating out the frequency components of a signal from its amplitude and is performed by computer.

2.5.2 Apodisation

After FT has been performed, the spectroscopic data is ready for display. In practice however the FID usually undergoes a small amount of filtering in order to improve signal-to-noise. This is another mathematical procedure known as apodisation whereby all the datapoints are multiplied by a set function. This has the effect of smoothing out the FID throughout its signal. The effect of this after fourier transformation is to produce broadening of the peak line-widths. The advantage of this (illustrated in Figure 2.6) is to smooth out the resonances and produce a less 'noisy' baseline. If however too much apodisation is applied to the FID then, after FT, the resonances from different metabolites may merge making quantification difficult (figure 2.7). The amount of apodisation which is necessary may vary depending on SNR and the line-widths of the metabolites. In the studies described in the following chapters, a 1- 1.5 Hertz (Hz) apodisation or line-broadening function has been applied.

2.5.3 Phase correction

After the NMR signal has undergone FT, a spectrum is produced similar to that shown in Figure 2.8. The peaks of the main metabolites are visible but they are not pointing in an an upright direction. This is due to the arbitrary phase relationship between the collected signal and

the reference RF frequency. Phasing can be performed manually to adjust the peaks till they are all upright as illustrated in Figure 2.8. This process is often carried out automatically by applying the phase information in the water reference signal to that of the water suppressed spectrum. Phasing may be performed in two steps. In the first step (or zero- order phasing) all the peaks are adjusted by the same amount. In the second step (or first-order phasing) the amount of correction increases linearly across the spectrum. In practice first-order phasing is seldom necessary.

2.5.4 Baseline correction

This is a post processing technique which allows for correction of the baseline which may be distorted by residual signal from what remains of the water peak. In the studies described in this thesis it was possible to quantify the data without applying baseline correction.

2.6 **PEAK ASSIGNMENTS**

The assignment of resonances to specific metabolites in the ^1H NMR spectrum of the human brain in-vivo can be determined in a number of ways.

2.6.1 Extract identification

The tissue of interest can be removed from the body and a tissue extract made. Making extracts allows narrower line widths to be obtained with in-vitro MRS (using higher field strengths) than is possible in vivo thus helping to separate out resonances from metabolites with a similar chemical shift. Furthermore, resonance assignments can be confirmed by adding quantities of the pure compound and observing an increase in intensity of the appropriate metabolite. It is also possible to use two dimensional NMR methods (for example 2D-COSY) to visualise coupling patterns between different Hydrogen groups within a given compound (Behar et al., 1991).

Editing techniques

J modulation

It is also possible to use 'editing' techniques in-vivo to identify or null particular metabolites. An example of this is the inversion of signal from a number of metabolites. This occurs as a result of J- coupling. J-coupling is the term used to describe any interaction which occurs between the magnetic fields of the nuclei themselves. Each nuclear magnetic moment has its own magnetic field which adds to or subtracts from the field of neighbouring nuclei. This produces a slight change in the chemical shift thus producing multiplet patterns from CH groups in the same molecule. Other manifestations of J-coupling include modulation of peak intensities and in some cases peak inversion in a spin-echo experiment. For example, lac produces a double resonance -or doublet- which are 7 Hz apart at 1.33 ppm in the ^1H NMR spectrum. The two resonances come from the CH and CH_3 groups which are adjacent within the lactate molecule (Figure 1.3b). When the lac signal is exposed to a spin-echo sequence, the doublet undergoes marked changes in phase and amplitude. At an echo-time of 270ms the lactate doublet demonstrates an in-phase signal and is therefore upright in the spectrum. However at 135ms, the doublet is out of phase and appears inverted (Figure 2.9). Other metabolites which possess this property include alanine GABA, glutamate and glutamine and J modulation can be used to highlight or suppress their signals.

2.7 METABOLITE QUANTITATION

2.7.1 Determination of peak areas

Peak integration is normally carried out by software provided with the MRS instrument. In this study peak areas were determined using a commercial package ("SA / GE", G.E. Milwaukee W.I.). The peak areas

were fitted to a gaussian line shape using a Marquardt fitting procedure. Although theoretically the resonances should have a Lorentzian line-shape, in practice, the peaks do not conform to this ideal shape. The fitting produced from a gaussian line shape proved more accurate and reproducible and was therefore used in the studies described in this thesis.

2.7.2 Relative quantitation

The majority of MRS studies have, to date, relied on an internal standard of reference for quantitation. The resonance from creatine/phosphocreatine at 3.2 ppm has been most frequently used in this role since theoretically these two compounds are in chemical equilibrium and would therefore be expected to remain constant in concentration. With this method, the data is converted into concentration units by calculating the area of signal produced from the creatine/phosphocreatine resonance and relating this to the other metabolites by simple proportion. This method was employed in chapters 3 and 6 of this thesis prior to the development of methods which allowed the application of absolute quantitation described below.

2.7.2 Absolute quantitation

More recently, it has proved possible to accurately quantitate the millimolar concentration of metabolites in vivo by MRS (Tofts and Wray 1988; Michaelis et al., 1993; Christiansen et al., 1993). The method of quantitation employed in chapters four, five and seven of this thesis is that described by Christiansen et al (1993). Metabolite concentrations are calculated by using the fully relaxed and unsuppressed water spectrum as an internal standard of reference. A number of correction factors are necessary. These take into account the concentration of water in the spectroscopic volume of interest, the number of protons in

each metabolite, T_1 and T_2 correction values and the difference in receive attenuator settings. These can all be expressed in the following equation,

$$\text{Met} = [\text{H}_2\text{O}] \times \text{PI} \times T_{1\text{corr}} \times T_{2\text{corr}} \times S_{0\text{Met}} / S_{0\text{H}_2\text{O}} \times 1/2^R$$

where $S_{0\text{Met}}$ and $S_{0\text{H}_2\text{O}}$ denote the signal intensities for metabolites and water respectively, $[\text{H}_2\text{O}]$ is the brain water concentration from the volume of interest. In the MS patients, the water concentration from the voxel of interest was calculated by comparing the signal intensity from the PD images in the basal ganglia (where no lesions were visible) with the signal intensity from the region of interest. The putamen was chosen since this region of the basal ganglia is not affected by heavy metal deposition in healthy controls (Olanow, 1992). Furthermore a recent study by Grimaud and colleagues (1995) has shown no evidence of hypointensity on T_2 -weighted images to suggest increased heavy metal deposition in the putamen of MS patients. The water concentration of normal appearing grey matter has been taken as 45.5M (Norton et al., 1966). In the control groups the concentration of water in white matter has been taken as 39.75M (Norton et al., 1966). $T_{1\text{corr}}$ and $T_{2\text{corr}}$ are T_1 and T_2 correction values based on published values for the metabolites studied (Frahm et al, 1989). T_1 and T_2 relaxation times were not measured in the following studies because of the prohibitively long examination times required. A T_1 or T_2 effect cannot therefore be excluded and for this reason the term apparent concentrations are used. PI is the proton index and $R = ((R_1 + R_2) \text{ metabolite} - (R_1 + R_2) \text{ water})$ accounts for different receive attenuator settings. For further theoretical discussion of this method see Appendix A.

Figure 2.1
 ^1H NMR spectrum of ethanolol ($\text{CH}_3\text{-CH}_2\text{-OH}$)

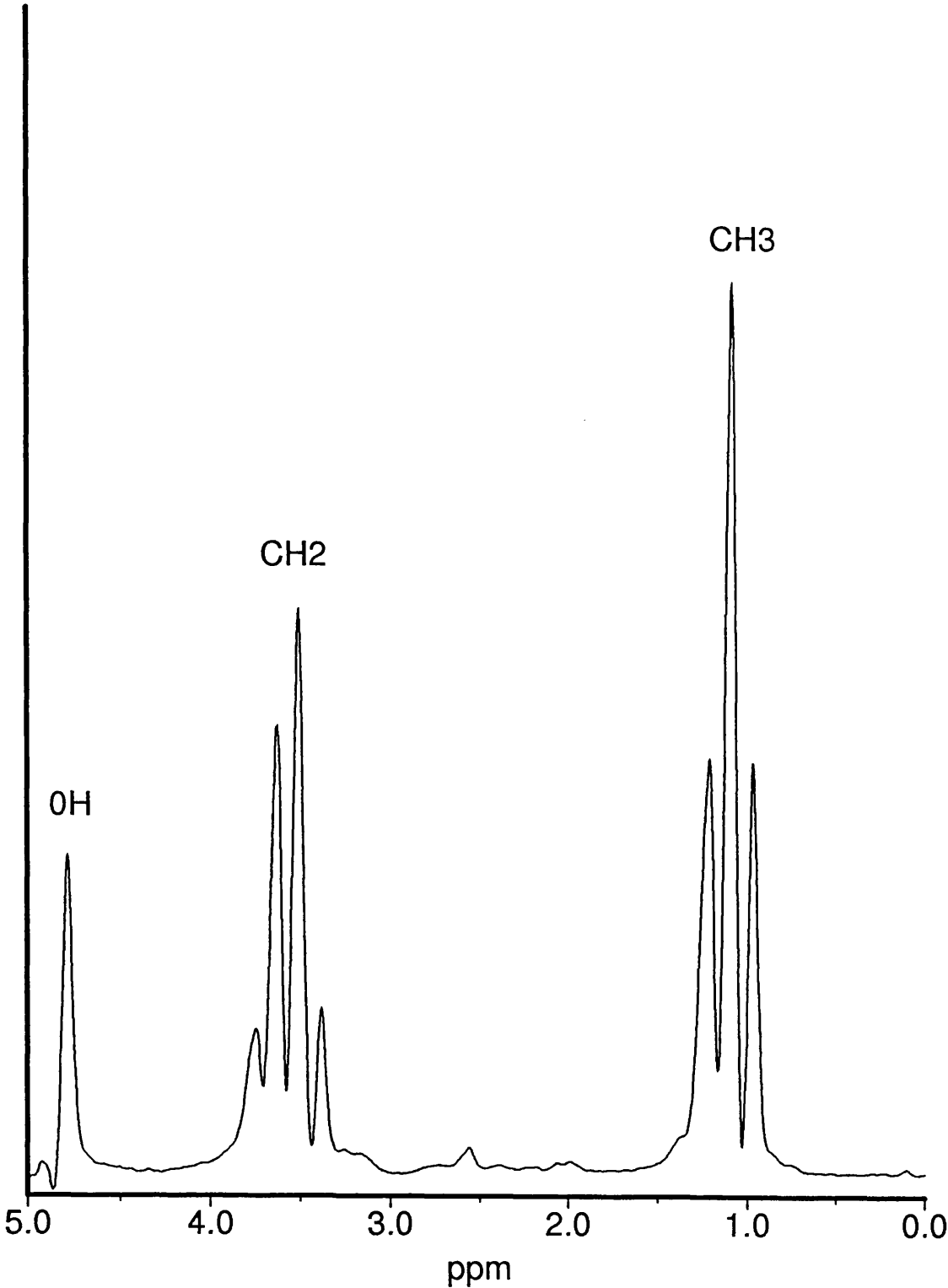


Table 2.1

Spin-lattice relaxation times (T_1) and spin-spin (T_2) relaxation times at 1.5 tesla of the major metabolites in the ^1H NMR spectrum from occipital white matter (Frahm et al., 1989b)

<u>Compound</u>	<u>ppm</u>	<u>T_1</u>	<u>T_2</u>
NAA	2.02	1450 ms	450 ms
Cr and PCr	3.04	1550 ms	240 ms
Cho	3.2	1150 ms	330 ms
Lactate	1.33	1550 ms	1200 ms
Myo-Inositol	3.54	900 ms	110 ms

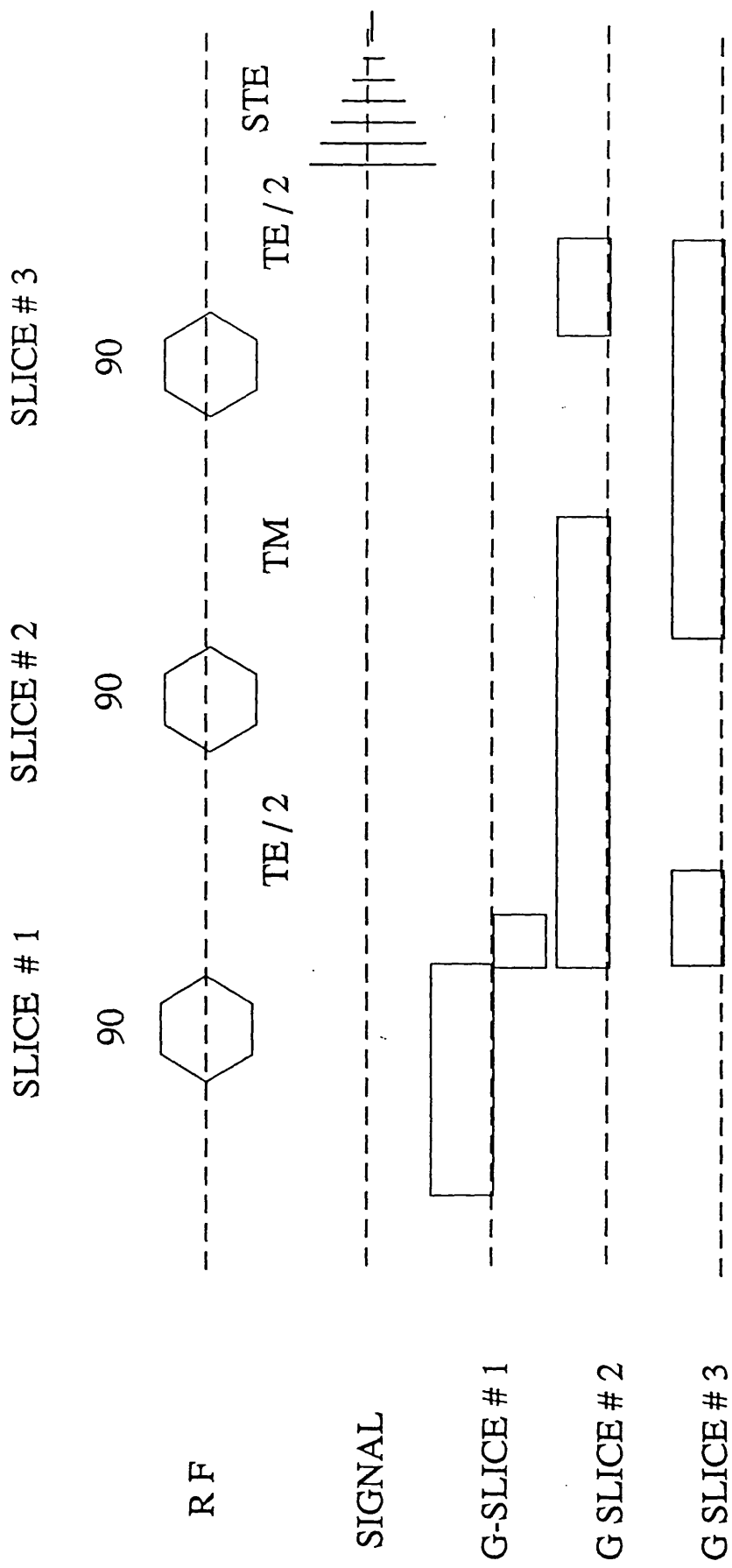
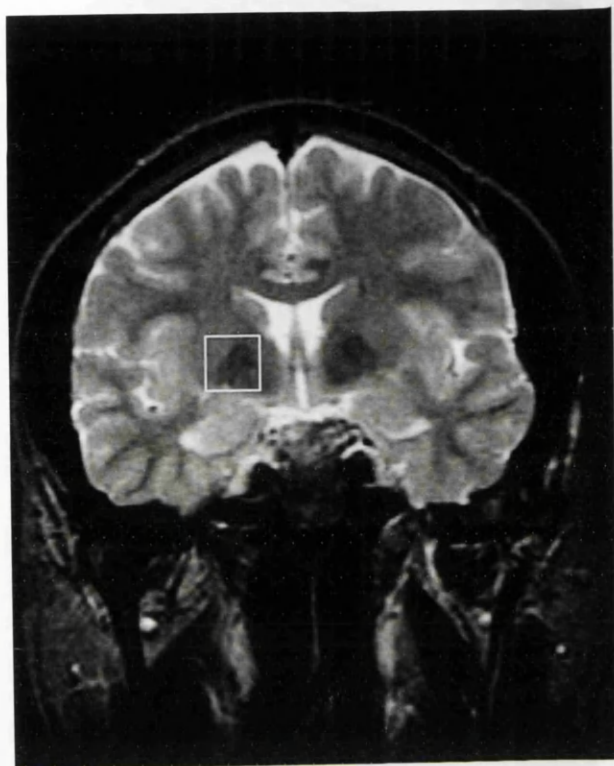


FIGURE 2.2 STEAM Localisation sequence

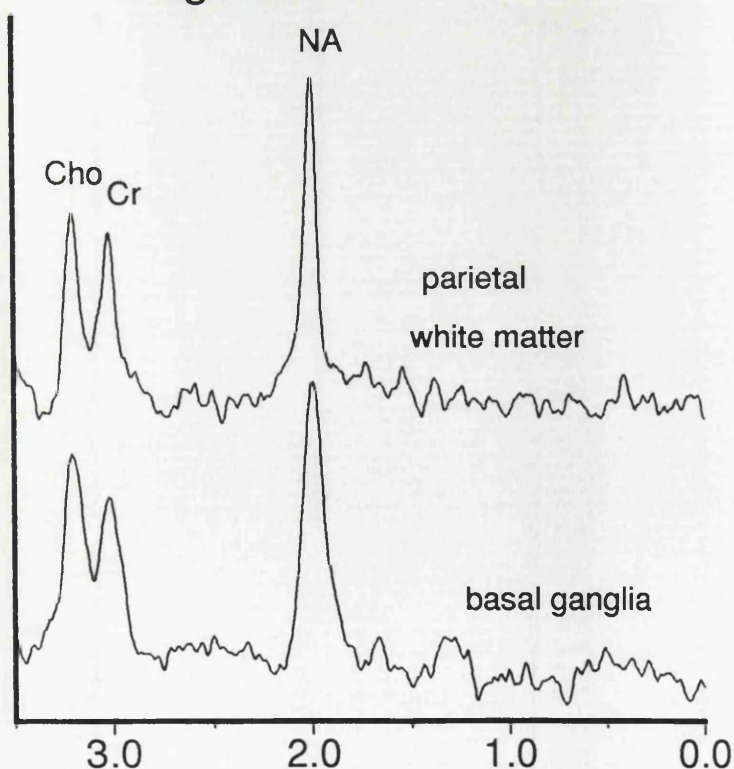
Figure 2.3

61



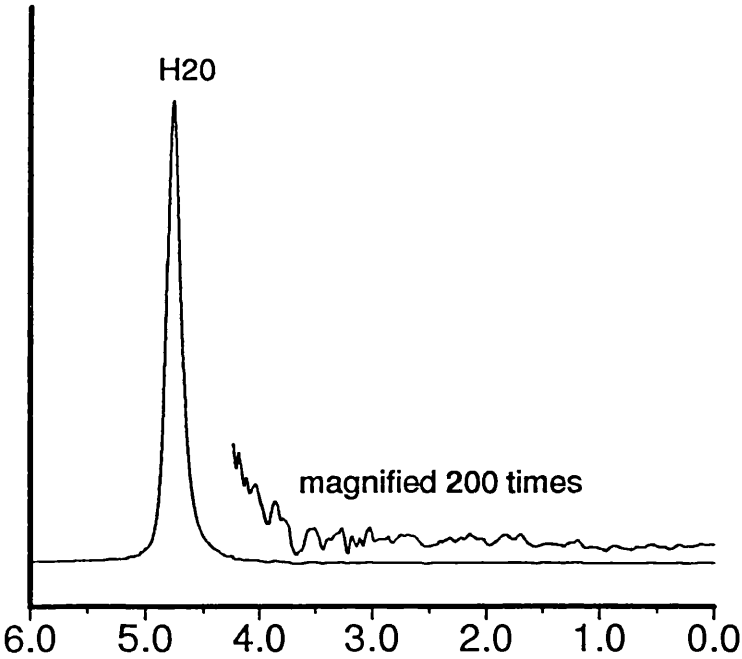
T2 weighted coronal MRI
with volume of interest
localised to the lentiform
nucleus

Figure 2.4



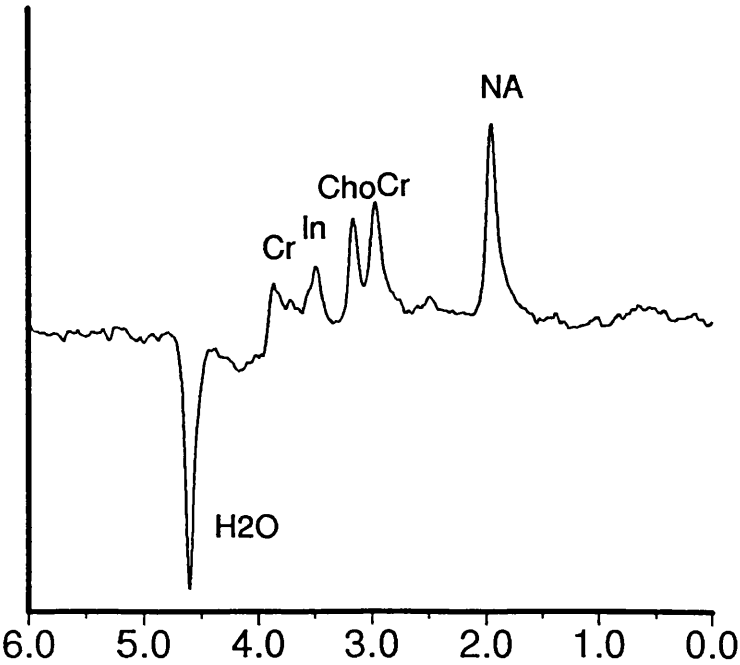
Comparison of spectra from the basal ganglia and the cerebral hemisphere.
The broader line-widths in the basal ganglia are the result of greater
magnetic field inhomogeneity due to iron deposition in this region of the brain.

Figure 2.5A



Unsuppressed water spectrum. While some metabolites are visible in the blownup spectrum, these are grossly distorted by the tail of the water peak.

Figure 2.5B



Spectrum from Figure 2.5A after water suppression showing remaining water signal and metabolites. TE 135ms

Figure 2.6
Effect of line broadening on NMR spectrum

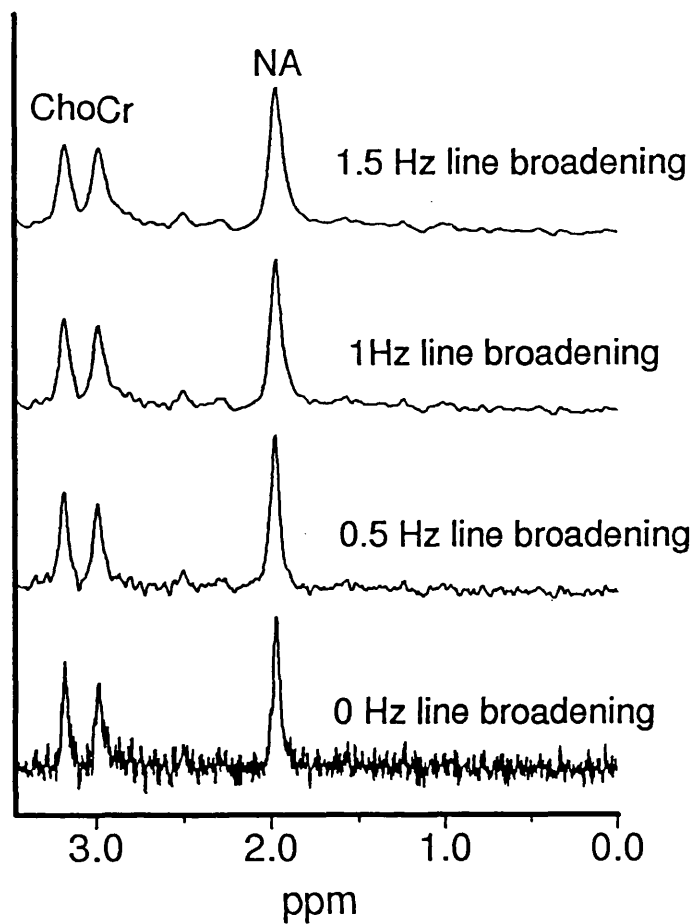


Figure 2.7
Merging of Cho and Cr with a line-broadening of 4 Hz

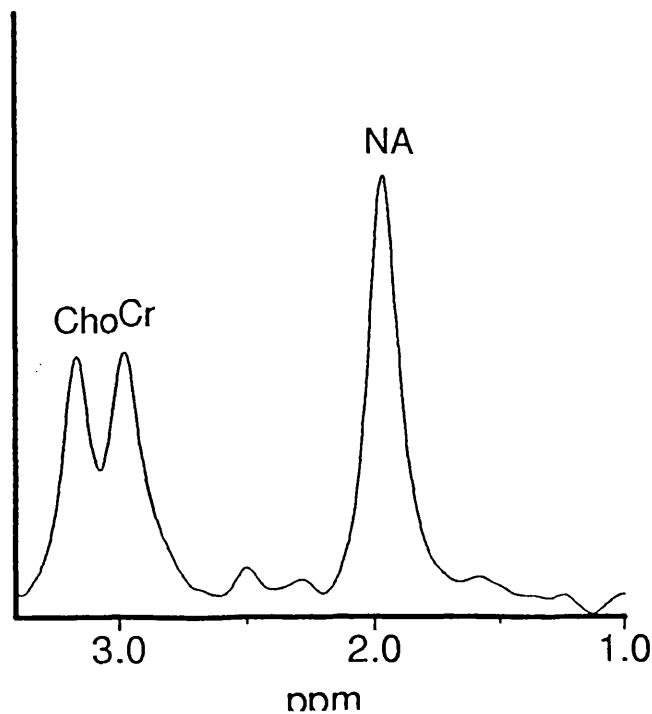
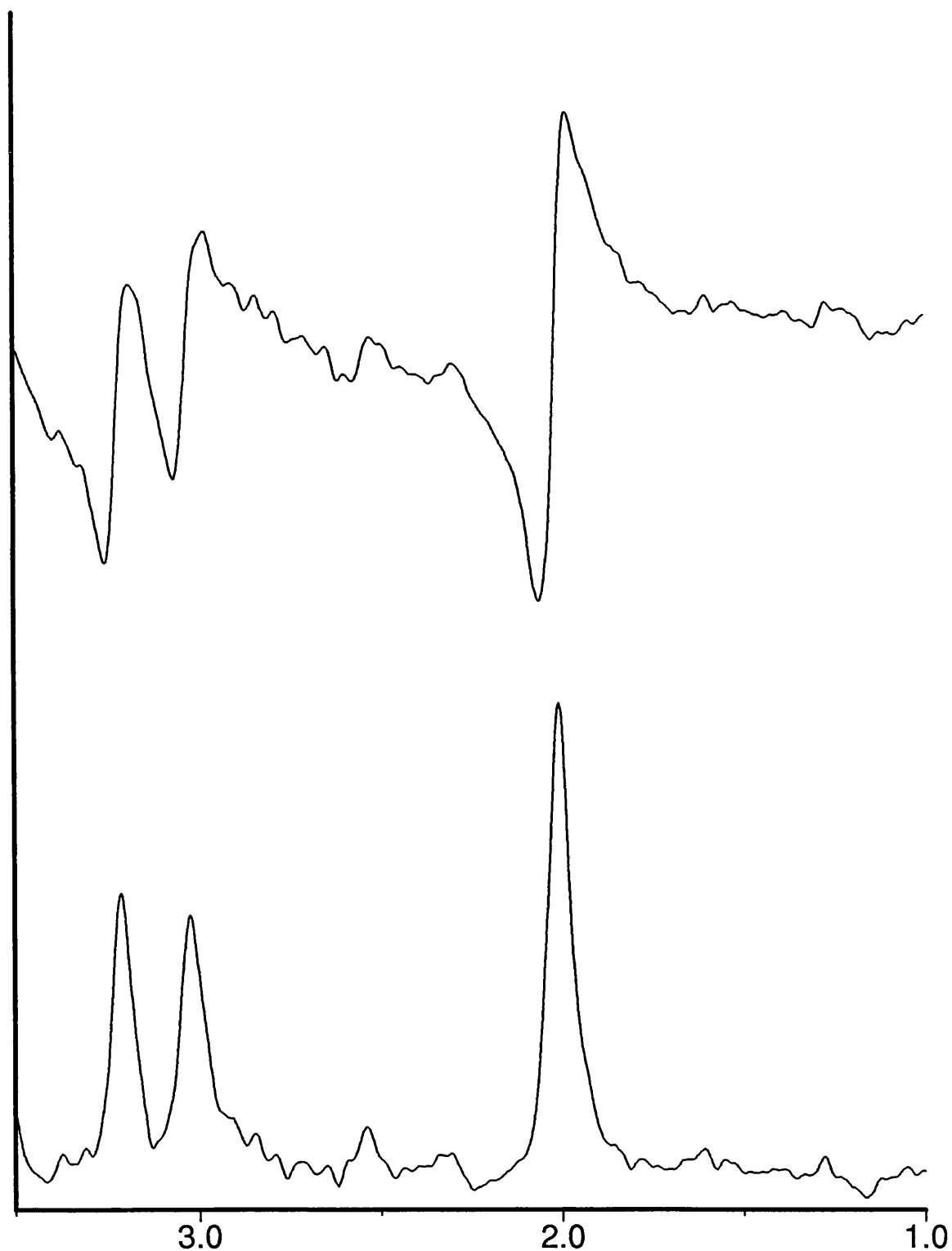


Figure 2.8

The effect of phasing on the ^1H NMR spectrum

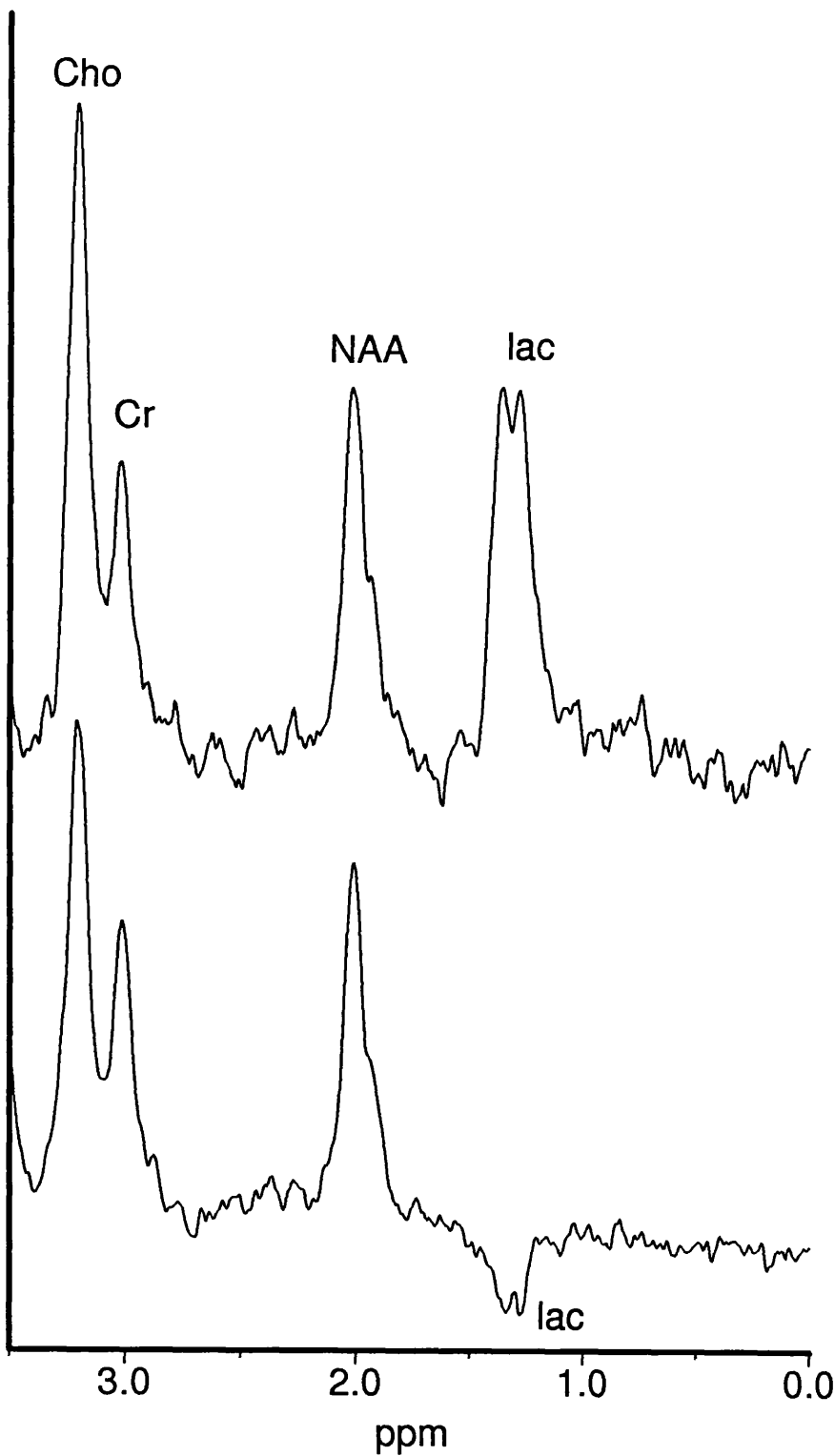


Upper spectrum – no phase correction

Lower spectrum manual phase correction applied

Figure 2.9

The effect of J modulation on the lactate signal



Upper spectrum TE 270ms with upright lactate doublet

CHAPTER 3

SERIAL PROTON MAGNETIC RESONANCE SPECTROSCOPY IN ACUTE MULTIPLE SCLEROSIS LESIONS

3.1 SUMMARY

Serial ^1H MRS, was carried out at one to two monthly intervals on 8 patients with MS who presented with evidence of a large acute cerebral white matter lesion. MRS was obtained from acute lesions (volumes of interest 4 to 12 mls), which at presentation showed Gd-DTPA enhancement, and from similar volumes of NAWM lateral to the lesion and nearer the scalp. Follow up ranged from 4 to 9 months (mean 6 months). Short echo spectra from acute enhancing lesions invariably showed the presence of large resonances at 0.9 and 1.3 ppm compared to NAWM and white matter from healthy age matched controls, indicating that these peaks were not the result of voxel contamination from scalp fat. These resonances, which probably represent lipid products of myelin breakdown, were detected in lesions which had been enhancing for less than one month and remained elevated for a mean of 5 months (range 4-8 months). The results provide evidence that short echo ^1H MRS can detect myelin breakdown products and that myelin breakdown occurs during the initial inflammatory stage of lesion development. The ratio of NAA - a neuronal marker- relative to Cr was reduced in acute lesions and in NAWM. In 6 of the lesions studied there was however a subsequent rise in the NAA/Cr ratio indicating that axonal loss is not the only mechanism of reduction in the NAA/Cr ratio.

3.2 INTRODUCTION

An important unresolved question about the pathogenesis of MS is when does demyelination occur ? Though it has long been known that both inflammation and demyelination can be present in the same lesion (Dawson 1916; Lumsden 1970; Allen 1991), the temporal pattern of evolution of each of these processes has not been elucidated by pathological studies which provide information only at a single time point. Serial Magnetic resonance imaging (MRI) studies (Kermode et al ., 1990) have shown that the earliest detectable event in the development of a new lesion is a breakdown of the blood brain barrier; there is experimental (Hawkins et al ., 1990) and post mortem evidence (Katz et al ., 1993) that this indicates the presence of inflammation. However, conventional MRI has not yielded information about the time course of demyelination since it does not reveal normal myelin or myelin breakdown products.

MRS at long echo times of 135 and 270 ms detects metabolites with long T_2 relaxation times such as NAA, Cho, Cr/PCr and lac. MRS at short TEs of 10-30ms detects additional metabolites with short T_2 relaxation times. These include mobile lipids, proteins, inositol, and a number of the neurotransmitters such as glu and GABA. The ability to detect mobile lipid resonances within MS lesions using proton MRS would provide, for the first time, a non-invasive tool with which to monitor myelin breakdown and to study the temporal relationship of inflammation and demyelination *in vivo*.

It has also been suggested that proton MRS may have a role in monitoring axonal loss (probably an important factor in the development of persistent disability in MS) since NAA, an amino acid clearly visible on proton MRS, is largely confined to neurones and their processes.

Recent technical advances in proton spectroscopy have improved its spatial resolution, allowing the study of volumes as small as 1 ml (Frahm et al., 1990)- a common size for multiple sclerosis lesions. Serial long-and short- TE proton MRS has therefore been performed on patients with MRI or symptomatic evidence of acute cerebral lesions. The aim was (1) to determine whether myelin breakdown products are spectroscopically detectable at short echo times within the acute lesion; (2) if they are, to determine whether they are the result of voxel contamination from overlying scalp; (3) to establish at what phase in the evolution of the lesion demyelination occurs; and (4) to elucidate the time course of changes in NAA.

3.3 MATERIALS AND METHODS

3.3.1 Subjects

Eight patients (age range, 20-48; mean age 28) were studied.

6 patients had clinically definite MS and two had laboratory supported definite MS (Poser CM *et al* ., 1983). The disease severity ranged from mild to severe as measured on the expanded disability status scale (Kurtzke 1983). Two patients had undergone treatment with intravenous methylprednisone one day prior to the first spectroscopic examination. Nevertheless, these lesions still enhanced after administration of Gd-DTPA, (Miller et al ., 1992b). The patients were followed at one to two monthly intervals. Follow up ranged from 4 to 9 months (mean 6 months). The patients were examined neurologically by the author at entry into the study and at each follow up session. The patients then underwent unenhanced MRI, localised proton MRS and finally Gd-DTPA enhanced MRI.

The study was approved by the Joint Ethics Committee at the Institute of Neurology and the National Hospital for Neurology and Neurosurgery,

London. Informed consent was obtained from all patients prior to each study. The patients were judged to have an acute lesion if 1) there was an area of increased signal intensity within white matter on MRI which displayed Gd-DTPA enhancement and which had not been present on MRI carried out in the previous month (4 patients). These patients had undergone monthly unenhanced and enhanced brain scans over the previous year as part of other longitudinal studies.

2) There had been an acute clinical relapse within the previous two weeks and there was an appropriately placed new lesion on MR imaging which enhanced after Gd-DTPA administration (4 patients).

Eight healthy age matched controls underwent MRI and localised proton MRS without administration of Gd-DTPA. A 17-year-old female with a lipoma in the quadrigeminal cistern was also studied.

3.3.2 Magnetic resonance imaging and spectroscopy

MRI and MRS were performed on a 1.5 T. G.E. signa whole body scanner using a standard quadrature head coil. The study commenced with a T_2 weighted fast spin echo imaging sequence (TR 3000 ms, TE_f 80 ms) (5mm slices with 2.5 mm gap, 256x256 matrix, echo train length 8). After imaging, a volume of interest ranging between 3.5 ml and 12ml was prescribed which in the patient group incorporated a new high signal lesion. Large lesions were chosen in order to minimise partial volume effects. An MR image of the voxel was then obtained to ensure accurate localisation. Water suppressed 1H spectra were obtained using a STEAM sequence (Frahm *et al* ., 1987 and 1989a). Acquisition parameters were TR 2000 ms, TM 12ms, TE 10 and 135ms. 256 averages were collected using an 8 step phase cycle in ~ 9 minutes. 1024 points were collected, with a spectral width of 750 Hz. Shimming to a line width of ~3Hz. and water suppression were re-optimised for each new location. In the control group, spectra were

collected from an area of periventricular white matter.

In the patient group, long and short TE spectra were acquired from acute lesions on the first study and at all subsequent examinations. At the first study only, a separate location containing NAWM was also examined which was lateral to the lesion and closer to the scalp. After collection of the spectroscopic data, Gd-DTPA, 0.1 mM./kg. was injected intravenously and T₁-weighted Gd-DTPA-enhanced images were obtained (TR 500 ms, TE 40ms).

Data processing included 1.5 Hz. line broadening for filtering, Fourier transformation, and zero order phase correction. No baseline correction was applied. Resonance areas were calculated by manual integration. Ratios for the various metabolites are expressed relative to creatine. NAA and choline ratios were calculated from the spectra collected at 135ms. Inositol ratios were calculated from spectra collected at 10ms. Statistical analysis was performed using Student's t test. Values are expressed \pm 1 SD together with a level of significance (p).

3.4 RESULTS

3.4.1 Controls

Representative short echo and long echo spectra from a healthy 28-year-old female control are shown in Figure 3.1A. All spectra collected at a short echo time from controls showed small resonances at 1.3 and 0.9 ppm (Davie et al., 1992) which have been assigned to macromolecules (Behar et al., 1994) and lipid (May et al., 1986; Callies et al 1993). The lipid assignments are corroborated by an experimental model, showing that signals appear at 0.9 and 1.3 ppm in the proton spectrum after the induced formation of lipid droplets in myeloma cells (Callies et al., 1993). *In vivo* confirmation of these assignments were obtained from

the 17-year-old female patient with a lipoma situated in the quadrigeminal plate (Figure 3.1B); large resonances were seen only at 0.9 and 1.3 ppm (Figure 3.1C).

A Spectrum at an echo time of 135ms confirmed that there was no contribution from lactate in the resonance at 1.3 ppm in healthy controls (Figure 3.1A). Lipid resonances were not observed at this longer echo time.

Resonances from the other metabolites have been assigned as follows (Behar and Ogino 1991, Frahm et al., 1989b); NAA at 2.02 ppm and 2.6ppm, Cr/PCr at 3.04 ppm. Cho at 3.2 ppm, In at 3.54 ppm, glu , gln and GABA between 2.1 and 2.45 ppm.

3.4.2 Short echo time spectra: patients

Short echo spectra in the patient group showed large resonances at 0.9 and 1.3 ppm from Gd-DTPA enhancing lesions (Figure 3.2), when compared to the small resonances seen in the regions of normal appearing white matter lateral to the lesion and in white matter from healthy controls. In one 36-year-old female with clinically definite MS it was possible to study a number of volumes from the lesion and surrounding normal appearing white matter. A spectrum (Figure 3.4 Spectrum A) was collected from a 12ml volume which included most of a region of high signal as shown on a T₂ weighted scan (Figure 3.3 image A). When the voxel was reduced to a volume of 4 ml and taken from the centre of the lesion (Figure 3.3 image B) , the changes were far more striking (Figure 3.4 Spectrum B); this region was subsequently shown to enhance (Figure 3.3 image D). A spectrum obtained from a 4ml volume incorporating part of the lesion lateral to the region of enhancement and including normal appearing white matter (Figure 3.4 spectra C and 3.3 image C) showed only small lipid resonances, consistent with the evidence that these non-enhancing areas

surrounding enhancing active lesions are the result of oedema (Larsson et al., 1988; McDonald et al., 1992). In addition, the small size of these lipid signals (which are at control levels) from a volume nearer the scalp makes it highly unlikely that the large resonances from the centre of the lesion are due to contamination from scalp fat.

In 7 patients, these abnormal lipid signals gradually resolved to control levels in from 4 to 8 months (mean ~ 5 months) (Figure 3.5), whereas Gd-DTPA enhancement had ceased in all patients by 2 months. One patient followed to date, for only four months, still has increased lipid resonances.

In 3 of the patients there was the suggestion of a separate resonance seen at 1.4 ppm (Figure 3.6). This resonance was only visible at relatively short echo times reflecting the short T_2 of its components.

In/Creatine ratios were elevated within acute enhancing lesions (0.95 ± 0.16) compared to areas of NAWM (0.7 ± 0.1 $p < 0.01$) and white matter from healthy age matched controls (0.62 ± 0.2 $p < 0.003$). The In/Creatine ratio in the lesion group remained elevated throughout followup. There was no significant difference between In/Creatine ratios in the control group and NAWM ($p < 0.2$)

3.4.3 Long echo time spectra: patients

There was a reduction of NAA/Cr ratios in acute enhancing lesions (1.35 ± 0.27 $p = 0.001$) and NAWM (1.6 ± 0.22 $p < 0.02$), compared to controls (1.84 ± 0.2). In 5 of these lesions there was a subsequent further reduction in NAA/Cr ratios (mean 1.16 ± 0.15) with maximum reduction seen between 1 and 4 months (mean 2.2 months). In 6 of the lesions, there was a later rise in the NAA/Cr ratio which began between 4 and 6 months (Figure 3.7). The mean NAA/Cr ratio at presentation in these 6 lesions was 1.41 ± 0.27 falling to 1.1 ± 0.15 , ($p = 0.006$) between 1 and 4 months and rising to 1.57 ± 0.22 , ($p = 0.001$)

between 4 and 8 months. The mean NAA/Cr ratio in all 8 lesions over time is shown in Figure 3.8.

The mean Cho/Cr ratio in the lesions when first studied was elevated (1.26 ± 0.26). This was significantly greater than in NAWM, (0.82 ± 0.13 , $p=0.006$) and controls, (0.92 ± 0.08 , $p=0.01$). With follow up, the Cho/Cr ratio returned to control levels in 5 out of 8 lesions over 2-6 months. Although the mean Cho/Cr ratio was lower in NAWM compared to controls, this was not statistically significant ($p<0.09$).

Two of the lesions showed evidence of lac production. In one, lactate was visible at the first study, 3 weeks after symptom onset (Figure 3.9). MRS one month later after Gd-DTPA enhancement had ceased showed resolution of the lac peak. In the second patient, spectra acquired from a large enhancing lesion 10 days after symptom onset showed no lac signal. However lactate was visible 1 month later when Gd-DTPA enhancement had ceased. The lac signal was no longer visible on spectroscopy 10 weeks after symptom onset.

3.5 DISCUSSION

The outstanding findings in this study are the regular detection of small lipid resonances in normal white matter using short echo time proton spectroscopy, the marked increase in lipid and protein resonances in association with the inflammatory phase of the new MS lesion and the partially reversible reduction in the NAA/creatine ratio in new MS lesions.

3.5.1 Increased lipid and protein resonances and the course of demyelination

This study has shown that small resonances at 0.9 and 1.3 ppm are a consistent finding in normal white matter of healthy individuals and MS

patients. However, in large acute MS lesions, there was a marked increase in these resonances which have been assigned to lipid and macromolecules (Callies *et al.*., 1993; Behar *et al.*, 1994).

When lipid peaks have been described in previous MRS studies in MS, no consistent relationship has hitherto emerged, either with the apparent age of the lesion or the presence of Gd-DTPA enhancement (Narayana *et al.*., 1992). Systematic serial observations have not however been performed. Moreover doubts have arisen as to whether the lipid peaks described have been due to extravoxel contamination from scalp. In the present study, two observations strongly suggest that these elevated peaks are not the result of scalp contamination: first, they were consistently and markedly higher in the acute lesions than from an area of NAWM closer to the scalp; and secondly they consistently decreased towards normal levels over several months.

There are a number of possible reasons why previous studies have not revealed increased lipid resonances in MS lesions. First, the lesions studied were often small and the voxels could have included a considerable proportion of NAWM resulting in partial volume effects. In the present study, large lesions were studied to avoid this problem. Secondly, a number of the non-enhancing lesions may have been chronic and the present study shows that abnormal lipid peaks will have disappeared in most lesions older than six months. Thirdly, a number of published studies have used echo times of 20 to 30 msec. Lipid has a very short T_2 (Figure 4) and the increased signal may therefore not be as obvious at these slightly longer echo times especially if the lesions are several months old.

In the present study, increased lipid/protein resonances were seen in all lesions which displayed Gd-DTPA enhancement. Indeed, when lesion size allowed more precise resolution this increase was maximal

in areas of enhancement (Figure 3.4 Spectrum B, Figure 3.3 Image B). Four lesions had not been apparent with or without enhancement on scans in the previous four weeks. Since in MS, enhancement indicates an increase in permeability of the blood-brain barrier in association with inflammation, (Katz et al., 1993; Kermode et al., 1990) it can be inferred that demyelination occurs during the inflammatory phase of lesion development. Just how early in this phase it occurs, or whether it might precede it, is unknown, though recent observations on acute optic neuritis have shown that delayed evoked potentials (indicating the presence of demyelination) can be seen in enhancing lesions within 48 hours of the onset of symptoms (S. Jones, R Kapoor, W.I. McDonald, unpublished observations). Since enhancement is the earliest detectable event in the evolution of a new lesion and may precede the onset of symptoms (Barrat et al., 1988). it may be concluded that demyelination occurs early in its development.

Increased lipid/protein peaks were detectable in new lesions for 4 to 8 months. Histopathological studies of demyelination (Adams et al., 1989) have shown lipid, in the form of triglyceride and cholesterol ester, in lesions (which were originally symptomatic) symptomatic for up to twenty-six weeks. Similar observations in cerebral infarction (Stehbens 1972) show lipid laden macrophages which are detectable for a minimum of 3 months and in larger lesions for several years. The time course of increased lipid signal detected by proton MRS is thus compatible with the histologically determined time course of disappearance of lipid laden macrophages from areas of acute myelin destruction. Such destruction is, of course, not peculiar to MS and it is likely that abnormal lipid resonances will be found in a wide range of pathological conditions, including vascular and granulomatous disorders. Whether a pattern of spectral changes will emerge which is

characteristic of Multiple Sclerosis remains to be seen.

A number of the acute lesions studied showed a resonance at 1.4 ppm. This resonance was more prominent at echo times of 20 and 30 msec (Figure 3.4) indicating that it either has a longer T_2 than the resonance at 1.3 ppm or is subject to J modulation (see Chapter 2). It is at present uncertain which metabolite this signal is due to, though the polypeptide thymosin β_4 , found in macrophages and in a subset of oligodendrocytes, produces resonances at this region of the spectrum (Kauppinen et al., 1992). There is also some preliminary evidence that other macromolecules such as myelin basic protein may also produce resonances in this part of the spectrum (S. Davies, unpublished observations).

3.5.2 Reversible reduction in the NAA/Cr ratio

Previous studies have reported a reduction in the NAA/Cr ratio both in acute (Arnold et al., 1992a, Bruhn et al., 1992, Miller et al., 1991) and chronic lesions (Matthews et al., 1991, Van Hecke et al., 1991) in MS. In this study a reduction in NAA/Cr ratios was observed from acute lesions which was partially reversible over four to eight months (Arnold 1992). A simple loss of axons cannot account for these reversible changes. A number of factors may be involved. First, alterations in the chemical environment of the lesion could alter the relaxation times of NAA thus affecting signal intensity. This however is unlikely. If one assumes an approximate T_1 value of 1500 ms for normal cerebral white matter (Frahm et al., 1989b), it would require a 75% increase in the T_1 of a lesion to explain the reduction in NAA signal observed in the current study. Such a change is improbable and spectroscopy of animals with acute EAE has shown no changes in the T_1 or T_2 values of NAA (Inglis et al., 1992).

Secondly, Cr/PCr has been used in this study as an internal standard of reference since these two compounds are in chemical equilibrium and their total concentration should accordingly remain constant. Frahm et al(1989b) have calculated the cerebral concentration of total creatine as between 10 and 11 mM. If there were a reduction in the total Cr/PCr concentration which continued to fall after stabilisation of NAA levels, the NAA/Cr ratio would rise. This hypothesis is not however in keeping with a study using ^{31}P MRS in which there was an increase in PCr levels in MS lesions compared to healthy controls (Minderhoud et al., 1992). Furthermore a recent study by Husted et al (1994) using spectroscopic imaging has shown an increase in the levels of Cr from MS lesions and NAWM.

Thirdly, oedema is a prominent feature of the acute Multiple Sclerosis lesion (McDonald et al., 1992) and it is possible that the relative number of axons per unit volume in the white matter affected by the lesion is at first reduced and later increases as the oedema is absorbed. Another possibility which is testable experimentally, is that the function of the mitochondria (where NAA is formed) (Patel and Clark 1979) is reversibly impaired during inflammation (Brenner et al., 1993b). Finally there is the possibility that adult O2A progenitor cells containing NAA proliferate locally or migrate into the lesion in order to promote remyelination. Though the latter is extensive in some lesions (Prineas *et al* ., 1993), it is not in others, and whether the magnitude of the change in NAA can be accounted for in this way is unknown.

3.5.3 Other observations.

The increase in Cho/Cr has previously been interpreted as evidence for demyelination because of the abundance of choline containing compounds in myelin. They are, however, abundant in all cell membranes (McIlwain and Bachelard 1985) and as the study of EAE (in

which there is inflammation, but no demyelination) shows (Brenner et al., 1993), a large increase in the Cho/Cr ratio can be produced by the increased membrane turnover associated with inflammatory cellular infiltration. This is likely to contribute to the changes in the Cho/Cr observed in this study and others (Matthews et al., 1991).

The elevation in the In/Cr ratio in the lesion group is in agreement with previous studies (Bruhn et al., 1992; Koopmans et al., 1993). The function of In (an osmolyte) is uncertain and it is not yet clear why the In/Cr ratio is increased in MS.

3.5.4 Implications for monitoring therapy

The reliable detection of lipid breakdown by spectroscopy has implications for monitoring treatment in MS. Beta interferon reduces the frequency of evidence of new disease activity as judged by unenhanced MRI (IFNB Multiple Sclerosis Study Group 1993, Paty *et al.*, 1993), but its mechanism of action is uncertain. It will be important to determine whether it (and future putative therapeutic agents) have differential effects on inflammation and demyelination. The former can be assessed by Gd-DTPA enhanced MRI. The results of this study would indicate that it may be possible to monitor demyelination by short echo time proton MRS. The observation of abnormalities in NAWM may be due to the presence of microscopic demyelination (Allen 1991) and is thus a potential measure of the extent of the disease process and possibly a prognostic indicator. Accordingly, it will be important in future studies to monitor not only the visible lesions, but the apparently uninvolved white matter as well.

LEGENDS

Figure 3.1A

Proton spectra from a healthy 28 year old female control taken from periventricular white matter. The upper spectrum is at an echo time (TE) of 10 ms. The lower spectrum is at a TE of 135 ms.

Figure 3.1B,C

T₂ weighted NMR scan (TR 3000 ms, TE_f 80ms) and short echo spectrum (Tr 2secs, TE 10ms.) from a 17 year old female with a lipoma in the quadrigeminal cistern. The spectrum taken from a voxel centred on the lipoma shows resonances from the methyl lipid group at 0.9 ppm and from the methylene group at 1.3 ppm.

Figure 3.2

Short echo time spectra (TR 2 secs, TE 10 ms) from a 48 year old female with clinically definite, relapsing remitting, Multiple Sclerosis. The upper spectrum is from a large gadolinium enhancing lesion which had been clinically symptomatic for 10 days. The lower spectrum is from an area of normal appearing white matter lateral to the lesion and nearer the scalp.

Figure 3.3 Images A,B,C and D.

Magnetic resonance images and spectra from a 36 year old female with clinically definite, secondary progressive, Multiple Sclerosis. Images A, B and C are T₂ weighted scans (TR 3000 ms, TE_f 80ms) which show the respective volumes of interest from which spectra A, B and C were obtained (see main text). Image D is a T₁ weighted scan (TR 500 ms, TE 40ms) showing the area of Gd-DTPA enhancement within the lesion from which Spectrum B was obtained. The increased lipid resonances are maximal in the area of Gd-DTPA enhancement.

Figure 3.4

Magnetic resonance spectra from an acute enhancing lesion. Spectra A is from a voxel encompassing the majority of the lesion. Spectra B is from the centre of the lesion as shown in Figure 3.3B showing marked evidence of myelin breakdown products. Spectra C is from the non-enhancing area shown in Figure 3.3 C showing normal resonances at 0.9 and 1.3ppm.

Figure 3.5

Serial short echo time spectra (TR 2secs, TE 10ms) at two monthly intervals taken from an acute lesion showing gradual resolution of lipid resonances over time. The lower spectrum is from an area of normal appearing white matter lateral to the lesion collected at the time of the first study - 10 days after symptom onset.

Figure 3.6

Proton spectra from the same lesion as Figure 3.2. These spectra were obtained at progressively increasing echo times from 10ms to 135ms and show the resultant decrease in lipid signal at 0.9 and 1.3 ppm as the echo time increases. They also show a resonance at 1.4 ppm at shorter echo times.

Figure 3.7

Serial long echo spectra (TR 2 secs, TE 135ms) taken at 1-2 monthly intervals from an acute lesion showing a fall in the NAA signal relative to creatine and then a subsequent rise over time. The lower spectrum is from a healthy age matched control.

Figure 3.8

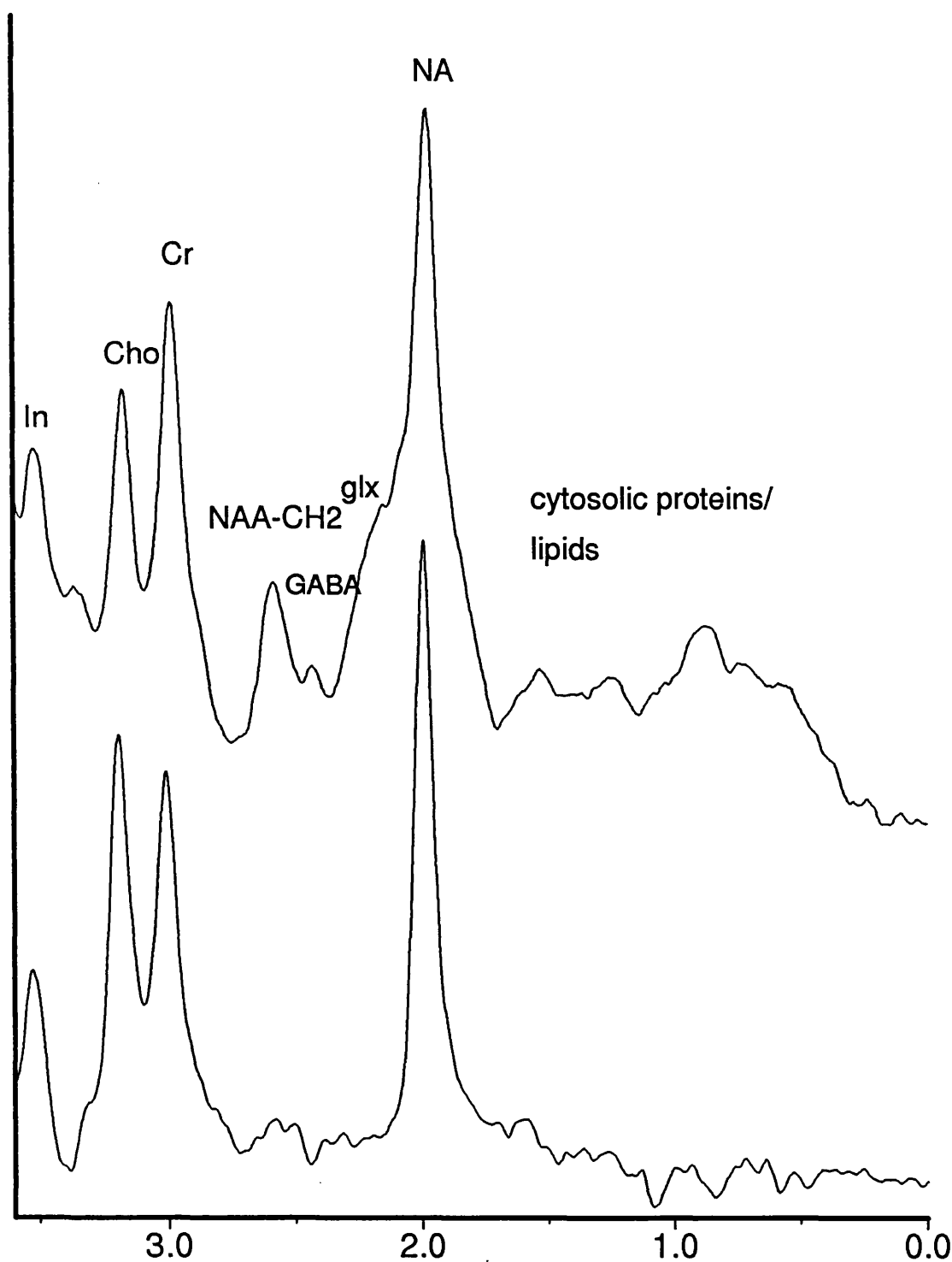
Mean NAA relative to creatine ratio of the 8 acute lesions studied over time.

Figure 3.9

Proton MRS (TE 270ms, TR 2000ms) from the centre of an acute lesion showing evidence of increased lactate at 1.3ppm.

Figure 3.1A

Proton MRS from healthy control
periventricular white matter TE 10ms/135ms TR 2.2secs



Upper spectrum TE 10ms

Lower spectrum TE 135ms



Figure 3.1B

T1 weighted axial image showing a lipoma in the quadrigeminal cistern. A voxel is shown from which the spectrum below was obtained

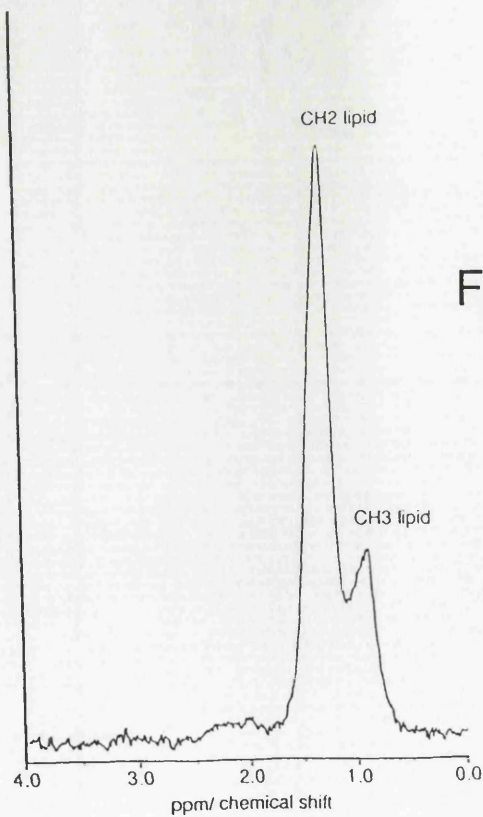


Figure 3.1C

Short echo spectrum (TE 10ms) of a lipoma in the quadrigeminal cistern showing lipid resonances at 0.9 and 1.3 ppm.

Figure 3.2

MRS from acute enhancing MS lesion
Volume 6mls TE 10ms TR 2secs

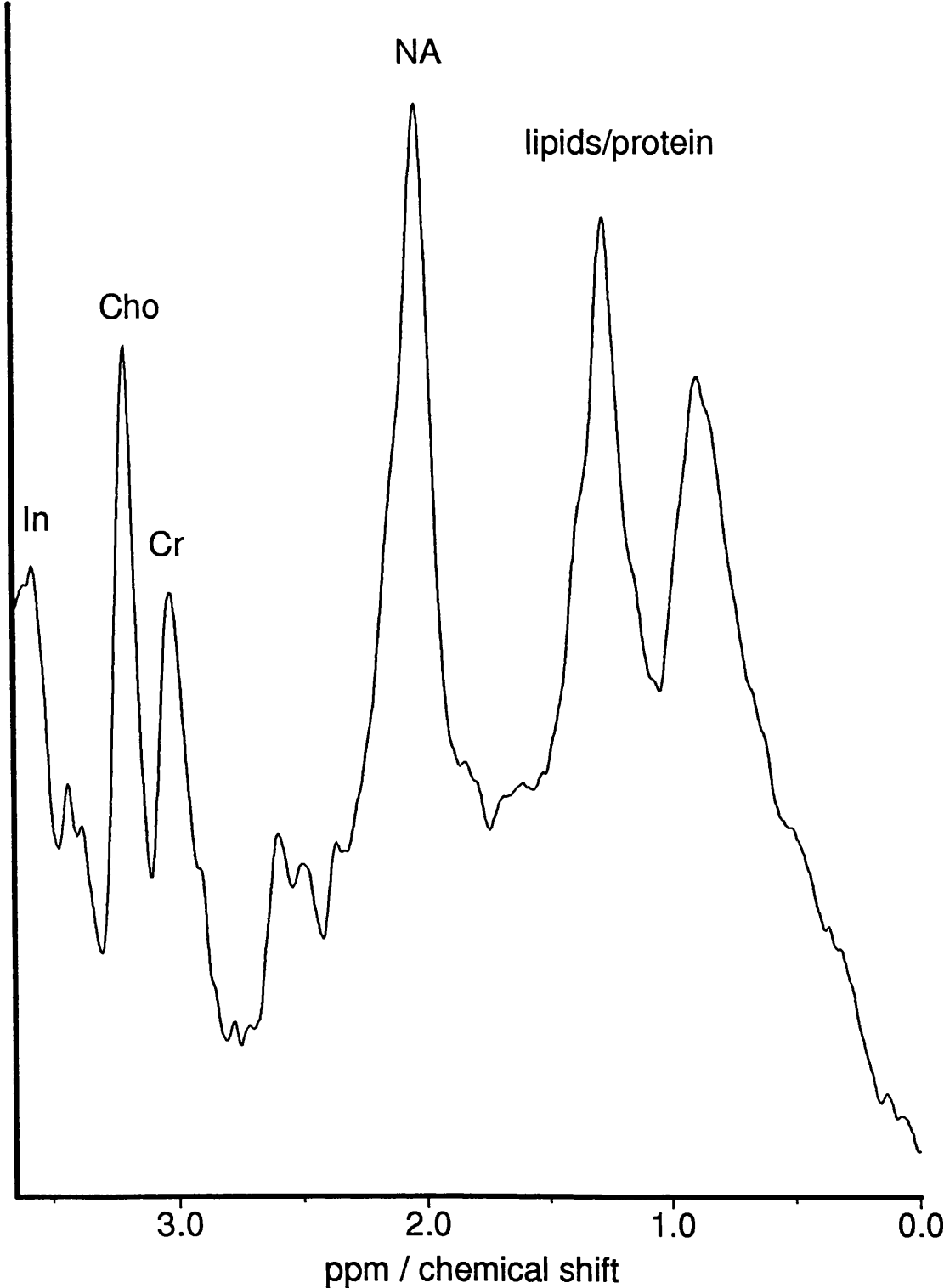


Figure 3.3



Image A



Image B

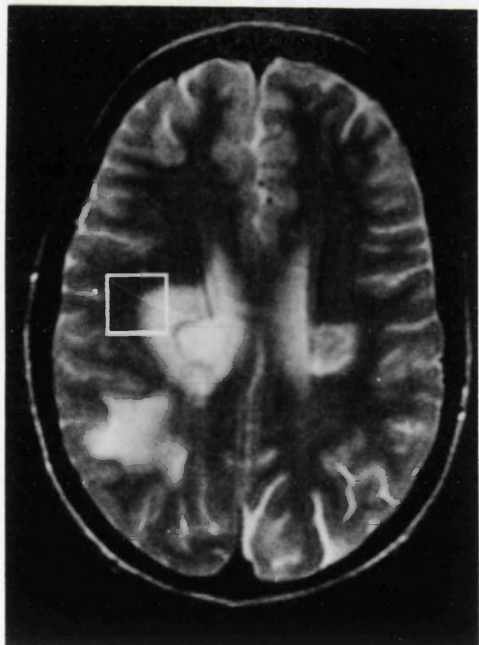
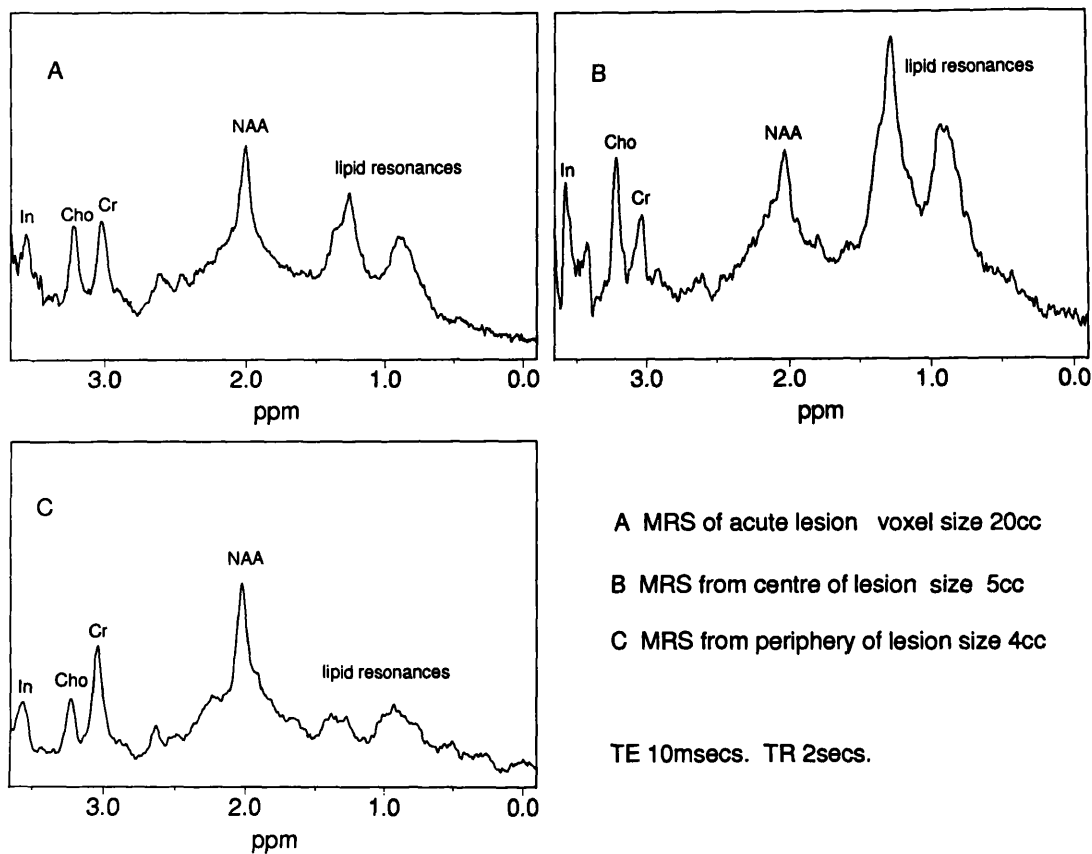


Image C



Image D

Figure 3.4



Short-echo spectra from acute demyelinating lesion

Figure 3.5
Serial MRS of acute MS lesion
Voxel 8 mls TR 2secs. TE 10msecs.

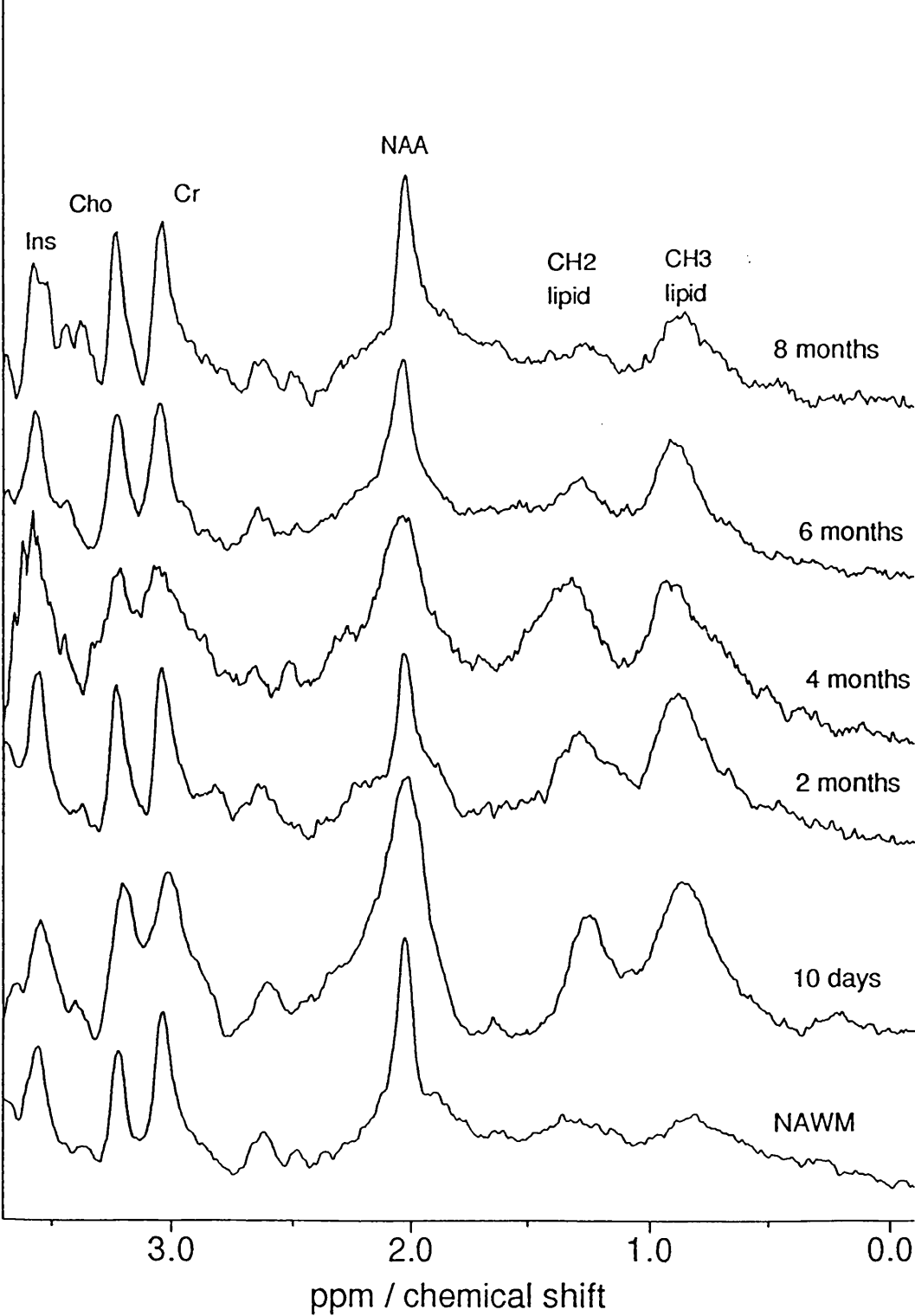


Figure 3.6

MRS of acute lesion at increasing echo times
Voxel 10ml. TR 2 secs.

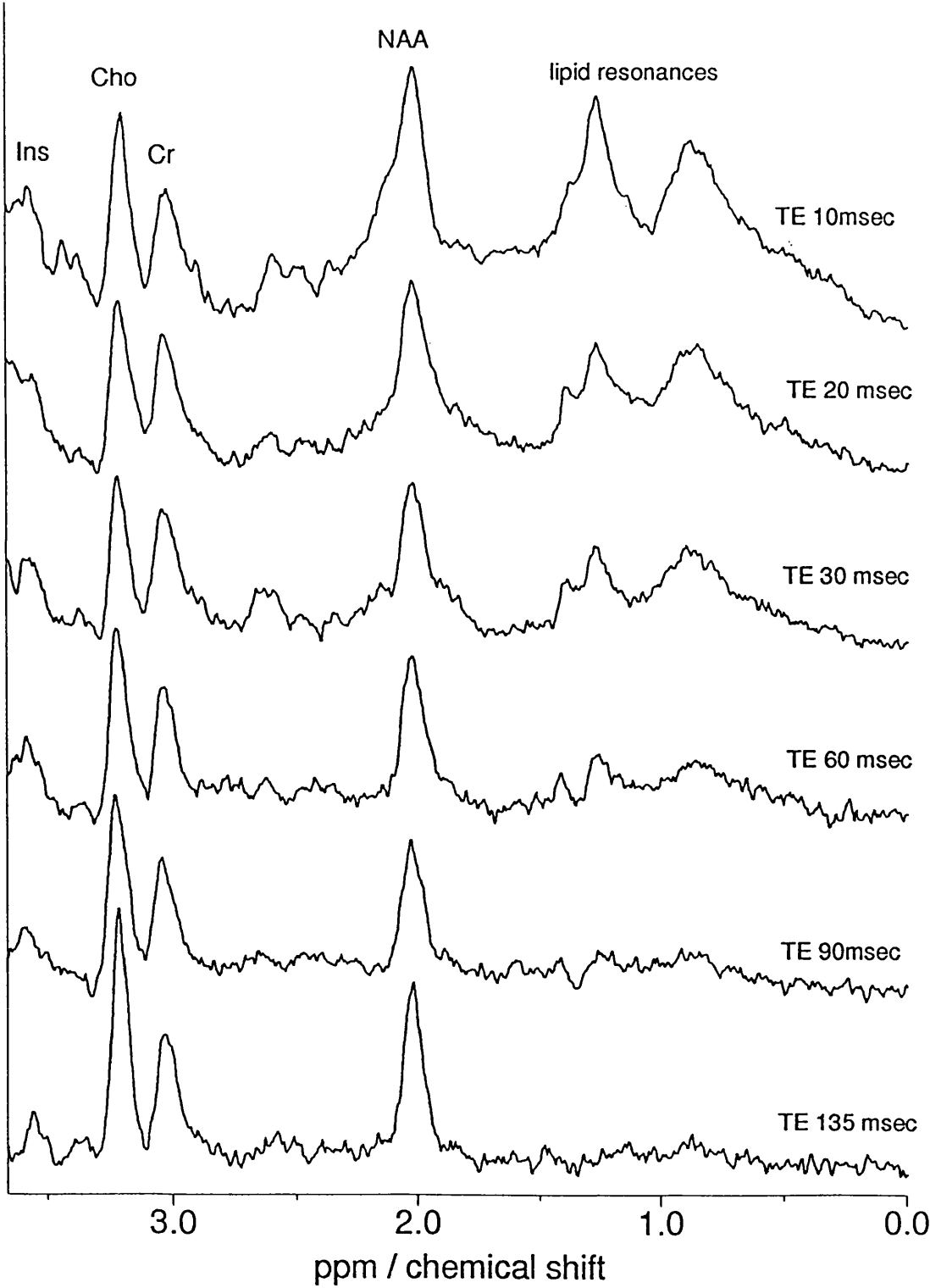


Figure 3.7

Serial proton MRS of acute lesion v control
Voxel 8 mls. TR 2 secs. TE 135 msec.

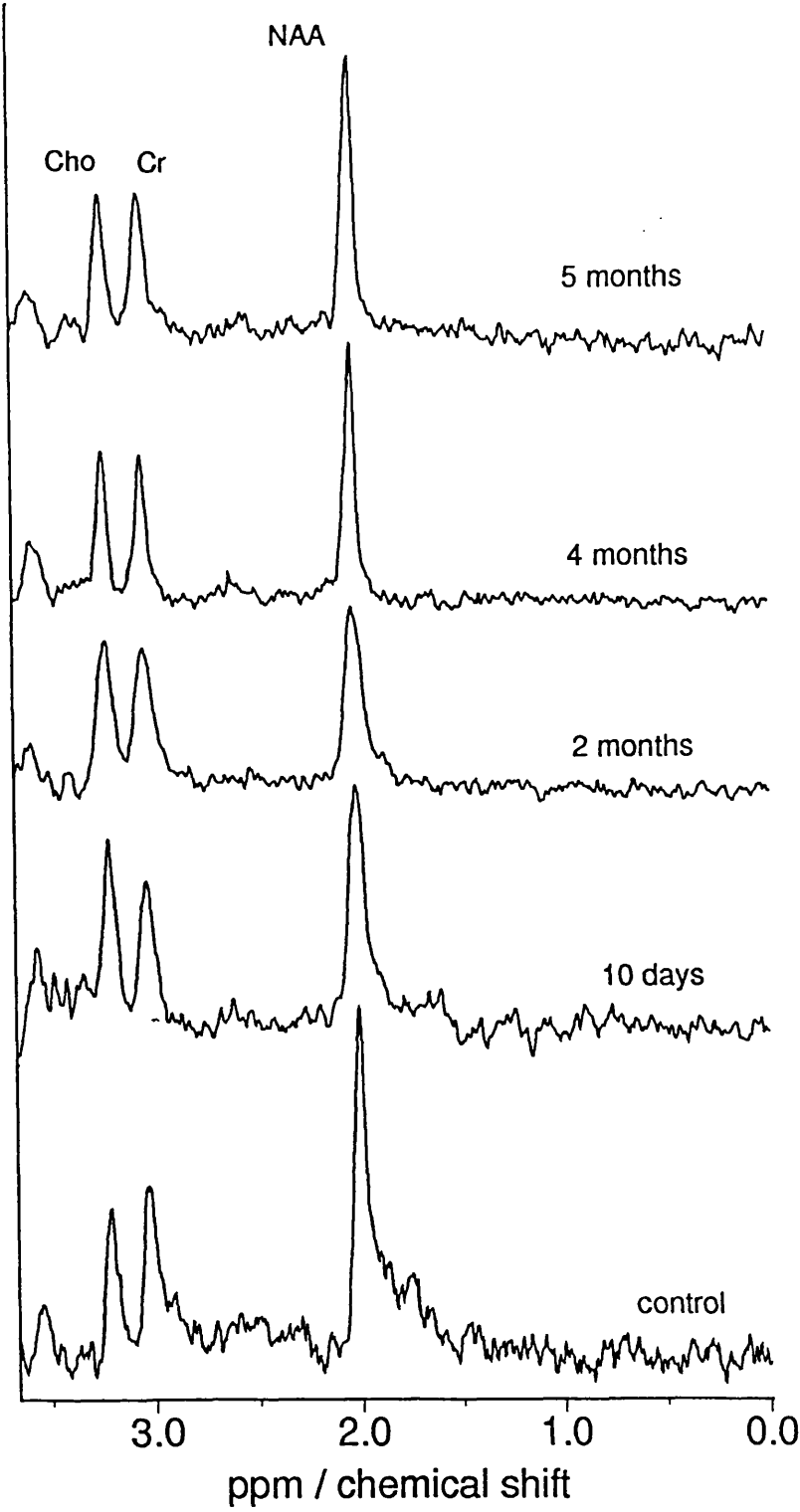


Figure 3.8

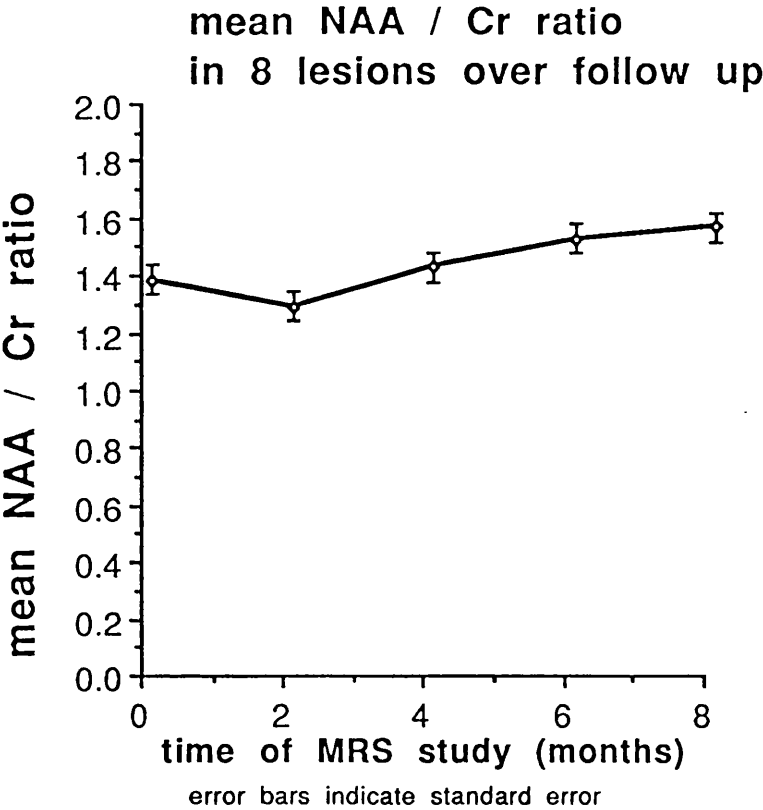
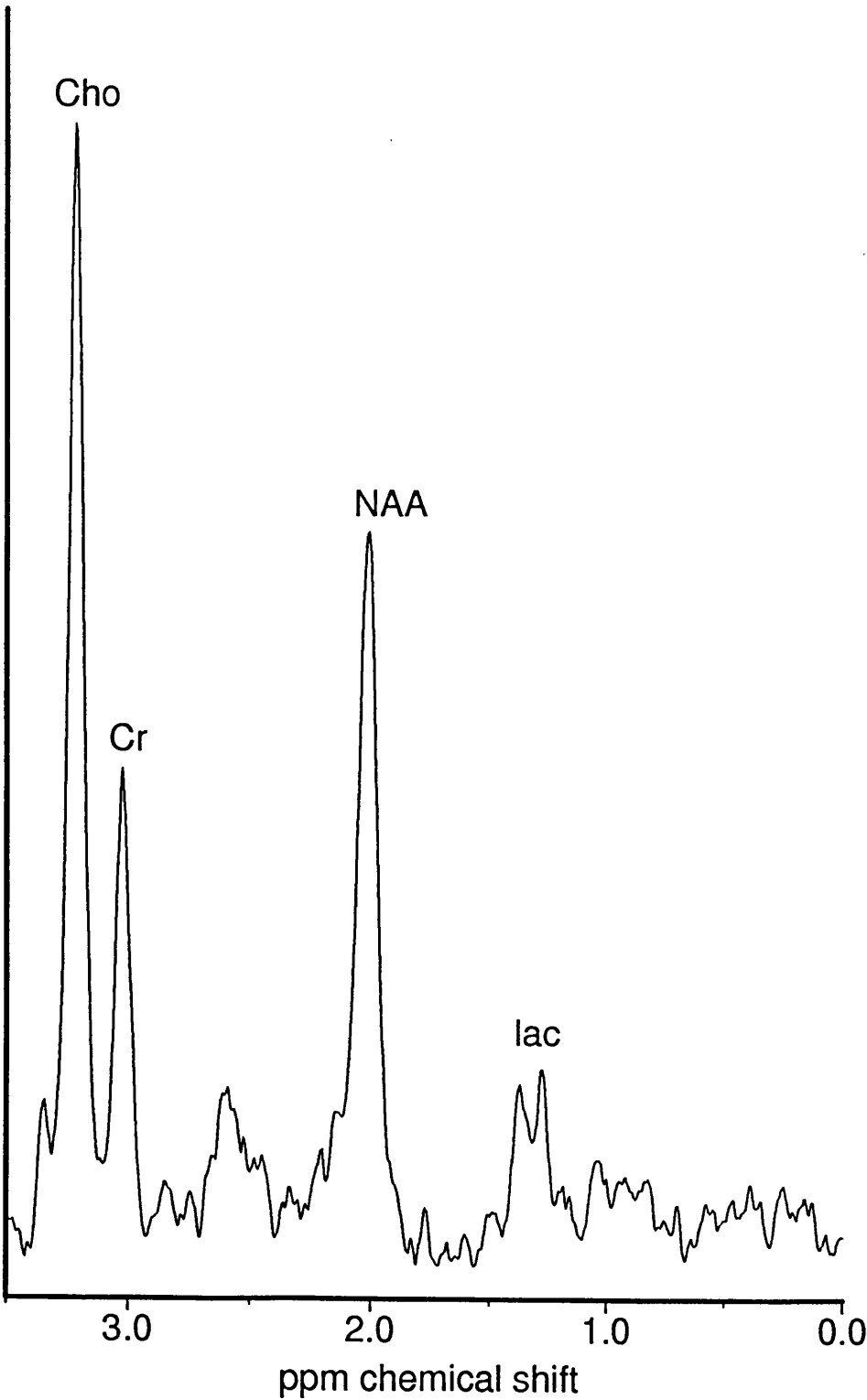


Figure 3.9

Lactate from acute enhancing MS lesion
TR 2secs TE 270msecs Volume 6mls



CHAPTER 4

PERSISTENT FUNCTIONAL DEFICIT IS ASSOCIATED WITH AXONAL LOSS IN MULTIPLE SCLEROSIS AND AUTOSOMAL DOMINANT CEREBELLAR ATAXIA

4.1 SUMMARY

Proton MRS and MRI were carried out in eleven patients with multiple sclerosis (MS) who had clinical evidence of severe cerebellar deficit, eleven MS patients (of similar age and disease duration) who had minimal or no signs of cerebellar involvement, eight patients with autosomal dominant cerebellar ataxia (ADCA) and in 11 healthy controls. In all subjects MRS was localised to cerebellar white matter (volumes of interest 3 - 6ml). Metabolite concentrations were calculated using the fully relaxed water spectrum as an internal standard of reference. The patients also underwent MR imaging to assess cerebellar volume and (in the two MS groups) lesion volume within the posterior fossa. MRS from cerebellar white matter showed a highly significant reduction in the concentration of N -acetylaspartate (NAA) (a neuronal marker) in the MS group with cerebellar deficit compared to the MS group with minimal or no signs of cerebellar involvement and healthy controls. Follow-up MRS performed in six of the MS patients nine months later showed no change in the [NAA]. The ADCA group showed a significant reduction of NAA from a region of cerebellar white matter and also a reduction in the concentration of Cho. The MS group with severe cerebellar deficit and the ADCA group both had significant cerebellar atrophy (suggesting axonal loss) compared to the MS patients with minimal or no signs of cerebellar deficit and the healthy controls. The MS patients with cerebellar deficit had a significantly greater lesion volume in the posterior fossa

although the proportion of the spectroscopic voxel occupied by lesion was small suggesting that the observed reduction in NAA is also due to axonal loss from NAWM.

These results support the hypothesis that axonal loss is important in the development of clinical disability in MS.

4.2 INTRODUCTION

The mechanisms producing permanent disability in MS are poorly understood. Although conventional MRI has provided a sensitive means of following the evolving pathological process, studies using MRI have shown only a weak relationship between brain MRI lesion load and clinical disability (Li et al 1984). This discordance may be due to several factors (Kermode et al., 1990, McDonald et al 1992). First, the location of lesions is likely to be important since many lesions occur in areas of the brain which are not clinically eloquent (Phadke and Best., 1983). Secondly, there may be inaccuracies in the measurement of lesion load. Thirdly the degree of disability may also be influenced by spinal cord involvement - as shown by the modest though significant correlation between clinical disability and cord atrophy (Kidd., et al 1993). Finally, there is considerable pathological heterogeneity between lesions (Dawson, 1916; Allen, 1991; Barnes., et al 1991).

Conventional MRI does not differentiate between the various

pathological processes occurring within an MS lesion which may include inflammation, oedema, demyelination, remyelination, gliosis and axonal loss. Of these, demyelination and axonal loss have been suggested as the main factors responsible for the development of disability. There is however electrophysiological evidence to suggest that demyelination may not contribute much to permanent loss of function; MS patients with optic neuritis may show marked prolongation in the visual evoked potential (indicating demyelination) despite normal visual acuity in the affected eye (Halliday et al., 1972). It is not yet proven whether axonal loss is the key pathological event which determines the development of disability in MS.

The aim of the present study is to determine using proton MRS whether the concentration of NAA in the cerebellum can differentiate between MS patients with signs of severe cerebellar deficit and those patients with little or no clinical evidence of cerebellar involvement. As a pathological control group in which cerebellar neurones are known to be lost (Schut and Haymaker 1951; Hoffmann et al., 1971) a number of patients with ADCA have also studied.

4.3 MATERIALS AND METHODS

4.3.1 Patients

Patients with clinically definite MS (Poser 1983) and ADCA (Harding 1982) were recruited from the National Hospital for Neurology and Neurosurgery . The study was approved by the Joint Ethics Committee at the Institute of Neurology and the National Hospital for Neurology and Neurosurgery, London. Informed consent was obtained from all patients prior to each study.

The patient groups were defined as follows:

(1) 11 MS patients with marked upper limb cerebellar incoordination and/or gait ataxia. These patients were classified on the Kurtzke (Kurtzke, 1983) functional cerebellar scale between 3-5. All patients in this group had evidence of marked cerebellar deficit for one year or more. These patients had a median age of 37 years (range 25 - 44) and a median disease duration of 6 years (range 2- 34 years).

(2) 11 MS patients with minimal or no signs of cerebellar deficit. These patients were classified on the Kurtzke functional cerebellar scale as 0 or 1. These patients had a median age of 32 years (range 22 - 56) and a median disease duration of 6 years (range 3 - 20 years).

(3) 8 patients with ADCA. These patients had type 1 ADCA (n=5), two

with the SCA 1 mutation (Giunti et al., 1994), two with the SCA 3 mutation (Kawaguchi et al., 1994), one with no known mutation and three patients with the pure form of cerebellar degeneration (type 3) using the classification devised by Harding (1982). The median age in this group was 46.5 years (range 25 -65 years) with a median disease duration of 6 years (range 3 years - 22 years)

In addition 11 healthy controls with a median age of 31 years (range 24-48 years) were studied. Each patient underwent a full neurological examination and in the MS patients a kurtzke cerebellar functional system and EDDS score were obtained.

4.3.2 Magnetic resonance imaging and spectroscopy

Both MRI and MRS were carried out on a Signa 1.5 Tesla system (General Electric, Milwaukee, WI) without contrast enhancement.

Sagittal images:

T₁ weighted 3mm contiguous slices covering the posterior fossa were collected [repetition time (TR) 640ms, echo-time (TE) 11ms].

Axial images:

A proton density weighted scan [TR 5000ms, effective TE (TE_{ef}) 18/78ms] (5mm slices, 2.5mm interspace, 256x256 matrix, echo train length 8) was collected. Finally, contiguous axial slices were collected through the posterior fossa [TR 2000ms TE_{ef} 17ms] (3mm, 256x256 matrix, echo train length 8). The axial posterior fossa scans of the two MS groups were analysed while unaware of the clinical details. All intrinsic lesions in the posterior fossa were documented. These were divided into anatomical site: cerebellar hemispheres and peduncles, medulla and pons and midbrain. Lesions that fell within the spectroscopic volume of interest were also recorded. A lesion load for the individual sites and total posterior fossa lesion load were then determined using a semi-automated contouring programme which segmented lesions ("Dispimage", DL Plummer, UCL, London, UK). The same contouring programme which allowed exclusion of cerebrospinal fluid (CSF) between the folia was then used on the T_1 weighted sagittal slices through the posterior fossa to determine the cerebellar volume. This was carried out by the authors who was unaware of patient identity at the time of analysis.

MRS

After imaging, a volume of interest localised to the cerebellar white matter was prescribed ranging in size from 3.5 to 6ml (Figure 4.1). In

the patient groups the cerebellar hemisphere ipsilateral to the more ataxic side was chosen. The size and shape of each volume was adjusted to avoid inclusion of grey matter and cerebrospinal fluid. In both MS groups the region of interest included lesions (when present) and NAWM. An MRI of the voxel was then obtained to ensure accurate localisation. Water suppressed ^1H spectra were obtained using a STEAM sequence. Acquisition parameters were TR 2000 ms, TM 12ms, TE 135ms. 384 averages were collected using an 8 step phase cycle in ~ 12 minutes. 1024 points were collected, with a spectral width of 750 Hz. Data processing included 1 Hz. line broadening for filtering, Fourier transformation, and zero order phase correction. Peak areas were determined using a line-fitting programme ("SA / GE", G.E. Milwaukee W.I.). Peaks were fitted to a Gaussian line shape using a Marquardt fitting procedure. Absolute concentrations for the metabolites were calculated using the fully relaxed water signal as an internal standard of reference (Christiansen et al 1993). Metabolite concentrations [met] were calculated as described in Chapter 2 and appendix A

Statistical analysis was performed with a Mann-Whitney confidence interval and test. Results are expressed as a median value together with the range and p value. A Spearman's rank correlation test was also used and results are expressed as an r value together with levels

of significance.

4.4 RESULTS

4.4.1 MRS

In the MS patients with severe ataxia, there was a highly significant reduction in the median concentration of N-acetylaspartate (NAA) (6.7mM, range 4.58 - 8.93mM) in the cerebellar white matter compared to the controls (9.6mM, range 8.3 - 10.8mM, $p=0.0002$) (Figure 4.2 and Table 4.1). In contrast, the concentration of NAA in the MS patients without cerebellar deficit (median 9.74mM, range 9.25mM - 11mM) showed no significant difference from the control group ($p>0.4$) (Figure 4.3 and Table 4.2). The patients with hereditary ataxia also showed a significant reduction in the median [NAA] from cerebellar white matter (6.82mM, range 3.55 - 7.96mM, $p=0.0003$) compared to the control group (Figure 4.4). The NAA values for the four groups are shown as a scatter graph (Figure 4.5). The Cho concentration showed no significant change in either MS group compared to the controls. The ADCA group, however, showed a significant median reduction in the Cho concentration (median 1.0mM, range 0.44 - 1.86mM) compared to the control group (median 1.56mM range 1.2 - 3.15mM, $p=0.04$) (Figure 4.4 and Table 4.3). There was no significant correlation between [Cho], and

[NAA], cerebellar volume or disease duration.

There was no significant difference between the median concentration of creatine in the cerebellar white matter from the control group (9.05mM, range 7.8 - 11.6mM) compared to the MS patients with cerebellar deficit (median 9.82mM, range 7.65 - 11.7mM, p.0.2) nor indeed the MS group without cerebellar deficit (median 9.8, range 7.98 - 11.0mM, p.0.2). The ADCA group also showed no significant difference in the median concentration of creatine (9.76mM, range 8.6 - 11.8mM) compared to the healthy controls.

Follow up MRS at nine months was carried out in 6 of the 11 clinically affected MS patients. The median concentration of NAA at follow up (median 7.42mM, range 5.04 - 8.73mM) showed no significant difference from the first study (median 7.45mM, range 5.88 - 8.93mM, p >0.4) (Table 4.1).

4.4.2 MRI

The cerebellar volumes for the MS patient groups are shown in Table 1 and 2. In the ataxic MS group, there was a highly significant reduction in the median cerebellar volume (107, 865 sq mm, range 101, 574 sq mm - 131, 421sq mm) compared to the control group (132, 003 sq mm, range 121, 278 - 143, 778 sq mm, p=0.0005). In contrast, the median cerebellar volume of MS patients who were clinically unaffected (

median 128, 037 sq mm, range 112, 008 sq mm - 135, 750 sq mm) showed no significant difference from the control group ($p>0.05$). The patients with ADCA also showed a significant reduction in the median cerebellar volume (94, 137 sq mm, range 61, 596 sq mm - 115, 434 sq mm, $p=0.0003$) compared to the control group (Table 4.3).

The posterior fossa lesion loads in the two MS groups are shown in Table 4.1 and 4.2. The median voxel lesion load in the MS group with cerebellar deficit (median 157sq mm, range 74 - 260 sq mm) was increased compared to the MS group without cerebellar deficit (median 117 sq mm, range 0 - 263 sq mm, $p>0.03$) though this did not achieve statistical significance. When corrected for voxel size, the percentage of voxel occupied by abnormal signal was found to be moderately higher in the MS group with cerebellar deficit (median 9%, range 5.2 - 15.7%) compared the patient group with no cerebellar deficit (median 5.9%, range 0 - 15.3%, $p<0.05$). There was also a significantly greater lesion volume in the total ipsilateral cerebellar hemisphere ($p<0.008$) and within the brainstem ($p<0.009$) in the MS patients with cerebellar deficit compared to the MS patients with no clinical cerebellar involvement.

Taking all MS patients together, there was a modest though significant negative rank correlation between the concentration of NAA from the cerebellum and both the Kurtzke extended disability status score

(EDSS) ($r -0.517, 0.02 > p > 0.01$) (Figure 4.6) and the Kurtzke functional cerebellar score ($r -0.49, 0.05 > p > 0.02$) (Figure 4.7). There was also a negative correlation between the concentration of NAA and lesion volume within the voxel ($r -0.527, 0.02 > p > 0.01$). Additionally, there was a positive correlation between [NAA] and cerebellar volume ($r 0.438, 0.05 > p > 0.02$). There was no rank correlation between lesion volume in the posterior fossa and kurtzke score though there was a significant correlation between the total posterior fossa lesion volume and the cerebellar functional score ($r 0.536, 0.02 > p > 0.01$).

4.5 DISCUSSION

The outstanding findings in this study are the persistent reduction of [NAA] from cerebellar white matter together with cerebellar atrophy in the MS patients with severe cerebellar deficit.

4.5.1 Decreased [NAA] and cerebellar atrophy in the MS group with cerebellar deficit

This study has shown a significant reduction of [NAA] from cerebellar white matter and cerebellar atrophy in a group of patients with ADCA, a syndrome in which neuronal loss is known to occur within the cerebellum, either as a result of pure cerebellar atrophy or as part of

olivopontocerebellar atrophy (Schut and Haymaker, 1951; Hoffmann et al., 1971). The finding therefore of reduced cerebellar [NAA] together with cerebellar atrophy in the ataxic MS group is perhaps the most convincing evidence to date that neuronal loss has occurred primarily in those MS patients with irreversible disability.

It has been established that there is a persistent reduction of NAA in chronic MS lesions (Arnold et al., 1994). However the serial studies of acute MS lesions described in the preceding chapter has shown partial reversibility of the NAA/Cr ratio over four to eight months suggesting that at least in the inflammatory phase of the disease, factors other than axonal loss are partly responsible for the observed reduction of NAA (Brenner et al., 1993b).

Previous MRS studies have failed to show a correlation between the reduction of NAA within a volume of interest and the degree of clinical disability (Arnold et al., 1994). One explanation for this may be that studies to date have concentrated primarily on lesions and NAWM within the periventricular white matter of the cerebral hemispheres. Lesions in this part of the brain are often 'clinically silent' (Phadke et al., 1983) and therefore of less importance in the development of disability, as measured by the Kurtzke EDSS score which is strongly influenced by locomotor function.

In the present study, a reduction of [NAA] has been observed from

cerebellar white matter in a group of 11 patients with severe cerebellar deficit, which in the six patients restudied after nine months was shown to be persistent. Such a persistent reduction makes axonal loss the most likely explanation for the low [NAA] observed in this group, supporting the hypothesis that axonal loss is an important mechanism in the development of irreversible clinical deficit in MS, a conclusion further supported by the observation of cerebellar atrophy in the MS group with cerebellar deficit.

An important issue to address is whether the MRS findings in this study are simply due to lesions within the region studied. This is unlikely for two reasons. First, only a modest increase in voxel lesion load was detected in the MS group with cerebellar deficit compared to the non-ataxic group and secondly, the median percentage of voxel occupied by abnormal signal in the ataxic patients was only 9%, compared with a median reduction in [NAA] of 30%. Such a disproportionate reduction of NAA may reflect axonal loss within the NAWM in the ataxic group. There was a significantly greater lesion volume in adjacent regions of the cerebellum and brainstem in these patients and therefore the decrease in NAA may in part arise from axonal damage by lesions located outside the spectroscopic volume of interest.

4.5.2 Other findings

An unexpected finding in this study was the reduction of [Cho] from cerebellar white matter in patients with ADCA. [Cho] was below the control range in four of the eight patients. This was not associated specifically with any mutation or type of ADCA or clearly correlated with [NAA], disease duration or cerebellar volume. However, although the patient group was small there was a tendency for the patients with the longest disease duration and greatest degree of cerebellar atrophy to have the lowest values of [Cho] (Table 4.3).

As discussed earlier, the resonance observed at 3.2 ppm in the proton spectrum is not one compound but the combination of signal from a number of metabolites. These include free choline, phosphocholine, glycerophosphocholine, acetylcholine, phosphatidylcholine sphingomyelin and betaine (Miller BL, 1991; Brenner et al., 1993a). Immunocytochemical studies have provided evidence for the existence of cholinergic transmission in the human cerebellum, with the detection of muscarinic receptors in the mossy fibres that terminate in the granular layer (Casanova et al., 1990). Mossy fibres account for about two thirds of the myelinated axons underlying the cerebellar cortex. It is conceivable that degeneration of these axons may explain the reduction of [Cho] that was observed in a number of patients with ADCA. Kish et al (1986) have shown a

significant reduction of choline acetyltransferase from the cerebral cortex in patients with ADCA, suggesting a loss of cholinergic neurones projecting from the nucleus basalis. It is not yet known whether cholinergic neurones are lost from the cerebellum in ADCA.

The reduction in [NAA] from a clinically eloquent location and its correlation with disability suggest that spectroscopy may emerge as a relevant tool for monitoring axonal loss in MS, particularly in the context of treatment trials. In order to do this effectively it would be desirable to survey the whole brain rather than a small localised volume. Spectroscopic imaging techniques are now able to achieve this and are already being used in the study of MS (Arnold et al., 1992; Husted et al., 1994).

LEGENDS

Figure 4.1

A proton density weighted scan [TR 5000ms TE 78ms] showing a volume of interest localised to the cerebellar white matter in an MS patient with no cerebellar deficit.

Figure 4.2

Magnetic resonance spectroscopy from cerebellar white matter in MS patient with severe cerebellar deficit (top spectrum) compared with healthy age-matched control.

Figure 4.3

Magnetic resonance spectroscopy from cerebellar white matter in MS patient with no cerebellar deficit (top spectrum) compared to healthy age-matched control.

Figure 4.4

Magnetic resonance spectroscopy from cerebellar white matter in patient with Autosomal dominant cerebellar ataxia (upper spectrum) compared to healthy control.

Figure 4.5

Scattergraph of apparent concentration of NA (mM) in multiple sclerosis patients, hereditary ataxia patients and controls.

Figure 4.6

Scattergraph of apparent concentration of NA (mM) compared to Kurtzke EDSS score in MS patients.

Figure 4.7

Scattergraph of apparent NA concentration (mM) compared to Kurtzke cerebellar functional score in MS patients

TABLE 4.1

MS patients with cerebellar deficit

	cerebellar volume (cu mm)	[NAA](mM) 1st study	[NAA](mM) follow-up	voxel lesion load (cu mm)	posterior fossa lesion load (cu mm)	ipsilateral cerebellum (cu mm)	pons/ midbrain (cu mm)	EDSS score	cerebellar functional score
1.	103,977	5.88	5.89	157	600	157	212	6.5	4
2.	131,421	7.9	8.0	187	1573	256	1072	5.5	5
3.	102,597	6.05	5.04	174	1390	332	581	6.0	5
4.	104,100	7.0	7.49	243	2563	285	1441	6.5	4
5.	105,510	8.5	8.73	191	773	225	305	8.5	5
6.	107,865	8.93	7.36	74	562	173	171	6.0	3
7.	101574	6.82	ND	140	967	248	425	6.0	4
8.	113,100	7.22	ND	137	644	193	402	4.0	3
9.	126,654	5.39	ND	260	2150	596	544	6.0	3
10.	122,454	6.65	ND	134	1066	250	660	8.0	5
11.	120.300	4.58	ND	117	1808	286	897	6.0	3

TABLE 4.2

MS patients without cerebellar deficit

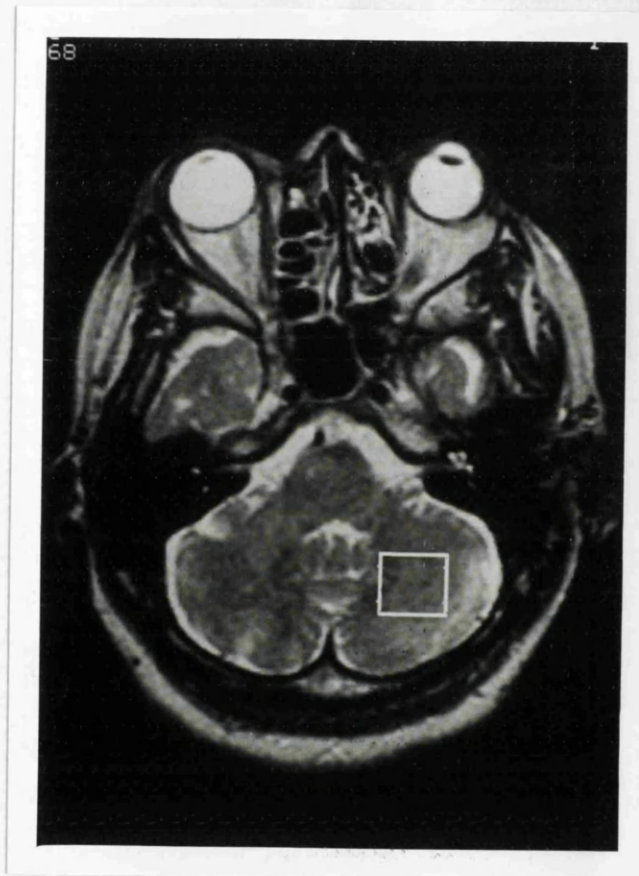
	cerebellar volume (cu mm)	[NAA](mM)	voxel lesion load (cu mm)	posterior fossa lesion load (cu mm)	ipsilateral cerebellum (cu mm)	pons/ midbrain (cu mm)	EDSS score	cerebellar functional score
1.	122,865	9.25	141	890	205	168	3.0	1
2.	128,037	9.74	263	856	379	290	5.0	0
3.	112,008	9.7	45	320	45	177	2.5	1
4.	135,750	9.48	117	713	140	235	1.0	1
5.	134,490	11	88	101	88	13	6.0	1
6.	131,520	9.5	121	748	204	439	4.0	0
7.	120,081	9.78	0	0	0	0	7.0	0
8.	113,973	11.2	35.1	910	172	307	7.0	0
9.	128,202	9.52	152	346	164	63	2.5	1
10.	134,106	10.48	0	116	0	22	2.0	0
11.	121,020	10.67	127	841	173	175	1.5	0

TABLE 4.3

Autosomal dominant cerebellar ataxia patients

	Age	Disease duration	classification	mutation	cerebellar volume (cu. mm)	[NAA]	[Cho]
1.	48	3 years	Type 1	SCA I	109,833	6.44mM	0.94mM
2.	45	5 years	Type 1	SCA I	89,523	5.65mM	1.36mM
3.	65	5 years	Type 1	SCA III	105,960	7.1mM	1.29mM
4.	25	5 years	Type 1	SCA III	115,434	7.96mM	1.90mM
5.	38	8 years	Type 1	not known	69,612	3.55mM	1.00mM
6.	50	22 years	Type 3	not known	61,596	7.0mM	0.44mM
7.	52	20 years	Type 3	not known	67,461	4.78mM	0.75mM
8.	24	6 years	Type 3	not known	82,176	7.7mM	1.86mM
control (median)					132,003	9.6mM	1.56mM

Figure 4.1



An axial MRI scan (TR 5000ms, TE 78ms) through the posterior fossa, showing a spectroscopic volume of interest localised to the cerebellar white matter in an MS patient with no cerebellar deficit.

Figure 4.2

MRS of cerebellar white matter in an ataxic MS patient
v control. Volume 3.5ml TE 135ms TR 2.135secs

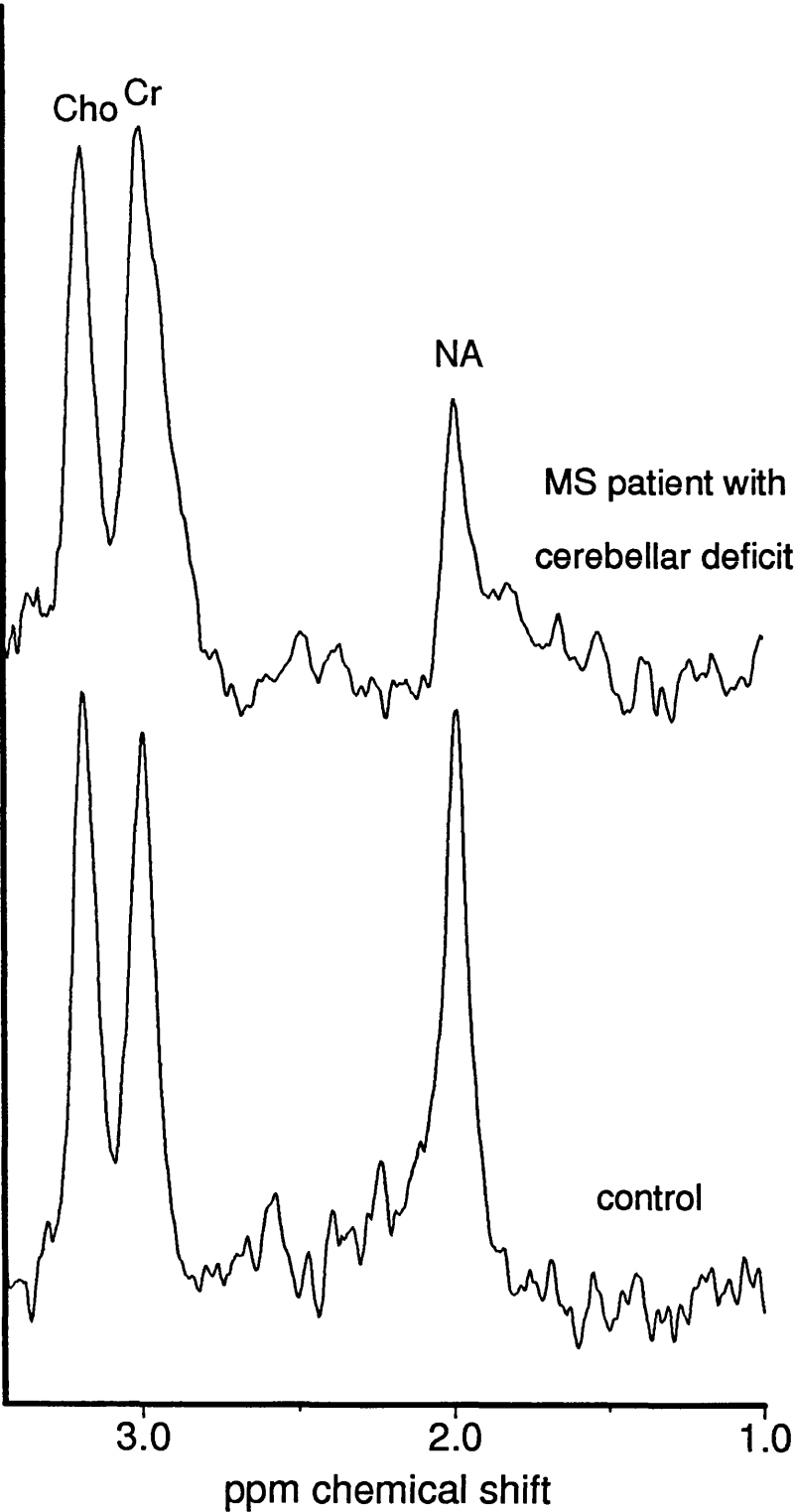


Figure 4.3

MRS of cerebellar white matter in MS patient (no ataxia) v control
Volume 3.5 mls TE 135 ms TR 2.135 secs

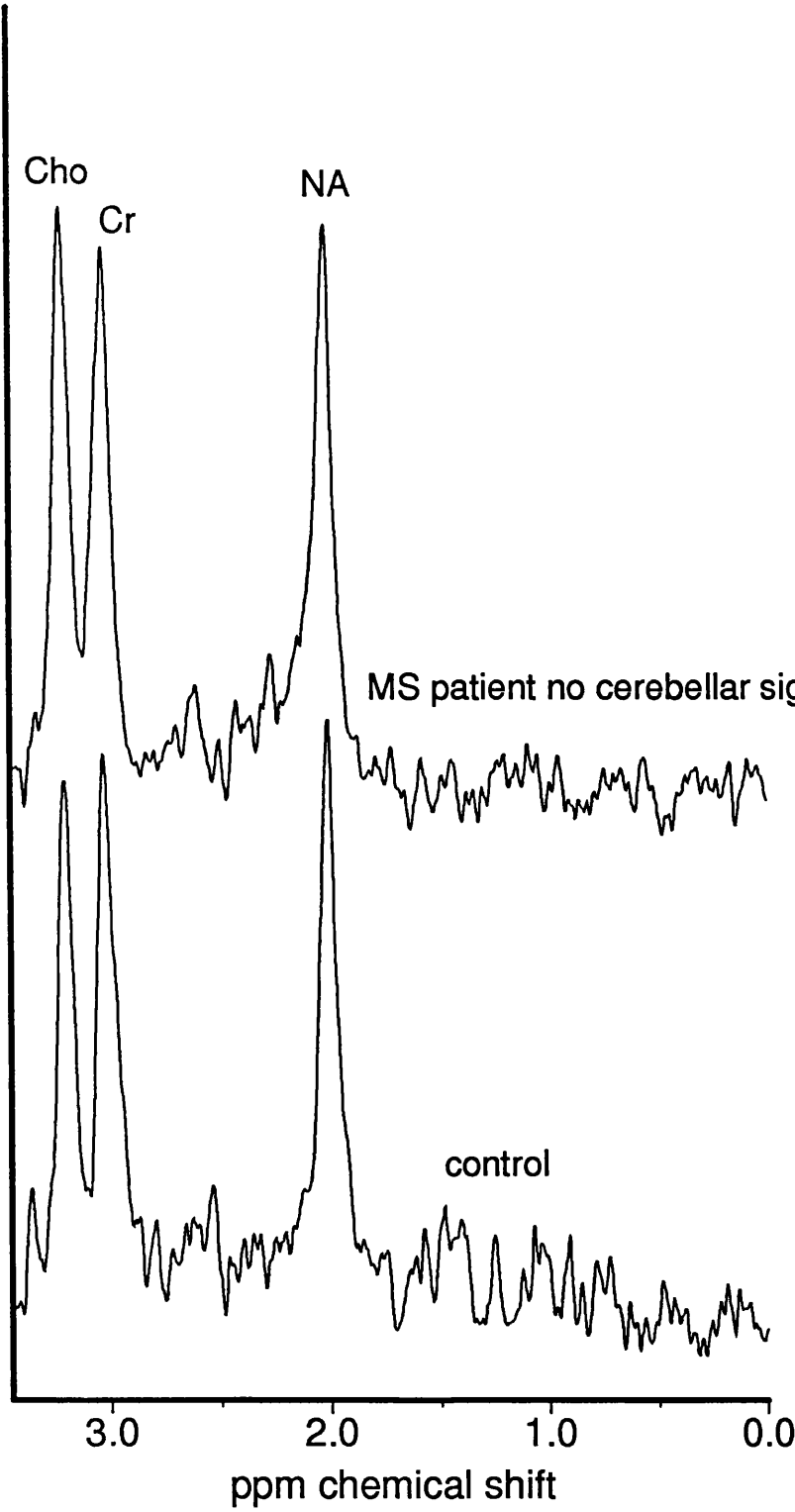


Figure 4.4

MRS in patient with ADCA Type 1 v control
cerebellar white matter TE 135ms TR 2.135 secs. Volume 3mls

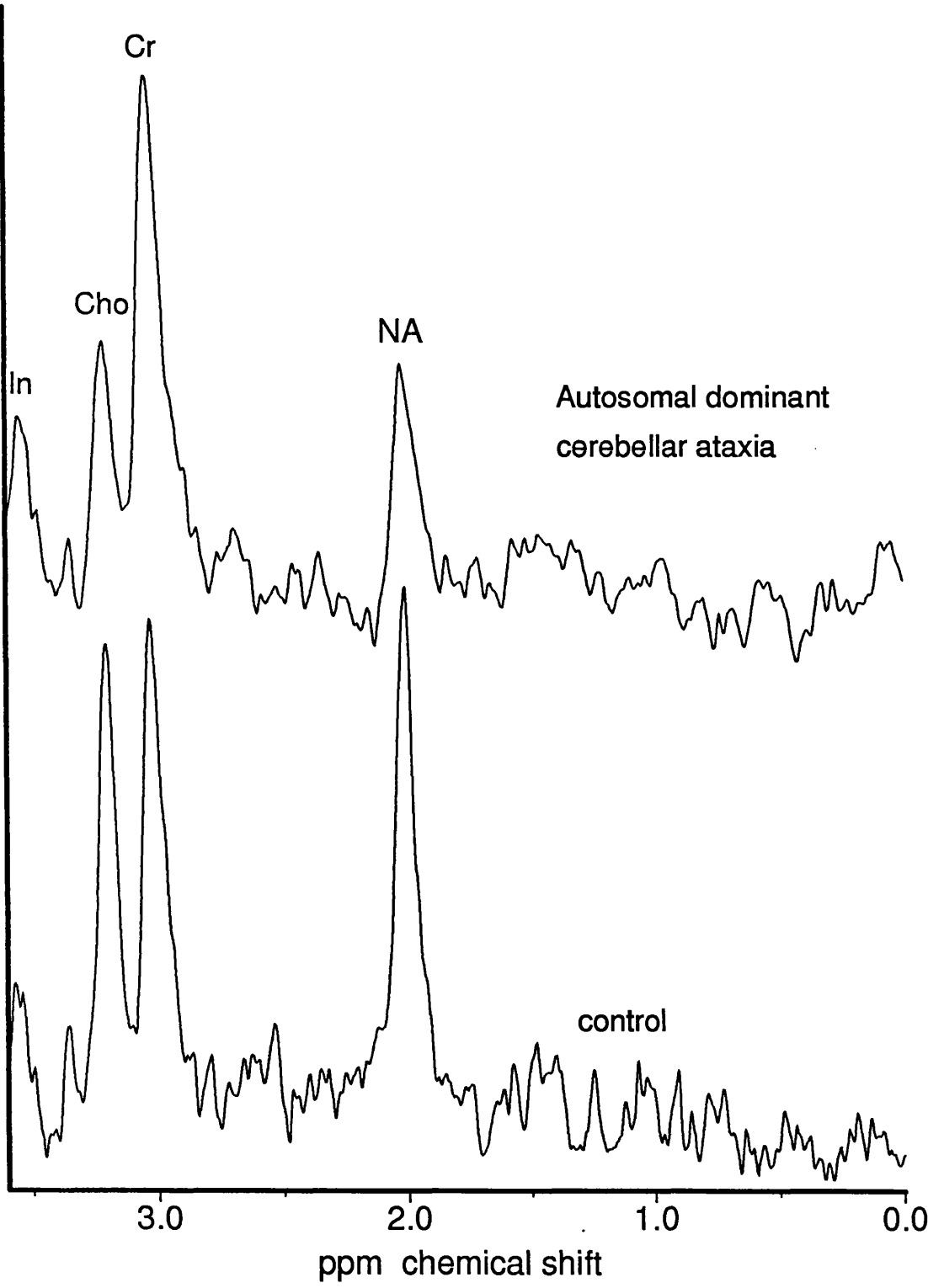


Figure 4.5

[NAA] values in patients and controls

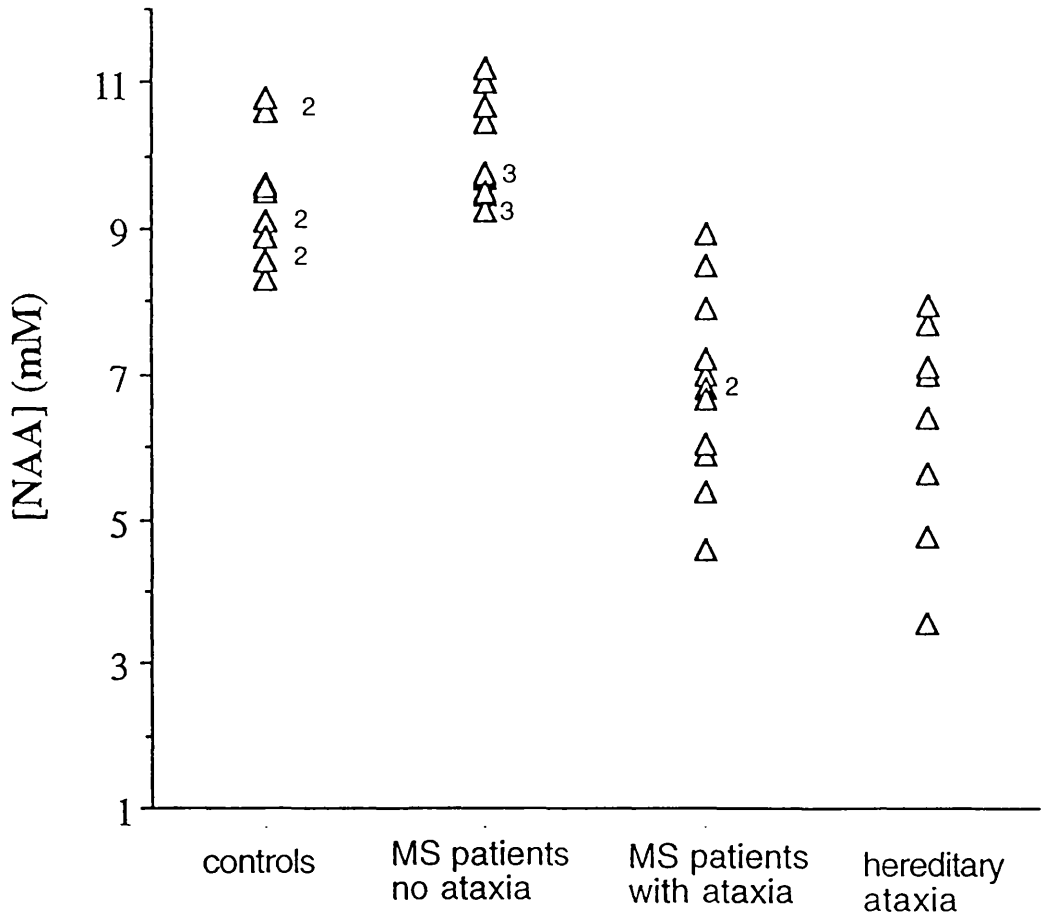


Figure 4.6

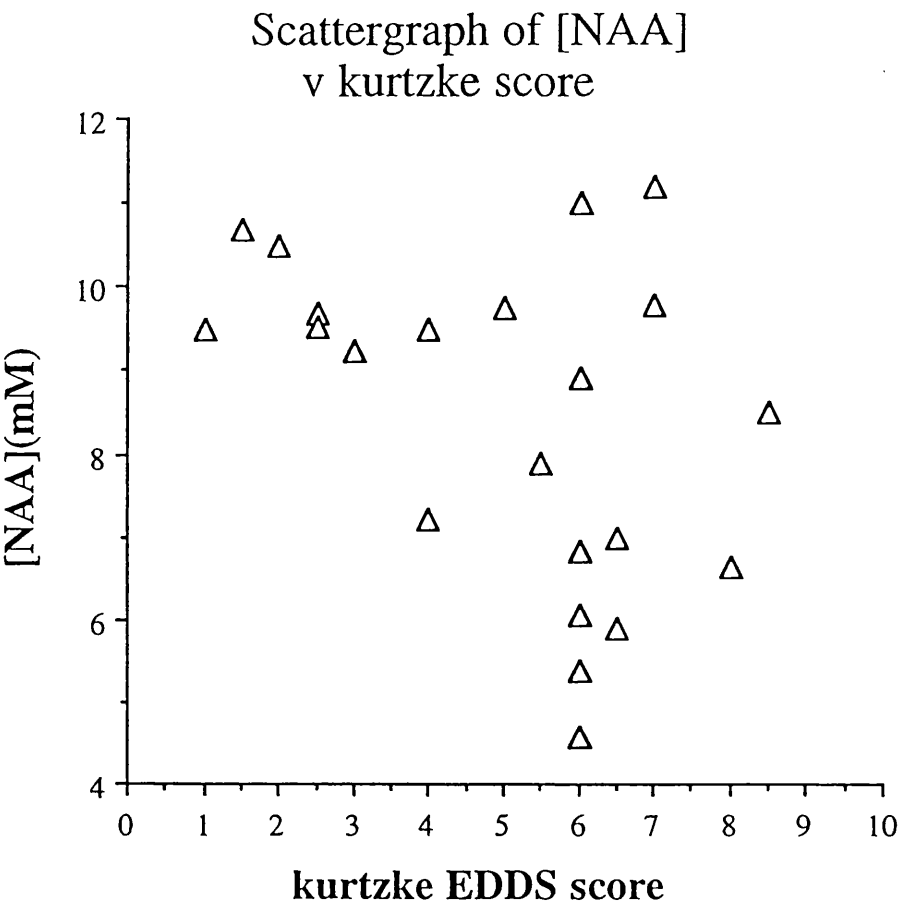
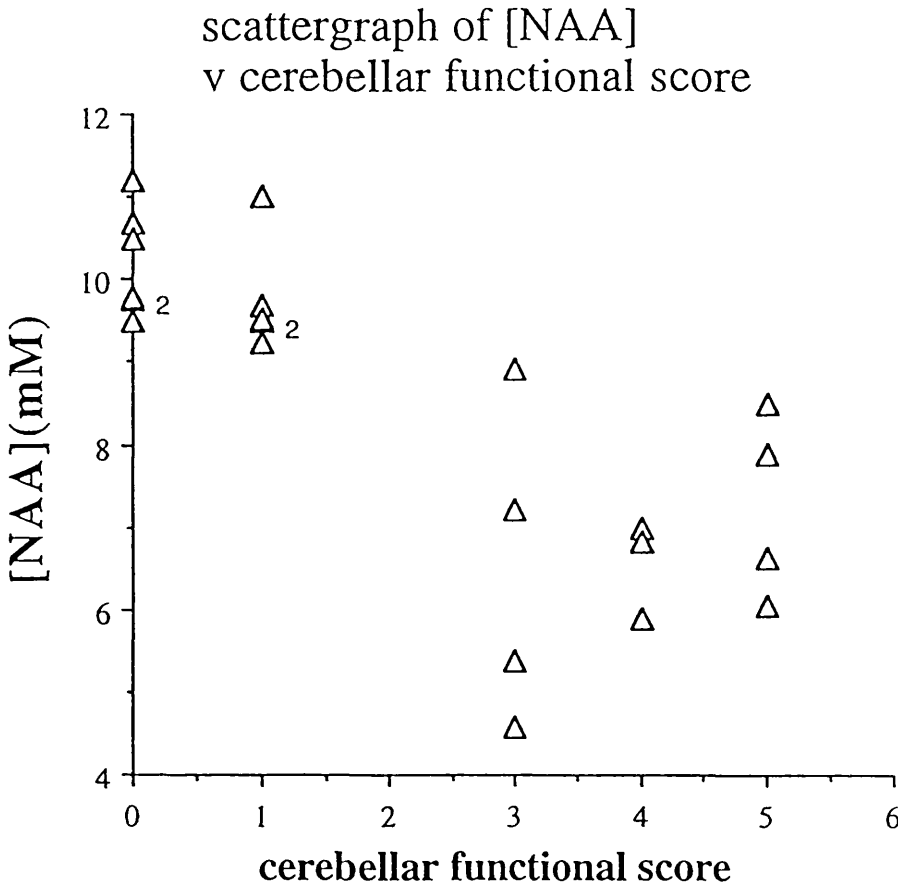


Figure 4.7



CHAPTER 5

¹H MAGNETIC RESONANCE SPECTROSCOPY OF CHRONIC CEREBRAL WHITE MATTER LESIONS AND NORMAL APPEARING WHITE MATTER IN MULTIPLE SCLEROSIS

5.1 SUMMARY

In order to explore further the hypothesis presented in the previous chapter that irrecoverable neurological deficit in MS is associated with axon loss, the apparent concentration of NAA (a neuronal marker) from cerebral white matter has been compared in four groups of MS patients classified as relapsing/remitting, secondary progressive, primary progressive, benign and a control group. In the MS patients with relapsing/remitting disease (n=9) there was a highly significant reduction of apparent NA (median 8.73mM, range 6.86mM - 10.74mM, $p=0.0008$) from an area of high signal compared to the control group (median 11.97mM, range 10.55-14.5mM). In the MS patients with secondary progressive disease (n=10), there was again a highly significant reduction of apparent NA (median 7.82mM, range 3.5mM - 10.3mM, $p=0.0003$) from an area of high signal compared to the control group. In the MS patients with primary progressive disease (n=6) there was once again a highly significant reduction of apparent NA (median 8.83mM, range 6.95mM - 9.89mM, $p<0.002$) from an area of high signal compared to the control group. In the MS patients with benign disease (n=6) however, there was no significant difference in the apparent NA (median 10.5mM, range 8.53mM - 12.8mM, $p>0.05$) from an area of high signal compared to the control group.

In the MS patients with benign disease (n=5) there was also no significant difference in the apparent NA (median 10.74mM, range

8.58mM - 13.4mM, $p > 0.3$) from an area of NAWM compared to the control group. In the MS patients with primary progressive patients however, there was a significant reduction of apparent NA from an area of NAWM (median 8.78mM, range 8.7mM - 12.38mM, $p < 0.025$) compared to the control group

There was a statistically significant inverse correlation between [NA] from lesions in the MS patients and disability as measured on the Kurtzke EDSS score $r = -0.364$, $0.05 < p < 0.02$

These findings support the hypothesis that axonal loss is important in the development of disability in multiple sclerosis. They also provide evidence for axonal loss in NAWM in patients with primary progressive disease

5.2 INTRODUCTION

It is well recognised that the clinical course of multiple sclerosis (MS) may follow a number of patterns. The majority of patients have a relapsing, remitting course at onset though after a variable interval many will develop progressive disability on a background of superadded relapses (Thompson et al., 1992). In approximately 30% of patients however, the disease adopts a benign course where minimal disability is observed after 10 years from symptom onset (McAlpine., 196, Kidd et al., 1994a). In 10 to 15% of MS patients the disease process is progressive from onset (1y progressive disease) (Thompson et al., 1991). These patients tend to be male, are older at the onset of symptoms and frequently present with a spastic paraparesis. Magnetic resonance imaging (MRI) studies in these patient groups have demonstrated important differences in the distribution, size and frequency of lesion development in these groups (Thompson et al., 1990, 1991, Kidd et al., 1994a) together with differing degrees of blood brain

barrier breakdown as evidenced by the presence of enhancement after the administration of gadolinium-DTPA (Kermode et al., 1990). However, to date there has been poor correlation between the degree of disability in the various MS patient subgroups and lesion load measured from conventional MR imaging (Li et al., 1984). From the results of the previous study (Chapter 4) it is possible to hypothesise that a sustained neurological deficit occurs in patients with primary and secondary progressive disease as a consequence of axonal loss occurring within lesions and also in areas of NAWM. A loss of neurones (cell bodies and axons) would be predicted to cause a persistent reduction in the concentration of NA in those patients with greatest disability. In order to test the hypothesis that irrecoverable neurological deficit in MS is associated with axon loss, the apparent concentration of NA has been compared in four groups of patients with differing degrees of disability classified as relapsing/remitting, secondary progressive, primary progressive and benign.

5.3 Materials and Methods

5.3.1 Patients

Patients with clinically definite MS (Poser 1983) were recruited from the National Hospital for Neurology and Neurosurgery. The study was approved by the Joint Ethics Committee at the Institute of Neurology and the National Hospital for Neurology and Neurosurgery, London. Informed consent was obtained from all patients prior to each study.

The patient groups were defined as follows:

1. Relapsing-remitting (n=9): a history of relapses and remission without gradual deterioration, excluding benign cases. The patients had a median age of 31(range 26 - 49 years) and a median disease duration of 3 years (range 1- 12 years). The median Kurtzke EDSS score was 3.5

(range 2.0 - 5.5)

2. Benign (n=9): relapsing-remitting disease of at least 10 years disease duration with a disability scoring on the Kurtzke Expanded Disability Status Score (EDSS) of less than or equal to 3.0. The patients had a median age of 45 (range 39 - 63 years) and a median disease duration of 20 years (range 10 years -35 years). The median Kurtzke EDSS score was 2.5 (range 1.0 - 3.0)

3. Secondary progressive (n=10): patients presenting with a relapsing-remitting course with evidence of progressive deterioration for at least six months with or without superimposed relapses. The patients had a median age of 46 years (range 21 - 55 years) and a median disease duration of 13.5 years (range 5- 25 years). The median Kurtzke EDSS score was 7.0 (range 4.0 - 8.0)

4. Primary progressive (n=8): patients with progressive deterioration from symptom onset without any relapses or remissions. The patients had a median age of 42 years (range 37 - 47 years) and a median disease duration of 4.5 years (range 1.5 - 19 years). The median Kurtzke EDSS score was 6.0 (range 5.0 - 7.5)

Nine healthy controls were also studied.

5.3.2 Magnetic resonance imaging and spectroscopy

MRI and MRS were performed on a 1.5 T. G.E. signa whole body scanner using a standard quadrature head coil. The study commenced with a T₂ weighted fast spin echo imaging sequence (TR 3000 ms, TE_f 80 ms) (5mm slices with 2.5 mm gap, 256x256 matrix, echo train length 8).

After imaging, a volume of interest ranging between 3.5 ml and 6ml was prescribed which in the patient group incorporated a chronic high signal lesion and or an area of normal appearing white matter (NAWM). Lesions were determined to be chronic if they were unchanged on imaging over a period of six months or greater. Large lesions were chosen in order to minimise partial volume effects. If a sufficiently large enough lesion could not be identified on imaging then spectra were collected from NAWM alone. In several of the patients it was not possible to collect spectra from an area of high signal and NAWM because of time constraints and patient compliance. An MR image of the voxel was then obtained to ensure accurate localisation. Water suppressed ^1H spectra were obtained using a STEAM sequence (Frahm *et al.*, 1987 and 1989a). Acquisition parameters were TR 2000 ms, TM 12ms, TE 135ms. 256 averages were collected using an 8 step phase cycle in ~ 9 minutes. 1024 points were collected, with a spectral width of 750 Hz. Shimming to a line width of ~1.5Hz. and water suppression were re-optimised for each new location. In the control group, spectra were collected from an area of periventricular white matter.

Data processing included 1.5 Hz. line broadening for filtering, Fourier transformation, and zero order phase correction. No baseline correction was applied. Peak areas were determined using a line-fitting programme ("SA / GE", G.E. Milwaukee W.I.). Peaks were fitted to a Gaussian line shape using a Marquardt fitting procedure. Absolute concentrations for the metabolites were calculated using the fully relaxed water signal as an internal standard of reference (Christiansen *et al* 1993) as outlined in Chapter 2 and Appendix A.

Statistical analysis was performed with a Mann-Whitney confidence interval and test. Results are expressed as a median value together

with the range and p value. A Spearman's rank correlation test was also used and results are expressed as an r value together with levels of significance.

5.4 RESULTS

5.4.1 MRS Lesions.

A spectrum from a healthy control is shown in Figure 1.

All patients in the relapsing-remitting and secondary progressive groups had lesions large enough to be studied with single voxel spectroscopy. In the benign group six patients had lesions large enough to study with MRS. Similarly in the primary progressive group, six patients had at least one lesion of sufficient size to study with spectroscopy.

Relapsing-remitting patients.

In the MS patients with relapsing remitting disease (n=9) there was a highly significant reduction of apparent NA (median 8.73mM, range 6.86mM - 10.74mM, $p=0.0008$) from an area of high signal compared to the control group (median 11.97mM, range 10.55-14.5mM). The apparent creatine concentration in the same group from an area of high signal was reduced (median 8.3mM, range 7.0mM - 12.1mM, $p=0.29$) compared to controls (median 9.05mM, range 8.1mM - 11.7mM) though this did not achieve statistical significance. There was no significant difference in the apparent choline concentration between the relapsing-remitting lesion group (median 1.73mM, range 1.27mM - 2.5mM, $p=1$) and controls (median 1.66mM, range 1.29mM - 1.91mM). (Figure 2).

Secondary progressive patients.

In the MS patients with secondary progressive disease (n=10), there was again a highly significant reduction of apparent NA (median 7.82mM, range 3.5mM - 10.3mM, $p=0.0003$) from an area of high signal compared to the control group. The apparent creatine concentration in the same group from an area of high signal was reduced (median 7.89mM, range 4.83mM - 10.3mM, $p=0.1$) though again this did not achieve statistical significance. There was no significant difference in the apparent choline concentration between the secondary progressive lesion group (median 1.78mM, range 1.36mM - 2.18mM, $p=0.48$) and controls. (Figure 3)

Primary progressive patients.

In the MS patients with primary progressive disease (n=6) there was once again a highly significant reduction of apparent NA (median 8.83mM, range 6.95mM - 9.89mM, $p<0.002$) from an area of high signal compared to the control group. The apparent creatine concentration in the same group from an area of high signal was reduced (median 7.39mM, range 6.47mM - 12.4mM, $p>0.08$) though again this did not achieve statistical significance. There was no significant difference in the apparent choline concentration between the primary progressive lesion group (median 2.0mM, range 1.3mM - 2.28mM, $p>0.20$) and controls. (Figure 4)

Benign patients

In the MS patients with benign disease however there was no significant difference in the apparent NA (median 10.5mM, range 8.53mM - 12.8mM, $p>0.05$) from an area of high signal compared to the control group. The apparent creatine concentration in the same group from an area of high signal was reduced (median 7.7mM, range 5.96mM - 11mM, $p>0.4$) though again this did not achieve statistical significance. There was no significant difference in the apparent choline concentration between the benign lesion group (median 1.75mM, range 1.08mM - 2.25mM, $p>0.34$) and controls. (Figure 5).

5.4.2 MRS normal appearing white matter

Benign patients.

In the MS patients with benign disease ($n=5$) there was again no significant difference in the apparent NA (median 10.74mM, range 8.58mM - 13.4mM, $p>0.3$) from an area of NAWM compared to the control group. The apparent creatine concentration in the benign group from an area of NAWM (median 9.15mM, range 8.68mM - 9.76mM, $p>0.9$) did not differ from the control group. There was no significant difference in the apparent choline concentration between the benign lesion group (median 1.82mM, range 1.72mM - 2.28mM, $p>0.12$) and controls.

Primary progressive patients.

In the MS patients with primary progressive patients however, there was a significant reduction of apparent NA from an area of NAWM (median 8.78mM, range 8.7mM - 12.38mM, $p< 0.025$) compared to the control group (Figure 6). The apparent creatine concentration in the primary progressive group from an area of NAWM (median 8.9mM, range

6.46mM - 9.49mM, $p>0.5$) did not differ from the control group. There was no significant difference in the apparent choline concentration from NAWM in the primary progressive lesion group (median 1.44mM, range 0.96mM - 2.53mM, $p>0.14$) and controls.

Due to time constraints, it was not possible to collect spectroscopic data from NAWM in the relapsing-remitting and secondary progressive patients.

There was a small but nevertheless significant inverse correlation between [NA] from lesions in the MS patients and disability as measured on the Kurtzke EDSS score $r = -0.364$, $0.05 < p < 0.02$

5.5 DISCUSSION

There are three findings of note in this study. The first is the relative preservation of [NA] from lesions in the benign MS patients compared to [NA] from lesions in the primary progressive, secondary progressive, relapsing remitting patients and NAWM from the control group. The second finding of note is small but nevertheless significant correlation between the reduction of [NA] from an MS lesion and the degree of disability measured on the Kurtzke score. Finally, this study has shown a reduction of [NA] from NAWM in the primary progressive group of MS patients compared to the preservation of [NA] from NAWM in the benign group of MS patients and healthy controls. These findings will now be discussed.

5.5.1 [NA] in MS lesions

Lesions from the patient groups with progressive and relapsing/remitting MS showed a significant reduction in the median

[NA]. The demonstration of a reduced [NA] from MS lesions in these patient groups is in keeping with the observations in Chapters 3 and 4 and is consistent with other reported studies (Arnold et al, 1990b, 1992a; Miller et al, 1991; Husted et al, 1994).

However an original observation in the present study is the relative preservation of [NA] from lesions in MS patients with benign disease. The incidence of benign MS varies in different series from between 15 and 40% (McAlpine., 1961, Confraveux et al., 1980, Thompson et al., 1986). The pathophysiological mechanisms that lead to a benign course are not fully understood. MRI studies in brain (Thompson et al., 1990) or spinal cord (Kidd et al., 1993) have shown little or no relation between disability and lesion load. It does seem however that new or enlarging MS lesions show significantly less gadolinium enhancement in MS patients with benign disease compared to relapsing remitting patients (Kidd et al., 1994a) suggesting a less marked inflammatory process in the evolution of the developing lesion in the benign group.

Given that the principal component of NA is N acetyl aspartate, an amino acid almost exclusively localised within neurones and their processes, the relative preservation of [NA] from lesions in the benign group may reflect a relative preservation of axons in these lesions. It may be that the less marked initiating inflammatory event in benign MS produces less axonal disruption and a preserved capacity for axonal repair.

The patients in the primary progressive and secondary progressive groups had a significantly higher median Kurtzke score compared to the patients in the benign group. Although the relapsing/remitting group showed a reduction in the median concentration of NA, three of these patients had a preserved concentration of NA (Figure 5.7) with minimal disability on the EDSS score. It is intriguing to speculate that these

patients may in fact have a benign form of the disease over time and thus would be expected to have a preservation of NA in lesions. An alternative explanation for this finding is that the patients in the relapsing/remitting group who had higher levels of NA tended towards a shorter disease duration, though not invariably so (Table 1, patient 10). Nevertheless, this observation at least raises the possibility that MRS may have some predictive role in determining disability in MS.

5.5.2 Correlation between the reduction of [NA] from an MS lesion and the degree of disability measured on the Kurtzke score

This study has also shown a weak correlation between the reduction of [NA] from MS lesions and increased disability as measured on the Kurtzke EDSS score (Figure 8). That such a modest correlation was found is not surprising. Previous investigators have failed to show a correlation between a reduction in NAA from chronic lesions and disability (Arnold 1994), probably because, as in the present study, lesions and NAWM in the periventricular areas were examined which are not clinically eloquent (Phadke and Best, 1983) except in relation to cognitive function (Rao et al., 1989 Feinstein et al., 1993). The study described in the previous chapter concentrated on an area of the brain that was clinically eloquent and showed a stronger correlation between a reduction of NAA and the Kurtzke EDSS score. Furthermore a spectroscopic study of acute symptomatic lesions showed a strong negative correlation between reduction of NAA and disability (De Stefano et al., 1995)

5.5.3 reduction of [NA] from NAWM in the primary progressive MS patients

The other finding of note in this study was the significant reduction of [NA] in NAWM in patients with primary progressive MS patients compared to NAWM from benign MS patients and white matter from healthy controls (Figure 6). In the study of acute lesions (Chapter 3) a reduction in the NAA/creatine ratio from normal appearing white matter was observed in patients with relapsing remitting MS. Such a reduction is likely to reflect microscopic abnormalities which have been documented in pathological studies (Allen, 1991). A diffuse pathological process in primary progressive MS may explain the tendency towards increased disability in these patients despite the relative lack of visible lesions observed with MRI (Thompson et al., 1991, Revescz et al., 1994).

5.5.4 Other findings

A post-mortem study by Davies and colleagues (1995) showed an absolute reduction of NA and creatine from MS lesions studied 48 hours after death whereas areas of NAWM studied showed normal metabolite levels. In the present study there was a tendency for the creatine concentration to be reduced in lesions from all MS groups though this did not achieve statistical significance. There was no significant difference between the creatine concentration from NAWM in the benign and primary progressive patients compared to controls.

LEGENDS

Figure 5.1

Magnetic resonance spectroscopy (TR 2000ms, TE 135ms) from parietal white matter in healthy control.

Figure 5.2

Magnetic resonance spectroscopy (TR 2000ms, TE 135ms) from a chronic parietal white matter lesion in a patient with relapsing remitting MS (disease duration 12 years, Kurtzke EDSS 5.0, [NA] 8.14mM).

Figure 5.3

Magnetic resonance spectroscopy (TR 2000ms, TE 135ms) from a chronic parietal white matter lesion in a patient with secondary progressive disease (disease duration 20 years, Kurtzke EDSS 7.5, [NA] 6.97mM).

Figure 5.4

Magnetic resonance spectroscopy (TR 2000ms, TE 135ms) from a chronic parietal white matter lesion in a patient with primary progressive disease (disease duration 4 years Kurtzke EDSS 6.0, [NA] 7.37mM).

Figure 5.5

Magnetic resonance spectroscopy (TR 2000ms, TE 135ms) from a chronic parietal white matter lesion in a patient with benign disease (disease duration 20 years, Kurtzke EDSS 3.0, [NA] 11.45mM).

Figure 5.6

Magnetic resonance spectroscopy (TR 2000ms, TE 135ms) from an area of normal appearing parietal white matter in a patient with primary progressive disease (disease duration 4 years Kurtzke EDSS 6.0, [NA] 9.9 mM).

Figure 5.7

Scattergraph of apparent [NA] compared to Kurtzke EDSS in MS patients with relapsing remitting disease.

Figure 5.8

Scattergraph of apparent [NA] from lesions compared to Kurtzke EDSS in MS patients from all subgroups.

Table 5.1

Disease duration, Kurtzke EDSS and [NA] in the MS lesion subgroups

Benign Patients	disease duration	EDSS	[NA]
1	20 years	3.0	11.45
2	19 years	2.0	12.8
3	14 years	2.0	9.01
4	25 years	2.5	9.9
5	15 years	2.5	8.53
6	29 years	3.0	10.5
Relapsing Remitting			
7	4 years	5.0	9.67
8	1 year	2.0	10.74
9	1.5 years	3.0	7.12
10	5 years	2.5	10.14
11	12 years	5.0	8.14
12	3 years	3.5	8.4
13	1.5 years	2.0	10.25
14	1 year	2.0	6.9
15	1 year	3.5	8.73

Table 5.1 (continued)

Disease duration, Kurtzke EDSS and [NA] in the MS lesion subgroups

2y progressive patients	disease duration	EDSS	[NA]
16	14 years	4.0	10.3
17	7 years	5.5	3.5
18	20 years	7.5	9.97
19	20 years	7.5	6.97
20	13 years	8.0	5.4
21	25 years	7.0	7.22
22	7 years	4.5	8.47
23	24 years	4.0	7.43
24	7 years	7.5	10.07
25	5 years	7.5	8.2
1y progressive patients			
26	8 years	7.5	9.89
27	3 years	6.0	9.02
28	4 years	5.0	9.84
29	1.5 years	5.5	6.95
30	4 years	6.0	7.37
31	9 years	6.0	8.64

Figure 5.1

MRS from NAWM parietal lobe healthy control
Volume 4mls TE 135ms TR 2000ms

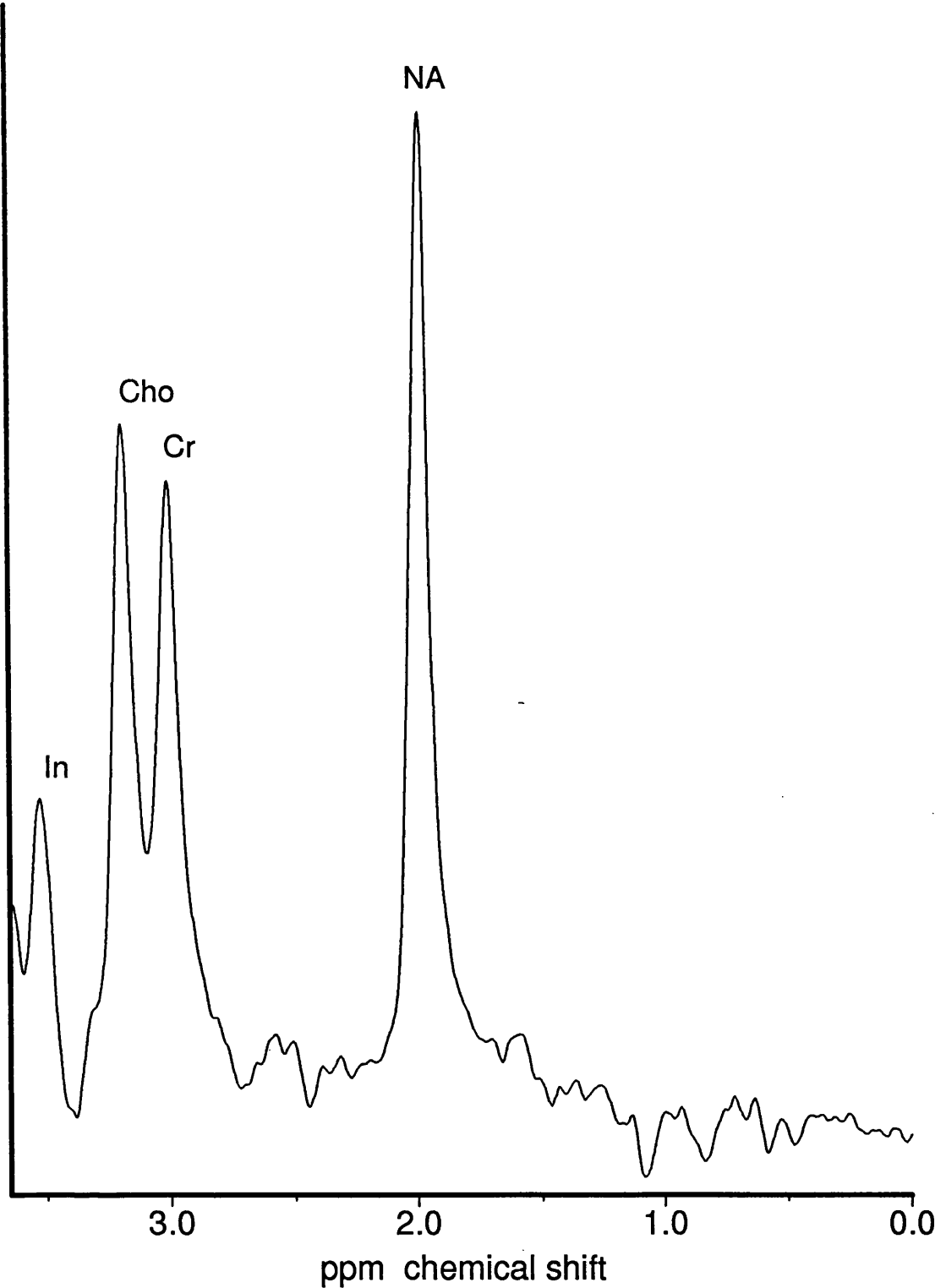


Figure 5.2

MRS from a white matter lesion in a relapsing-remitting MS patient

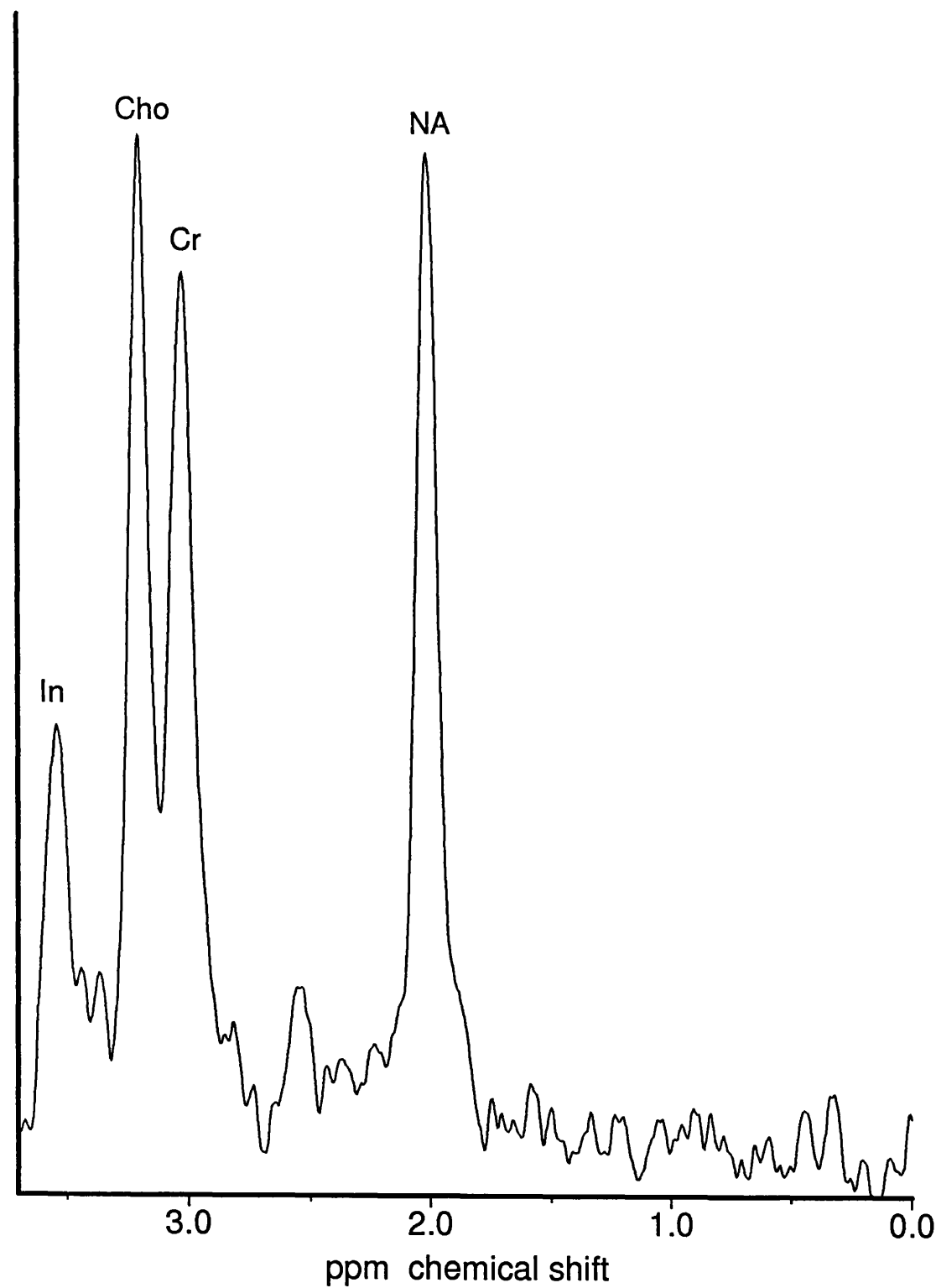


Figure 5.3

MRS from a chronic WM lesion in a patient with 2y progressive MS

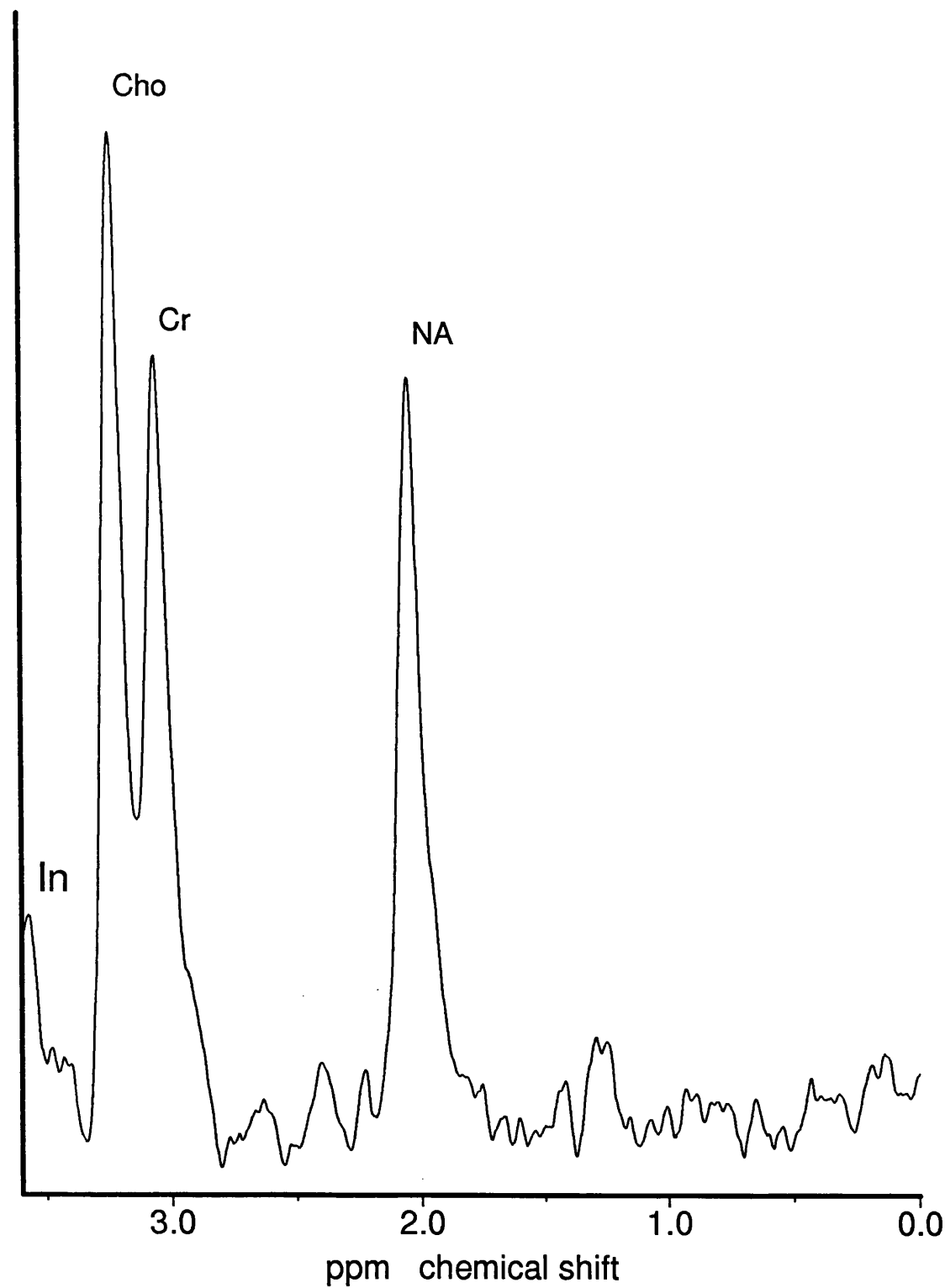


Figure 5.4

MRS from a chronic WM lesion in a primary progressive MS patient

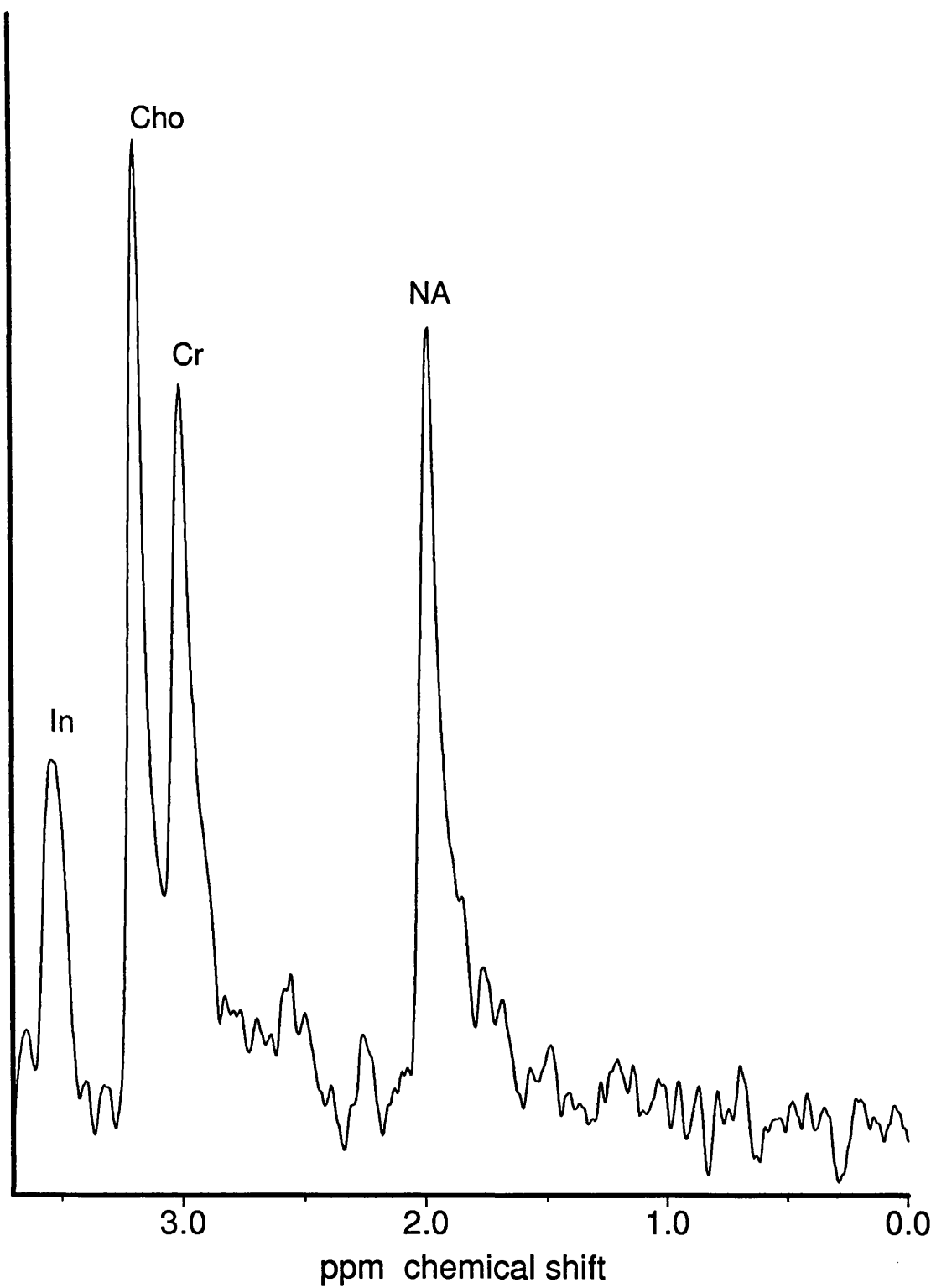


Figure 5.5

MRS from a lesion in a patient with benign MS

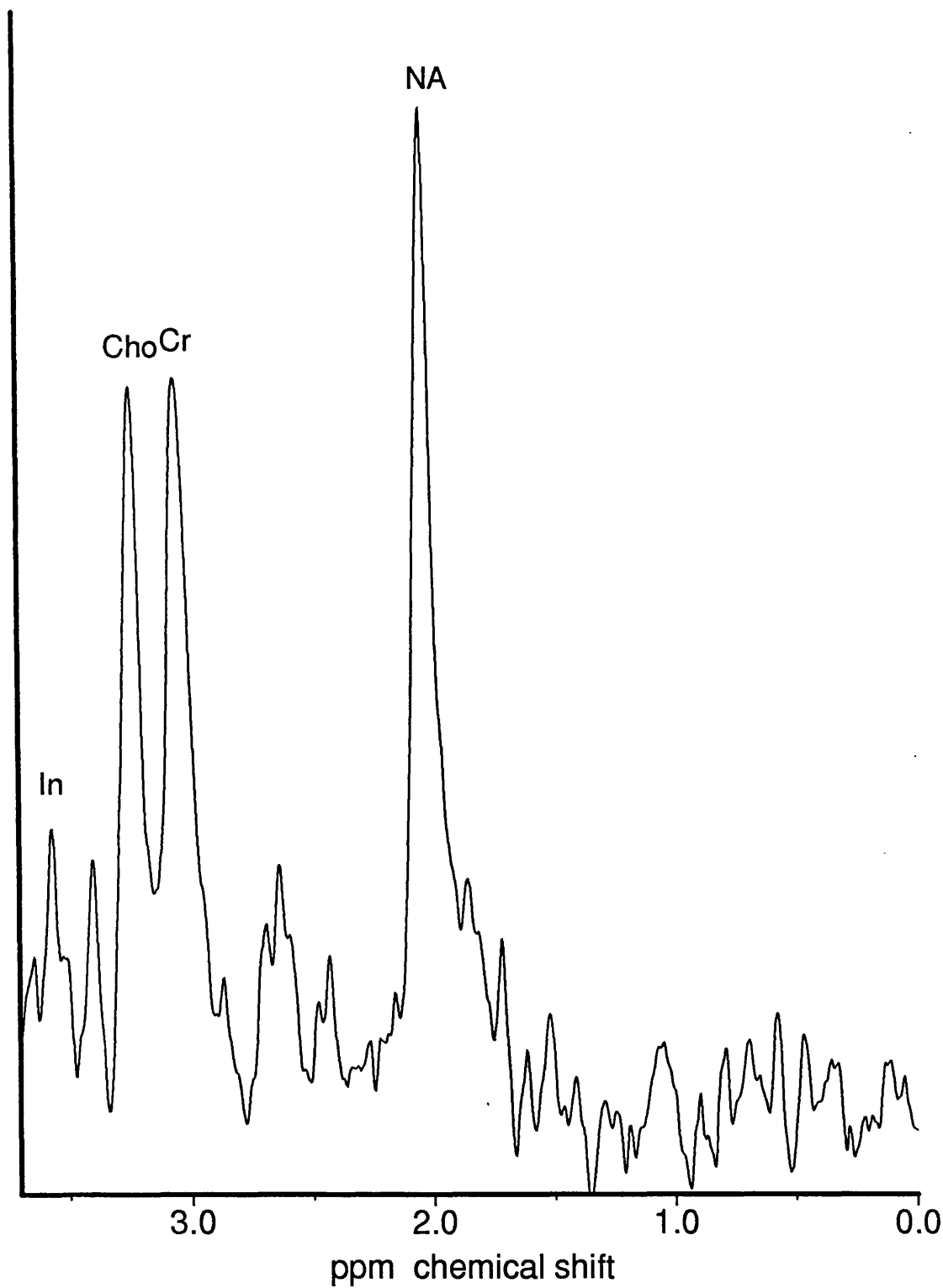


Figure 5.6

MRS from NAWM in a primary progressive MS patient

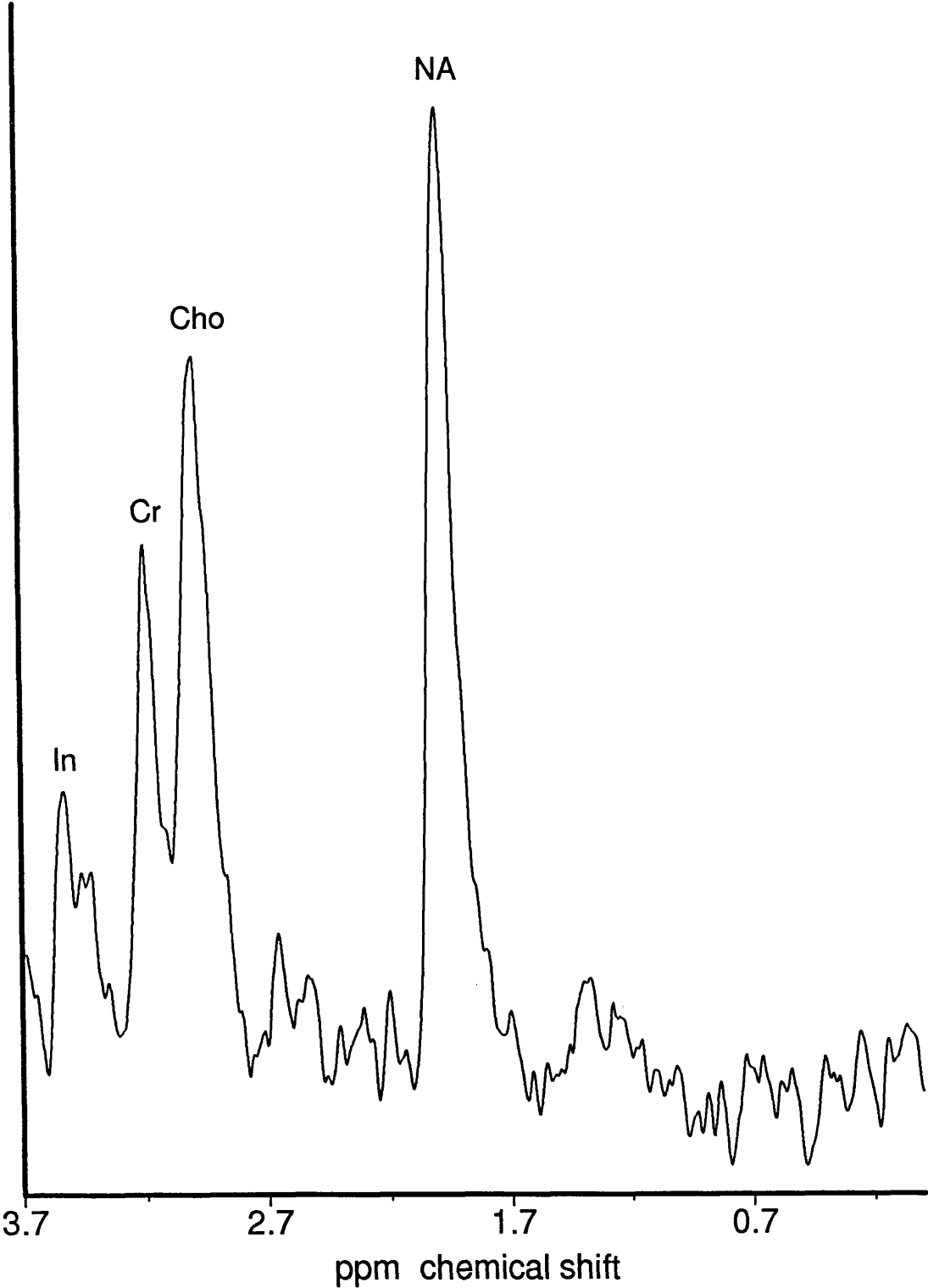
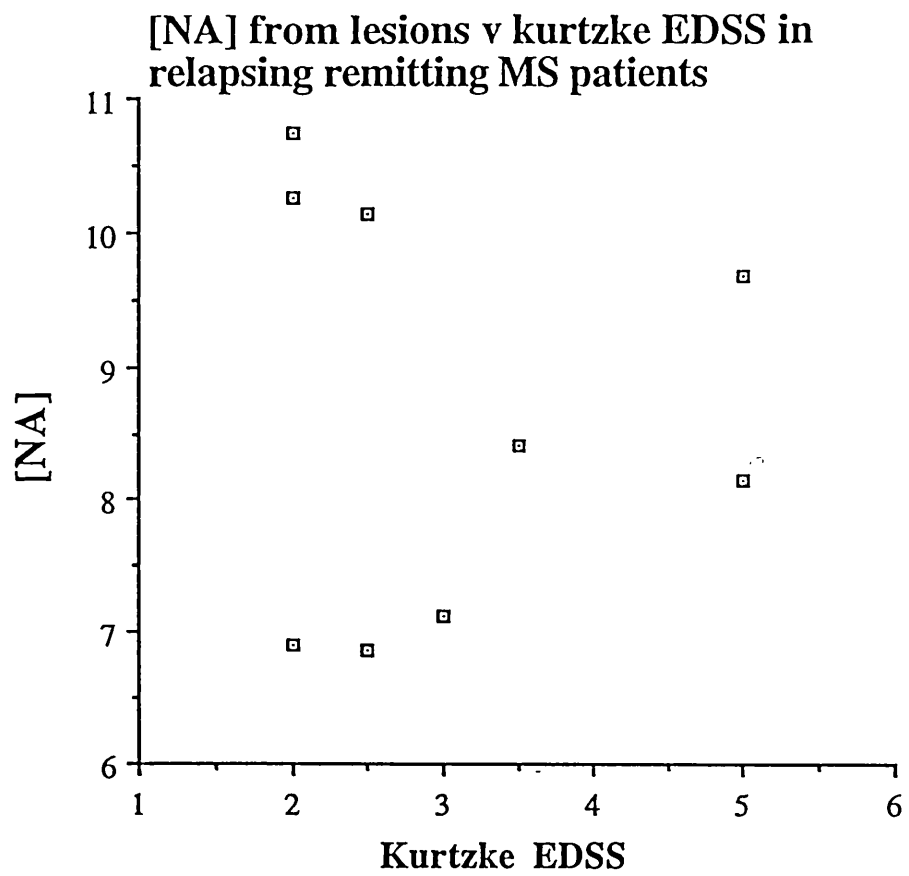
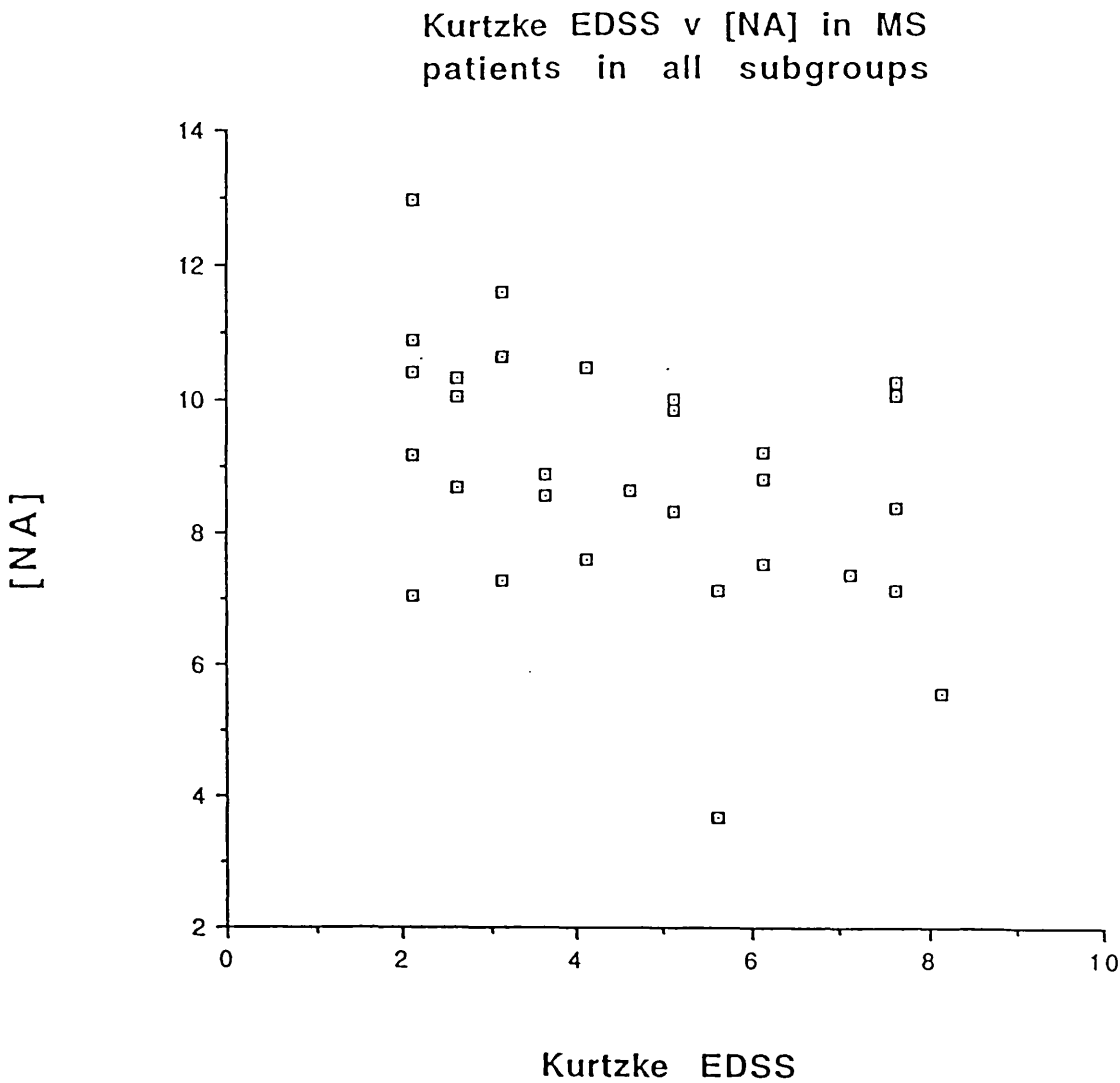


Figure 5.7





CHAPTER 6

¹H MAGNETIC RESONANCE SPECTROSCOPY OF SYSTEMIC LUPUS ERYTHEMATOSUS INVOLVING THE CENTRAL NERVOUS SYSTEM

6.1 SUMMARY

In this study 13 patients with neurological manifestations of SLE with previous and/or current neurological or psychotic episodes were studied by MRI and ¹H MRS together with psychiatric and cognitive assessment. MRI was abnormal in 7 patients, showing high signal lesions in the white matter and/or cerebral atrophy. Proton MRS centred on white matter lesions in 5 patients showed a reduction in the (NAA)/creatine ratio compared to NAWM in the SLE group and in 10 healthy controls. This pattern of abnormality does not allow differentiation of SLE lesions from the chronic plaques occurring in MS. There was a very high frequency of current psychiatric morbidity in the SLE group: occurring in 12 of the 13 patients. There was no correlation between the presence of current psychiatric involvement and/or cognitive dysfunction and abnormalities detected with MRI or MRS.

6.2 INTRODUCTION

SLE is an autoimmune disease which frequently involves the nervous system (Johnson and Richardson; 1968 Harris and Hughes, 1985). Neurological manifestations include seizures, strokes or transient ischaemic attacks, cranial neuropathies, depression, psychosis and cognitive impairment (Baker, 1973). Some manifestations (e.g. optic neuropathy, transverse myelopathy) resemble those of MS. Brain MRI may show a variety of abnormalities including large infarcts or

multifocal grey and/or white matter lesions, most commonly multifocal white matter lesions. This appearance is not specific (Miller et al., 1992) and similar lesions may be seen in MS, arteriosclerotic cerebrovascular disease and granulomatous disease.

A conservative estimate suggests that cognitive dysfunction occurs in approximately a quarter of patients with SLE attending an out-patient clinic (Hanly et al., 1992). This figure rises to 40% when active brain involvement is present and significantly exceeds that for related disorders without cerebral involvement, such as rheumatoid arthritis (Hanly et al., 1992). Similar prevalence figures have been found in children with SLE (Papero et al., 1990) suggesting that the degree of cognitive dysfunction is not age related. A wide array of cognitive abnormalities are found, but the most noticeable deficits are seen with tests of attention (Ginsburg et al., 1992).

In addition to the cognitive changes, psychiatric abnormalities frequently occur in SLE. Point prevalence has ranged from 21% (Hay et al., 1992) to approximately 60% (Lim et al., 1988) with both studies showing a firm correlation between the presence of more minor psychiatric disturbance (anxiety and depression) and social stress. An earlier study (Lim et al., 1988) failed to find a correlation between affective and anxiety symptoms and the presence of cerebral pathology as demonstrated by MRI.

¹H MRS has been carried out in a group of SLE patients with neurological involvement. The aims of the study were:

- (i) to assess the value of MRS in the differential diagnosis of MS and SLE and
- (ii) to determine if there was a correlation between spectral abnormalities on the one hand and neuropsychiatric manifestations on the other.

6.3 PATIENTS AND METHODS

6.3.1 Patients

13 patients (10 women and 3 men) aged 22 - 58 (median 43 years) and 10 healthy controls aged 20-55 years (median 38 years) were studied. SLE was diagnosed using the 1982 American Rheumatism Association criteria (Tan et al., 1982). Patients were recruited from two hospital departments of rheumatology on the basis of a past and/or current neurological or psychotic episode (see Table 1). In 12 there was a history of neurological symptoms in keeping with a diagnosis of cerebral SLE. These included acute episodes of ataxia and diplopia, dysphasia, hemiparesis or sensory disturbance and episodes of altered behaviour in keeping with complex partial seizures. Patient 12 had a history of psychotic illness without any definite neurological signs or symptoms attributable to SLE although there was a history of late onset migraine. In 10 patients there was evidence of neurological deficit at entry into the study. These included hemiparesis, myelopathy and brain stem involvement. Time since onset of neurological symptoms ranged from 6 months to 30 years (median 6.5 years). Patients underwent formal neuropsychological, psychiatric and neurological examination. Three patients exhibited a parkinsonian syndrome, something not hitherto associated with SLE. In one this was possibly attributable to neuroleptic treatment. In the other two it was felt possible that it was either due to to coincidental idiopathic Parkinson's disease or an unusual manifestation of cerebral lupus. The latter may be more likely since one of these patients exhibited signal change in both basal ganglia and Gd-DTPA enhancement in the right caudate nucleus on MRI (Figure 6.2), abnormalities which are not seen in idiopathic Parkinson's disease.

6.3.2 Magnetic resonance imaging and spectroscopy

MRI and MRS were performed on a 1.5 T. whole body imager using a standard quadrature head coil. The study commenced with a T_2 -weighted fast spin-echo imaging sequence (TR 3000 ms, TE_f 80 ms) (5mm slices with 2.5 mm gap, 256x256 matrix, echo train length 8). In the patient group, spectra were then acquired from a volume of interest (3.5 - 6ml) centred on a white matter lesion if present and if not, from an area of normal appearing frontal white matter. On each occasion an MR image of the voxel was obtained to ensure accurate localisation. Water suppressed 1H spectra were obtained using a STEAM sequence. Acquisition parameters were, TR 2000 ms, TM 12ms, TE 10 and 135ms. 256 averages were acquired using an 8 step phase cycle in ~ 9 minutes; 1024 points were collected, with a spectral width of 750 Hz. Shimming to a line width of ~3Hz. and water suppression were re-optimised for each new location. In the control group, spectra were collected from an area of frontal white matter. After collection of the spectroscopic data, in the patient group only, Gd-DTPA 0.1 mM./kg. was injected intravenously and T_1 -weighted Gd-DTPA-enhanced images were obtained (TR 500 ms, TE 20ms). The MRI and MRS examination took approximately 90 minutes.

Data processing included 1.5 Hz. line broadening for filtering, Fourier transformation, and zero order phase correction. No baseline correction was applied. Resonance areas were calculated by manual integration. Ratios for the various metabolites are expressed relative to Cr. NAA and Cho ratios relative to creatine were calculated from the spectra collected at 135ms. Inositol ratios were calculated from spectra collected at 10ms. Statistical analysis was performed using a Mann-Whitney test. Values are expressed as a median together with the range.

6.3.3 Psychiatric assessment

All 13 patients underwent psychiatric evaluation. Prior to undergoing psychiatric assessment, demographic data was collected on all subjects. This included marital and employment status, a family history of mental illness and previous or family history of psychiatric illness and/or substance abuse.

Subjects were then interviewed using the Present State Examination (PSE) and symptoms present only during the past month were noted. The 140 items of the PSE embrace both neurotic and psychotic psychopathology with the first 107 questions devoted to assessing subjective complaints and the remainder assessing objective evidence of mental state disturbance. The data generated by the PSE was then analysed using the CATEGO software programme (Wing et al., 1974)

6.3.4 Neuropsychological assessment

Cognitive assessment was carried out by a psychologist on 11 patients using measures of general intellectual ability and focal cognitive tests. Evidence of general intellectual deterioration was obtained by analysing discrepancies between estimates of optimal levels of general ability (premorbid I.Q.) and measures of general ability at the time of assessment (current I.Q.). Estimates of optimal levels of general ability were based on the patients' reading vocabulary using the National Adult Reading Test (Nelson, 1971) and/or the Schonell Reading Test (Schonell 1942).

Focal cognitive deficits were defined on the basis of tests of memory, language, visual perception and "executive skills". In addition, tests of speed and attention and tests considered to be sensitive to frontal lobe dysfunction were used i.e. word fluency tests (Benton, 1968) and a

modified version of the Wisconsin Card Sorting Test (Nelson, 1976). Patients who scored below the 10th percentile for their age group or showed a significant discrepancy between their performance on focal tests and measures of general intelligence (I.Q.) were considered to have specific focal cognitive deficits.

6.4 RESULTS

6.4.1 MRI

MRI was performed in 13 patients and reported by a senior neuro-radiologist. In seven patients, there were abnormalities on T₂ weighted scans. In six of these patients there were discrete periventricular and/or subcortical white matter high signal lesions (Figure 6.1). Patient 10 also showed evidence of patchy high signal in the basal ganglia on T₂ weighted imaging which enhanced after Gadolinium on T₁ weighted imaging (Figure 6.2). In four patients (three of whom also had white matter lesions) there was evidence of mild generalised cerebral atrophy.

6.4.2 MRS

Spectroscopic data was collected from 12 patients, one patient being unable to remain in the scanner for the length of the spectroscopic examination. In five of the patients studied, MRS was localised to focal lesions seen on MRI and in the other seven from an area of NAWM. The lesions studied occupied 40-60% of the spectroscopic volume.

There was no significant difference in the mean inositol/creatine ratio from the spectra collected at 10ms in SLE lesions (median 0.59, range 0.3-0.78) compared to NAWM in the SLE group (median 0.64, range 0.30-0.99, $p>0.6$) and NAWM from healthy controls (median 0.65, range 0.45-1.01 $p>0.8$) (see Figure 3).

The median Cho/Cr ratio was also normal in the SLE lesions (median 1.08, range 0.97-1.17) compared to frontal NAWM in the SLE group (median 1.06, range 0.76-1.4, $p>0.8$) and control NAWM (median 1.00, range 0.77-1.22, $p>0.6$). There was however a significant reduction in the NAA/Cr ratio in lesions (median 1.3, range 1.12-1.68,) compared to NAWM in the SLE group (median 1.74, range 1.6-2.08, $p=0.01$) and control NAWM (median 1.76, range 1.49-2.06, $p<0.03$) (see Figure 6.4). Only two patients had evidence of frontal lobe dysfunction on neuropsychological testing. These patients showed no evidence of frontal lobe lesions or atrophy on MRI and no reduction of the NAA/Cr ratio from an area of frontal NAWM compared to controls. Neither lac nor abnormally elevated lipid/protein peaks were observed in lesions or NAWM in the SLE patients or in the control group.

6.4.3 Psychiatric assessment

A family history of psychiatric illness was present in the first degree relatives of four subjects and second degree relatives of one more. No patients had a history of substance abuse, though 10 had a past history of psychiatric problems necessitating consultation with a psychiatrist in all but one case. At the time of the study only one had insufficient psychopathology to warrant a psychiatric diagnosis. Of the remainder, four had had a psychotic illness within the past month (schizophrenia {1}; mania {1}; paranoid psychosis {1}; and psychotic depression {1}). While 8 subjects had experienced non psychotic disorders (anxiety states {2}; neurotic depression {2} and retarded depression {4}) during this period.

A closer look at the nature of the psychopathology was undertaken by collapsing the 140 individual PSE items into discrete categories such as anxiety (PSE items 11-18), concentration difficulties (19-22),

depression (23-27), perceptual disorders (49-54). The symptoms which occurred most frequently are shown in Table 6.2.

Overall, there was no correlation between the presence of a psychiatric disorder (psychotic or neurotic) and abnormalities on MRI or MRS. Too few MRI lesions were present to allow any meaningful correlations between specific psychiatric symptoms and the location of brain lesions.

Of the four patients with a history of psychotic illness, three had normal imaging and one mild generalised atrophy. The one subject with normal PSE had no lesions on MRI and normal spectroscopy.

Significantly, 3 of the 4 psychotic patients as opposed to 1 of 8 neurotic patients had a positive history of psychiatric illness in a first degree relative.

6.4.4 Neuropsychological assessment (Table 6.3)

In four of the 10 patients who underwent cognitive assessment there was a significant degree of deterioration on measures of general intellectual ability. Most of the patients with focal cognitive deficits showed a degree of general intellectual deterioration. However in one patient with evidence of visual memory impairment there was no observed deterioration in her general level of functioning. Patients who failed on one or more of the speed tests also showed impairment on general ability or focal cognitive testing. In five patients there was no evidence of deficit on any of the neuropsychological tests. In two patients with evidence of neuropsychological deficit MRI revealed high signal abnormalities on imaging. In two of the five patients with completely normal cognitive testing there were also discrete white matter lesions on imaging. There was no correlation between neuropsychological deficit and the NAA/Cr ratio of lesions or of NAWM. Of two patients who showed impairment on tests sensitive to frontal

lobe dysfunction, one had generalised cerebral atrophy with no white matter lesions present in the brain. The other patient had a normal MRI.

6.5 DISCUSSION

In this study of 13 patients with SLE and neuropsychiatric involvement it was found that:

- (i) MRS showed a reduction of the NAA/Cr ratio in white matter lesions. There were no metabolic differences on MRS between NAWM in SLE and white matter from healthy controls.
- (ii) There was no correlation between neurological, psychiatric or cognitive involvement and MRI or MRS abnormalities. These findings are now discussed in turn.

6.5.1 Spectroscopy findings in SLE

In SLE, the areas of signal change observed on MRI probably represent areas of ischaemic infarction secondary to vasculopathy, the most frequent pathological finding at post mortem (Johnson and Richardson, 1968; Hume-Adams and Duchon, 1992). A number of mechanisms are likely to contribute to the vascular changes seen in cerebral SLE, including hypertension, coagulopathy, embolism from cardiac vegetations and immune complex vasculitis (Berry and Hodges, 1965). The reduction of the NAA/Cr ratio observed in this study from areas of signal change may be the result of axonal dysfunction or more likely axonal loss in these regions given that the pathological basis of these lesions is probable infarction. Conversely, the normal NAA/Cr ratio from frontal NAWM in the SLE patients suggests that there is unlikely to be a substantial degree of axonal dysfunction or loss in these regions.

In contrast to an earlier report (Haseler et al., 1991), there was no

elevation of lac or lipids in any of the lesions studied, nor were significant changes seen in the ratio of Cho/Cr in either lesions or in NAWM. The lack of elevation of the Cho/Cr ratio in the SLE lesions suggests that they were not inflammatory or that cellularity was not increased at the time they were studied. This is in contrast to the elevation of Cho/Cr ratio observed in acute MS lesions (Chapter 3). It is likely, however, that most of the SLE white matter lesions observed in the present study were longstanding, since only one patient showed evidence of contrast enhancement on imaging. It is not possible from this study therefore to exclude an increase in Cho during the early stage of lesion development in SLE.

A low NAA/Cr ratio is very non specific and has been reported in a large number of neurological disorders including acute and chronic MS lesions (see Chapters 3,4 and 5). It would seem that MRS has little diagnostic value in evaluating chronic lesions in SLE. In MS, acute lesions may be associated with increases in choline, inositol, lipids and lactate. A study of similarly aged lesions in SLE is needed.

6.5.2 Lack of correlation between spectroscopic, neuropsychological and neuropsychiatric features

The fact that the majority of patients had recent or current evidence of psychiatric involvement suggests that psychiatric phenomena in SLE cannot, at least in most instances, be ascribed to structural brain disease detectable on MRI or MRS. This is in keeping with the findings of a previous study of 40 patients with SLE and psychiatric and neurological manifestations (Lim et al., 1988) which also found no correlation between abnormalities on MRI and the presence of psychiatric symptoms. In the same study by Lim et al, a weak correlation was found between the presence of neurological disease and

abnormalities on imaging. In the present study, no association was found between neurological involvement and the presence of abnormalities on MRI. This may reflect a smaller patient group or that the neurological disease in the patients in the present study was quiescent. Nevertheless, it is recognised that there may be marked discordance between the clinical findings in SLE and the neuropathological changes. As Berry (Berry, 1971) has observed “despite neurologic involvement clinically, there is often a disconcerting lack of gross and even microscopic findings in the nervous system on post mortem examination.” The pathogenesis of many of the cognitive, neurological and psychiatric syndromes in SLE remains poorly understood. It may be that other factors including genetic predisposition and the degree of perceived social and personal stress are of relevance.

In summary, proton MRS has shown a non-specific reduction in the NAA/Cr ratio within brain lesions in patients with neuropsychiatric SLE probably indicating axonal loss or dysfunction due to ischaemia or infarction. This pattern of abnormality does not allow differentiation of SLE lesions from the chronic plaques occurring in MS, a condition with which it may be confused clinically. It remains to be determined whether MRS can help differentiate lesions in these two conditions when they present acutely.

Legends

Figure 6.1

T₂-weighted MRI in a patient with SLE (patient 2), showing mild cerebral atrophy and high signal lesions in the periventricular and subcortical white matter.

Figure 6.2

T₁-weighted MRI of a patient with active neurological SLE (patient 11) showing patchy gadolinium enhancement centred on the right caudate nucleus.

Figure 6.3

Short echo time (TE 10ms) spectrum from patient 11 showing no change in the inositol/creatine and choline/creatine ratios in a periventricular white matter lesion compared to an area of NAWM in the same patient and from an age matched control. There is also no elevation of signal in the lipid region.

Figure 6.4

Long echo time (TE 135ms) spectrum from patient 12 showing a low NAA/creatine ratio from a volume centred on a white matter lesion compared to NAWM in the same patient and an area of white matter from an age-matched control.

Table 6.1

Clinical, MR and psychiatric data of SLE patients

<u>Patient</u>	<u>age</u>	<u>sex</u>	<u>past</u>	<u>neurology</u>	<u>current deficit</u>	<u>current psychiatric state</u>	<u>MRI</u>	<u>(NAA/Cr) lesion</u>	<u>NAWM</u>	<u>frontal lobe tests</u>
1	32	F	left CVA 6 y.		none	retarded depression	atrophy, WM lesions	not done		normal
2	35	M	brainstem episode 10 y. signs		brainstem	anxiety state	atrophy,WM lesions	1.3	1.76	normal
3	44	F	L AION 3y		sensory level T2 L optic atrophy	normal	normal	-	1.7	normal
4	36	F	cerebritis 7 y.		R hemiparesis	paranoid psychosis	atrophy	-	2.08	impaired
5	58	F	brainstem episode 5 y.		brainstem signs	anxiety state	small WM lesions	1.68	-	normal
6	52	F	brainstem episode 10 y.		none	depressive psychosis	normal	-	1.8	normal
7	44	F	parkinsonism 3 y.		parkinsonian	retarded depression	normal	-	1.6	normal
8	55	F	brainstem episode 1 y.		brainstem signs	neurotic depression	WM lesions	1.5	-	impaired
9	22	F	epilepsy 3 y.		normal	neurotic depression	normal	-	1.65	normal
10	29	F	brainstem episode 6 m.		brainstem signs parkinsonian	retarded depression	atrophy, WM lesions	1.12	-	not done
11	43	M	seizures 2y. myopathy 2y.		limb weakness	retarded depression	basal ganglia(Gd+) lesions	1.28	-	not done
12	47	M	migraine 3 y.		none	mania with psychotic symptoms	normal	-	1.84	not done
13	38	F	cerebritis parkinsonism 6m.		pyramidal signs parkinsonian	schizophrenia	normal	-	1.72	not done

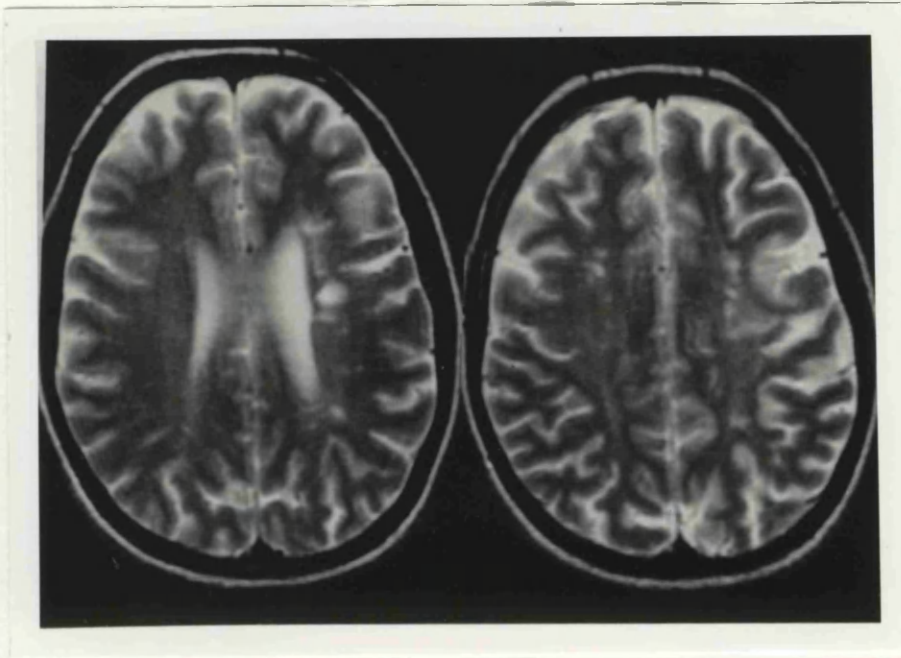
abbreviations: NAWM Normal appearing white matter, CVA -cerebrovascular accident, AION -anterior ischaemic optic neuropathy, WM-white matter y -years since neurological episode, m - months since neurological episode. Gd+ - Gadolinium enhancement.

Table 6.2

Commonest occurring psychiatric symptomatology.

symptom		No. of subjects (13)
1.	worry	13
2.	anxiety	11
3.	concentration difficulties	11
4.	vegetative depressive features (ie. sleep, appetite disturbance)	10
5.	irritability	6
6.	obsessive-compulsive symptoms	5
7.	perceptual abnormalities	5
8.	depersonalisation	4
9.	auditory hallucinations	3
10.	visual hallucinations	3
11.	olfactory hallucinations	2
12.	delusions of reference	1
13.	persecutory delusions	1

Figure 6.1



T₂ weighted axial MRI in SLE patient showing periventricular high signal lesions

Figure 6.2



T₁weighted axial MRI in SLE patient showing enhancing lesion in the head of the right caudate nucleus.

Figure 6.3

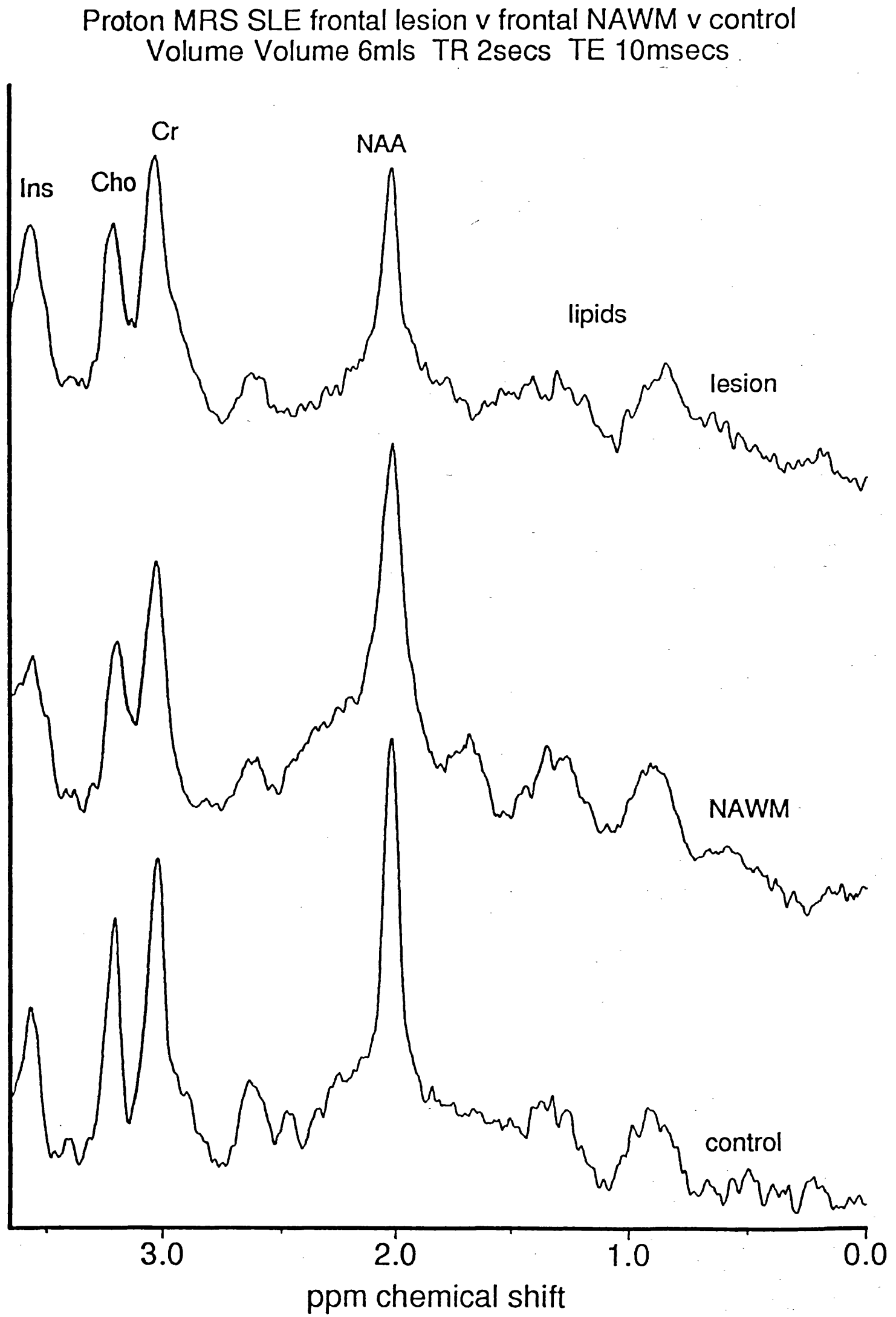
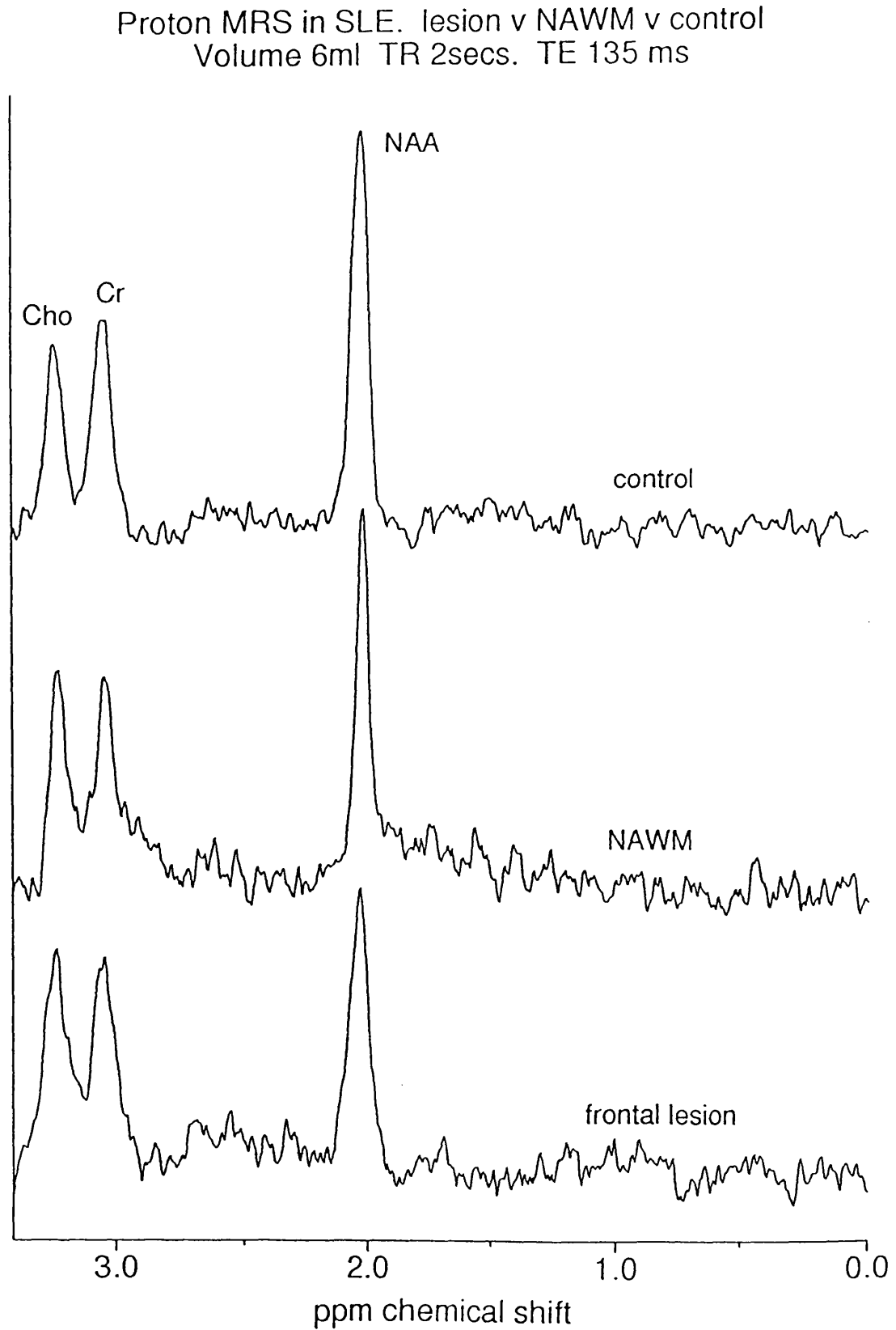


Figure 6.4



CHAPTER 7

1H MAGNETIC RESONANCE SPECTROSCOPY AND MAGNETISATION TRANSFER IN ADULT CASES OF PHENYLKETONURIA

7.1 SUMMARY

Proton MRS, magnetization transfer (MT) and MRI were carried out in five patients with PKU and in eight healthy controls. MRS and MT were collected from areas of signal abnormality in the posterior trigone and NAWM. Metabolite concentrations were calculated using the fully relaxed water spectrum as an internal standard of reference. There were no statistically significant differences in the metabolite concentrations of NAA, Cho and Cr from lesions or NAWM in the PKU patients compared to controls. Quantifiable levels of phenylalanine (phe) were not detected using MRS in the PKU patients. A modest reduction in the median MT ratio was observed from areas of high signal on MRI in the PKU group compared to NAWM in the same patients and white matter of healthy controls. These findings strongly suggest that the lesions visible on MRI in adults with PKU are due primarily to oedema rather than demyelination or axonal loss.

7.2 INTRODUCTION

It is now well established that some degree of intellectual impairment may occur in patients with PKU despite early treatment (Smith et al., 1990; Thompson et al., 1990b). Neurological deterioration has also been documented recently in a number of patients in whom diagnosis was delayed or who had relaxed or discontinued their diet (Thompson et al., 1993). These patients invariably have white matter abnormalities on MRI. Similar, though usually less marked changes on MRI may occur in patients who have no obvious neurological dysfunction

(Thompson et al., 1993). There is also some evidence to suggest that the severity of MRI change in such patients correlates with the degree of hyper-phenylalaninaemia at the time of investigation and with the duration of exposure to high levels of phe (Bick et al., 1991a). It has been suggested on the basis of early pathological studies, carried out on patients with severe neurological involvement, that these MRI abnormalities may represent areas of dysmyelination and/or demyelination (Poser and van Bogaert 1959;) though more recently, a reversible component to the MRI abnormalities has been demonstrated suggesting that oedema may also be involved in lesion pathogenesis (Thompson et al., 1990; Bick et al., 1991b) or that remyelination occurs. At present conventional MRI is unable to provide specific information regarding the various pathological processes occurring within lesions and normal appearing white matter in PKU. The high signal areas visible on conventional MR images are the result of a non-specific increase in water content and therefore may occur secondary to a number of processes including oedema, gliosis, demyelination and axonal loss.

As discussed in previous chapters, proton MRS provides information regarding the chemical pathology occurring within the brain. Magnetisation transfer (MT) is another NMR technique which relies on the transfer of energy between highly bound protons within structures such as myelin and the very mobile protons of free water. This effect can be quantitated as a magnetisation transfer ratio (MTR) - and shows promise in being able to differentiate between the MRI changes of demyelination (Dousset et al 1992; Gass et al., 1994) from that of oedema (Dousset et al., 1992).

These two NMR techniques, MRS and MT, have been used in the present study in five adult patients with PKU and abnormalities on MRI.

7.3 MATERIALS AND METHODS

7.3.1 Patients

The study was approved by the Joint Ethics Committee at the Institute of Neurology and the National Hospital for Neurology and Neurosurgery, London. Informed consent was obtained from all patients prior to each study.

Patient details are shown in Table 7.1. Two of the patients were diagnosed by routine neonatal screening and had no neurological signs or symptoms. Three patients were diagnosed in early childhood because of developmental delay and had evidence of late neurological deterioration including cognitive impairment and pyramidal signs. Eight healthy controls were also studied

7.3.2 NMR Techniques

MRI, MRS and MT were performed on a 1.5 T. G.E. signa whole body scanner using a standard quadrature head coil. The study commenced with a T₂ weighted fast spin echo imaging sequence (TR 5000 ms, TE_f 80 ms) (5mm slices with 2.5 mm gap, 256x256 matrix, echo train length 8). After imaging, a volume of interest localised to the posterior trigone was prescribed ranging in size from 3.5 to 8ml (Figure 1). The size and shape of each volume was adjusted to avoid inclusion of grey matter and cerebrospinal fluid. The region of interest included lesions and NAWM. An MRI of the voxel was then obtained to ensure accurate localisation. Water suppressed ¹H spectra were obtained using a STEAM sequence. An MR image of the voxel was then obtained to ensure accurate localisation. Acquisition parameters were repetition time (TR) 2.135 ms, mixing time (TM) 12ms, TE 10 and 135 msec. 256 averages were collected using an 8 step phase cycle in approximately 13 minutes. 1024 points were collected, with a spectral width of 750 Hz. Spectra were then collected from an area of normal

appearing white matter in the centrum semi-ovale of the parietal lobe using the same parameters. Shimming to a line width of about 3Hz. and water suppression were re-optimised for each new location. After collection of the spectroscopic data, Gd-DTPA, 0.1 mM./kg. was injected intravenously and T_1 -weighted images were obtained (TR 500 ms, TE 40ms). Spectroscopic data processing included 2Hz. line broadening for filtering, Fourier transformation, and zero order phase correction. Data processing included 1 Hz. line broadening for filtering, Fourier transformation, and zero order phase correction. Peak areas were determined using a line-fitting programme ("SA / GE" , G.E. Milwaukee W.I.). Peaks were fitted to a Gaussian line shape using a Marquardt fitting procedure. Absolute concentrations for the metabolites were calculated using the fully relaxed water signal as an internal standard of reference as set out in chapter 2 and Appendix A.

Magnetization transfer

MT images were obtained in the PKU patients and in eight healthy age-matched controls. Eight axial slices through the the hemispheres were obtained which covered the regions of brain from which MRS had been performed.

Dual spin-echo images were obtained (SE = 1,500/32/80, 8 slices, 5mm thickness, 2.5mm gap, 256 x 128 matrix, scan time = 10 min), with and without the application of a saturation prepulse to saturate the broad resonance of immobile macromolecular protons. The applied pulse was a 4-lobed, 64msec sinc pulse, 2-kHz off-water resonance. The energy deposited by this pulse ensured a good signal-to-noise in the calculated MT image. To ensure exact coregistration of the saturated and unsaturated images, scans with and without saturation were interleaved for each phase encoding step. From the two images, i.e.,

without (M_0) and with (M_s) saturation pulse , quantitative MT ratio images were derived pixel by pixel according to the equation: $MT\ ratio = (M_0 - M_s / M_0)$. Signal intensities in the calculated image represented the amount of MT between the free and bound water pool.

In the healthy controls and PKU patients, MT ratios were calculated from an area of white matter from the occipital trigones and from parietal white matter in the centrum semi-ovale. The areas from which MT were calculated approximated in size and location to the spectroscopic volumes of interest in the PKU patients.

In the patient group the total lesion area was calculated from the proton density-weighted images using a semi-automated lesion detection programme .

Statistical analysis was performed with a Mann-Whitney confidence interval and test. Results are expressed as a median value together with the range and p value.

7.4 RESULTS

7.4.1 MRI

MRI revealed diffuse high signal abnormalities on T2 weighted images in all five patients. In four of the patients these changes were of a moderate degree and seen predominantly around the trigones. One patient aged 34, who had been off a restricted diet since age 10 and had evidence of recent neurological deterioration with cognitive impairment and gait ataxia showed more widespread white matter changes (Figure 7.1). There was no evidence of Gd-DTPA enhancement on the T_1 weighted images in any of the patients studied.

7.4.2 MRS

MRS showed a normal concentration of NAA in areas of MRI abnormality (median 11.54mM, range 10.56 - 11.75mM, $p>0.09$) and from areas of

normal appearing white matter (median 11.54mM, range 10.85 - 11.57mM, $p>0.15$) in the PKU patients compared to age matched controls (median 12.3mM, range 10.77- 13.7mM). The concentration of Cho in the MRI lesions (median 1.66mM, range 1.3 - 1.88 mM, $p> 0.3$) and NAWM (median 1.84mM, median 1.33 -2.31mM, $p>0.3$) was also normal compared to control white matter (median 1.83mM, range 1.48 - 2.28mM). The Cr concentration was lower in the lesion areas (median 7.83mM, range 6.0 - 9.01mM, $p>0.065$) and from NAWM (median 8.18mM, range 6.5mM - 9.33mM, $p>0.07$) in the PKU patients compared to the white matter in the healthy controls (9.98mM, range 7.73 - 11.83mM) though this did not achieve statistical significance. No abnormal peaks were observed which could be attributed to phe or to myelin breakdown products in the PKU patients.

7.4.3 MT

There was a modest reduction of the MT ratio from the area of high signal observed on MRI at the occipital trigones (median 28.1, range 25.8 - 28.7) compared to the occipital white matter from healthy controls (median 29.7, range 28.9 - 32.4, $p <0.02$) (Figure 4). There was no difference in the MT ratio from parietal NAWM in the PKU patients (median 30.1,range 28.6 - 31.1, $p>0.09$) and from parietal white matter in the control group (median 31.3, range 330.5 - 31.55)

7.5 DISCUSSION

The findings of interest in this study are,

- (1) the preservation of [NAA] and other brain metabolites in brain lesions and NAWM in adult patients with PKU and
- (2) the modest reduction of MT in brain lesions in the same group

7.5.1 Normal [NAA]

The preservation of NAA in patients with PKU suggests that there is

very little axonal loss occurring either within the MRI visible lesions or in the NAWM. Such a 'non-destructive' pathological process is also suggested by the resolution of MRI lesions which has been demonstrated with strict dietary control (Thompson et al., 1993).

7.5.2 Moderate reduction of MT in PKU

There is good experimental evidence to suggest that MT is able to differentiate between oedema and demyelination. Dousset and colleagues (1992) were able to show a modest reduction of the MT ratio from brain lesions in guinea pigs after the induction of EAE (a condition in which there is inflammation and oedema in the absence of demyelination). In contrast, a significant reduction in the MT ratio was observed from lesions in patients with MS. A study by Gass et al (1994) has shown that the degree of MT reduction in patients with MS correlates with clinical disability indicating that a low MT ratio is indicative of a more destructive pathological process.

In the present study, only a modest reduction in the MT ratio from lesions in patients with PKU. This degree of change is consistent with an increased water content of white matter which is known to be elevated in the post-mortem brains of patients with PKU compared to controls (Crome et al., 1962). Such a modest reduction of MT also suggests that there is little demyelination or axonal loss occurring within lesions or NAWM in the PKU patients.

7.5.3 Other findings

Quantifiable levels of phe which is assigned at 7.37 ppm in the proton spectrum were not detected in the brains of PKU patients in the present study. Recent work by Kreiss et al (1994b) has suggested that it is possible to detect and measure phe concentration in vivo. This was

achieved by collecting spectra from large volumes of interest (18 - 80ml), collating the spectra from a number of PKU patients and then producing a "difference spectrum" from the PKU patients against that of a control. The voxel size in the present study was rather small (ranging from 4-6ml) and may explain the inability to detect phe in the PKU group.

There was no spectroscopic evidence of myelin breakdown products in the form of increased lipid or macromolecule resonances such as those observed in acute multiple sclerosis lesions (Chapter 3) suggesting again that active myelin breakdown is not a prominent pathological feature in PKU lesions.

In this study a normal concentration of Cho was found in lesions and NAWM in the PKU patients. When this data was initially analysed (Davie et al., 1994b) using metabolite/Cr ratios an increase was observed in the Cho/Cr ratio within lesions and NAWM. This can now be attributed to an absolute reduction of Cr in the PKU patients (which did not quite achieve statistical significance) rather than an absolute increase in the concentration of Cho. The normal concentration of NAA, Cho and creatine in the present study is in keeping with the preliminary spectroscopic findings in PKU of Kreiss et al (1994b).

Proton MRS has shown no significant alteration in [NAA], [Cr] and [Cho] from areas of signal abnormality and NAWM in five adults with PKU. MT has shown a moderate though significant reduction of the MT ratio from an area of signal abnormality in the same group. These findings suggest that the lesions occurring in patients with PKU are the result of oedema rather than demyelination or axonal loss.

LEGENDS

Figure 7.1

Axial MRI (TR 5000ms TE 80ms) in patient with phenylketonuria showing predominant high signal lesions in the posterior trigones. A spectroscopic volume of interest over the posterior trigone is shown.

Figure 7.2

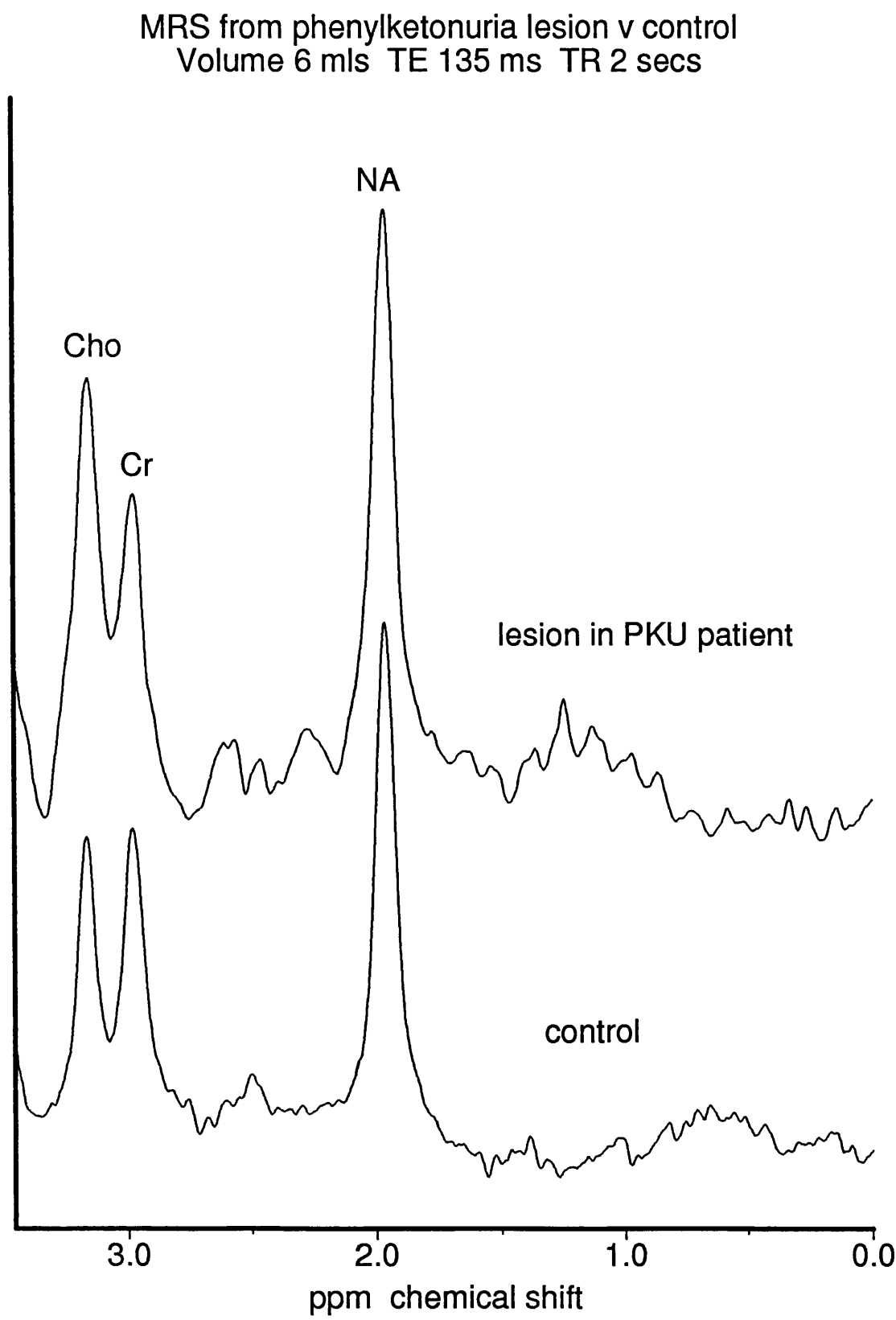
Magnetic resonance spectroscopy from lesion in posterior trigone in patient with phenylketonuria (upper spectrum) compared to control.

Figure 7.1



T₂ weighted axial MRI in a patient with phenylketonuria. There are areas of high signal in the white matter which is most marked at the posterior trigones. A localised volume of interest where spectroscopic data was collected from (Figure 7.2) is shown.

Figure 7.2



CHAPTER 8

CONCLUSIONS AND IMPLICATIONS FOR FUTURE RESEARCH

8.1 CONCLUSIONS AND IMPLICATIONS FOR FUTURE RESEARCH

Over the last 10 years ^1H MRS has become established as a reliable, non-invasive *in-vivo* technique which has advanced our understanding of many conditions affecting the central nervous system. One particular advantage that MRS has over other techniques is that it provides unique quantitative information regarding a variety of normal metabolites and macromolecules and the effects of disease on the brain at a biological level.

In this thesis I have demonstrated that ^1H MRS is able to identify biological markers of myelin breakdown in the form of cytosolic proteins and lipids early on in the evolution of the acute MS lesion. Furthermore these changes can be observed over time until their resolution. This provides a great advantage over conventional MR imaging which is unable to visualise normal myelin or the products of myelin degradation. The ability to detect demyelination is clearly important for a number of reasons. First, it may permit the unravelling of the precise relationship between inflammation and demyelination and whether these two processes invariably occur in all lesions. Secondly, it potentially provides a means of monitoring the effect of drugs on the two aspects of the pathological process - demyelination and axonal loss - which are most likely to be responsible for the development of disability in MS.

MRS has also provided a means of assessing neuronal dysfunction and loss by the measurement of NAA- a neuronal marker. In the preceding

chapters it has been shown that NAA falls within acute MS lesions and that at least in some lesions one can demonstrate a partial recovery of NAA. This observation is significant since it implies that neuronal dysfunction may occur in the acute phase of the MS lesion and that such neuronal dysfunction has the potential to recover. It seems likely however that this potential for recovery is limited at least in those patients who go on to develop disability. In the study of MS patients with persistent functional deficit described in Chapter 4 the concentration of NAA was reduced and remained low after followup for greater than six months. This suggests that at some stage in the development of clinical progression axonal loss occurs. The precise relationship between reversible neuronal dysfunction and the development of axonal loss is as yet unclear. A further spectroscopic study following patients with early relapsing remitting MS who subsequently enter the progressive phase of the disease would clearly be useful in addressing this issue. It is also evident from the studies described in this thesis (Chapters 4 and 5) that there is a strong relationship between the presence of disability and loss of axons within MS lesions and normal appearing white matter as evidenced by a persistent reduction of NAA. The mechanisms that produce such axonal loss are unclear.

MRI has suggested that an inflammatory process is the first detectable event in the development of the majority of acute MS lesions. However it is not yet known whether this inflammatory process may occur as an isolated event without the subsequent development of demyelination. It is also not known whether axonal loss or demyelination (either in lesions or in NAWM) may occur in the absence of any preceding inflammatory phase. Spectroscopy may be able to help in addressing these issues since this technique can provide specific evidence of

demyelination and axonal loss and can thus be compared with various markers of inflammation such as the development of gadolinium enhancement on MRI, an increase in the production of circulating cytokines or using ^1H MRS and the elevation of choline containing products which (from animal studies in experimental allergic encephalomyelitis) are known to be elevated during inflammation in the absence of demyelination.

One limitation of the studies described in this thesis is that they have provided information on relatively small areas of the brain. In a multifocal disease it would clearly be beneficial to have biological information from other lesions and areas of NAWM. The development of chemical shift imaging (CSI) now allows the acquisition of spectroscopic data from several brain slices simultaneously. Instead of information from one voxel it is now possible to collect data from a 32×32 square providing over 900 spectra which can be examined individually and also collated to make a metabolite image. Each individual voxel has a volume of approximately 1ml. The accompanying chemical shift image shows the concentration of NAA through a slice of brain at the level of the ventricles. Further such studies using CSI and MRI should help unravel the precise relationship between inflammation, demyelination, axonal dysfunction and / or loss and the evolving clinical course.

The degree of spinal cord involvement in MS is also likely to be an important factor in the development of disability. As with studies of the brain however, there remains poor correlation between the presence of lesions visible on conventional MRI and persistent functional deficit. There does nevertheless seem to be a strong association between spinal cord atrophy and disability. It seems probable that such atrophy in the spinal cord is secondary to axonal loss. A spectroscopic

study of the spinal cord may be useful in supporting this hypothesis. Spectroscopy is however technically far more demanding in the spinal cord than the brain. The voxel size has to be less due to the smaller area involved. The spinal cord is subject to greater mobility making data acquisition less reliable and the surrounding epidural fat produces large resonances which swamp the signal from cord metabolites. These problems are nevertheless surmountable (Figure 8.1.) A future spectroscopic study of the spinal cord in MS would be of interest particularly in patients with primary progressive disease in whom a proportionately greater extent of the disease load is found in the spinal cord

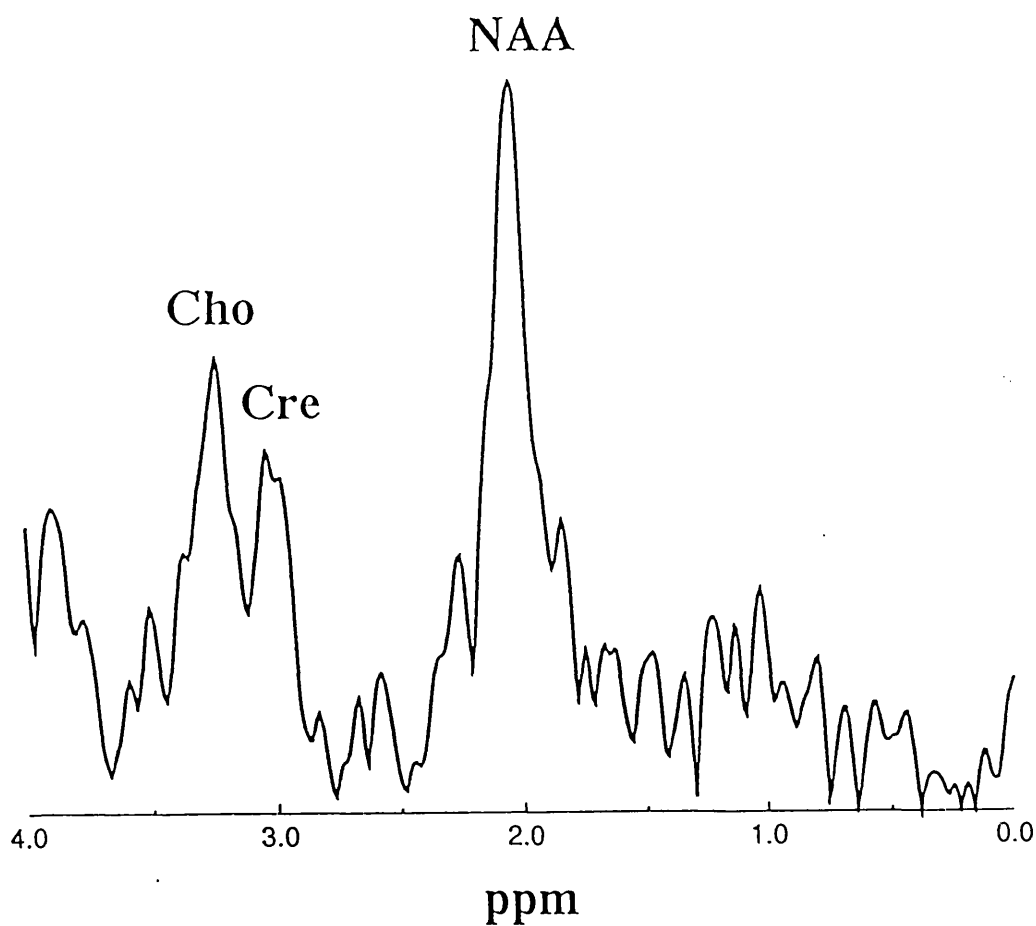
Finally, MRS may have a role to play in the differential diagnosis of MS. Distinct MRS abnormalities were found in the cerebellum in patients with autosomal dominant cerebellar ataxia and in the cerebrum in patients with phenylketonuria. This was not the case in the spectroscopic study of lesions in patients with neuropsychiatric manifestations of SLE described in chapter 6. One possible explanation for the lack of discriminatory findings with MRS in SLE is that only patients with chronic lesions were studied. A study of patients with acute enhancing SLE lesions would be worthwhile to determine whether there are any specific changes between the MR lesions seen with MS and those occurring in SLE. Clearly there are many other conditions which may mimic MS either clinically or radiologically where spectroscopic information might be useful in diagnosis. A spectroscopic study in patients with small vessel microvascular disease visible on MRI would be particularly useful since coincidental (presumed ischaemic) lesions are frequently seen when scanning patients who are in their fifties or older. Similarly, an MRS study of patients with neurosarcoidosis and Behçet's disease might provide

further information allowing greater diagnostic specificity. Whether a pattern of spectral changes will emerge which is absolutely characteristic of multiple sclerosis remains to be seen.

LEGEND**Figure 8.1**

Magnetic resonance spectroscopy (TR 2000ms, TE 270ms) from a volume of cervical spinal cord in a healthy control.

Figure 8.1



Proton magnetic resonance spectroscopy obtained from the cervical spinal cord of a healthy control. (3mls, TR 3000ms, TE 144ms) using a PRESS sequence.

REFERENCES

Ackerman JJH, Grove TH, Wong GG, Gadian DG, Radda JK. Mapping of metabolites in whole animals by P-31 NMR using surface coils. *Nature* 1980; 283:167-170.

Adams CWM, Poston RN, Buk SJ. Pathology, histochemistry and immunocytochemistry of lesions in acute multiple sclerosis lesions. *J Neurol Sci* 1989; 92: 291-306.

Allen IV. Pathology of multiple sclerosis. In: Matthews WB, Compston A, Allen IV, Martyn CM, editors. *McAlpine's multiple sclerosis*. Second edition. Edinburgh: Churchill Livingstone, 1991: 341-378.

Arnold DL, Matthews PM, Radda GK. Metabolic recovery after exercise and the assessment of mitochondrial function in vivo in human skeletal muscle by means of ^{31}P NMR. *Magn Reson Med* 1984;1:307-315.

Arnold DL, Shoubridge EA, Villemure JG, Feindel W. Proton and phosphorus magnetic resonance spectroscopy of human astrocytomas in vivo: preliminary observations on tumour grading. *NMR Biomed* 1990a;3:184-189.

Arnold DL, Matthews PM, Francis G, Antel J. Proton magnetic resonance spectroscopy of human brain in vivo in the evaluation of multiple sclerosis: assessment of the load of disease. *Magn Reson Med* 1990b;14:154-159.

Arnold DL. Reversible reduction of N-acetylaspartate after acute central nervous system damage. In: Proceedings of the eleventh annual meeting of the Society for Magnetic Resonance in Medicine (abstract) 1992a;1:643.

Arnold DL, Matthews PM, Francis GS, O'Connor, Antel J. Proton magnetic resonance spectroscopic imaging for metabolic characterisation of demyelinating plaques. *Ann Neurol* 1992b; 31: 235-241.

Arnold DL, Riess GT, Matthews PM, Francis GS, Collins DL, Wolfson C., et al. Use of proton magnetic resonance spectroscopy for monitoring disease progression in multiple sclerosis. *Ann Neurol* 1994; 36: 76-82.

Baker M Psychopathology in systemic lupus erythematosus: 1. Psychiatric observations. *Seminars in arthritis and rheumatism* 1973; 3: 95.

Barnes D, Munro PMG, Youl BD, Prineas JW, McDonald WI. The longstanding MS lesion. A quantitative MRI and electron microscopic study. *Brain* 1991;114: 1271-1280.

Barratt HJ, Miller D, Rudge P. The site of the lesion causing deafness in multiple sclerosis. *Scand Audiol* 1988; 17: 67-71.

Beckmann N, Turkalj I, Seelig J, Keller U. ¹³C NMR for the assessment of human brain glucose metabolism in vivo. *Biochemistry* 1991;30:6362-6366.

Behar KL, Ogino T. Assignment of resonances in the ¹H spectrum of rat

brain by two-dimensional shift correlated and J-resolved NMR spectroscopy. *Magn Reson Med* 1991; 17: 285-303.

Behar KL, Rothman DL, Spencer DD, Petroff OAC. Direct measurement of macromolecule resonances in short-TE localized ^1H NMR spectra of human brain in vivo at 2.1 Tesla [abstract]. In: *Proceedings of the Society of Magnetic Resonance* 1994; 1: 310.

Benton AL. Differential behavioral effects in frontal lobe disease. *Neuropsychologia* 1968; 6: 53-60.

Berry RG, Hodges JH. Nervous system involvement in systemic lupus erythematosus. *Transactions of the American Neurological Association* 1965 90: 231-233.

Berry RG. Lupus erythematosus. In, Minckler J. *Pathology of the Nervous System*. 1971 McGraw-Hill, New York, pp 1482-88.

Bick U, Fahrenndorf G, Ludolph AC, Vassallo P, Weglage J, Ullrich K. Disturbed myelination in patients with treated hyperphenylalaninaemia: evaluation with magnetic resonance imaging. *Eur J Pediatr* 1991a; 150: 185-189.

Bick U, Ullrich K, Stöber U, Möller H, Fahrenndorf G, Ludolph AC, et al. MRI white matter abnormalities in patients with treated hyperphenylalaninaemia: disturbed myelination or toxic oedema? *Neuropediatrics* 1991b; 22: 174.

Birken DL and Oldendorf WH. N-acetyl-L-aspartic acid: A literature review of a compound prominent in ^1H -NMR spectroscopic studies of brain. *Neurosci Biobehav Rev* 1989;13:23-31.

Blakely RD, Robinson MB, Thompson RC, Coyle JT. Hydrolysis of the brain dipeptide N-acetyl-L--aspartyl-L-glutamate :subcellular and regional distribution, ontogeny, and the effect of lesions on N-acetylated-alpha-linked acidic dipeptidase activity. *J Neurochem* 1988;50:1200-1209.

Brenner RE, Munro PMG, Williams SCR, Bell JD, Barker GJ, Hawkins CP, et al. The proton NMR spectrum in acute EAE: the significance of the change in the cho:cr ratio. *Magn Reson Med* 1993a; 29: 737-745.

Brenner RE, Munro PMG, Williams SCR, Barker GJ, Miller DH, Landon DN et al. Abnormal neuronal mitochondria: a cause of reduction in NA in demyelinating disease [abstract]. In: the 12th Proceedings of the society of magnetic resonance in medicine 1993b;1:281.

Bruhn H, Frahm J, Gyngell M, Merboldt KD, Hänicke W, Sauter R, et al. Cerebral metabolism in man after acute stroke: new observation using localized proton NMR spectroscopy. *Magn Reson Med* 1989; 9: 126-131.

Bruhn H, Frahm J, Merboldt KD, Hänicke W, Hanefield F, Christen HJ, et al. Multiple sclerosis in children:cerebral metabolic alterations monitored by localised proton magnetic resonance spectroscopy in vivo. *Ann Neurol* 1992; 32:140-150.

Burri R, Steffen C, Herschkowitz N. N-Acetyl-L-aspartate is a major source of acetate groups for lipid synthesis during rat brain

development. *Dev Neurosci* 1991; 13: 403-411.

Cady EB, Costello AMdeL, Dawson MJ, Delphy DT, Hope PL, Reynolds EOR, et al. Non-invasive investigation of cerebral metabolism in newborn infants by phosphorus nuclear magnetic resonance spectroscopy. *Lancet* 1983; i: 1059-1062.

Callies R, Sri-Pathmanathan RM, Ferguson DYP, Brindle KM. The appearance of neutral lipid signals in the ^1H -NMR spectra of a myeloma cell line correlates with the induced formation of cytoplasmic lipid droplets. *Magn Reson Med* 1993; 29: 546-552.

Casanova MF, Zito M, Weinberger DR, Kleinman JE. An immunocytochemical and autoradiographic study on the cellular localisation of cholinergic markers in the human cerebellum [abstract]. *Soc Neurosci abstr* 1990; 16: 535.

Chance B, Eleff S, Leigh JS. Non invasive, non destructive approaches to cell bioenergetics. *Proc Natl Acad Sci* 1980; 77: 7430-7434.

Chang L, Mehringer CM, Buchthal SD, Miller BL, Myer H, Satz P, et al. Decreased N-acetyl compounds and increased myo-inositol in cocaine and polysubstance abusers. In: *Proceedings of the Society of Magnetic Resonance* 1994; 2: 579.

Chong WK, Sweeney B, Wilkinson ID, Paley M, Hall-Craggs MA, Kendall BE, et al. Proton spectroscopy of the brain in HIV infection: correlation with clinical, immunologic and MR imaging findings. *Radiology* 1993; 188: 119-124.

Christiansen P, Larsson HBW, Henriksen O. Time dependence of N-acetylaspartate and choline containing compounds in multiple sclerosis [abstract]. 12th meeting of The proceedings of the Society of magnetic resonance in medicine. 1993;1:279.

Christiansen P, Henriksen O, Stubgaard M, Gideon P, Larsson HBW. In vivo quantification of brain metabolites by ^1H -MRS using water as an internal standard. *Magn Reson Imaging* 1993; 11: 107-118.

Confavreux C, Aimard G, Devic M. Course and prognosis of multiple sclerosis assessed by the computerised data processing of 349 patients. *Brain* 1980; 103: 281-300.

Crome L, Tymms V, Woolf LI. A chemical investigation of the defects of myelination in phenylketonuria. *J. Neurol Neurosurg Psychiatry* 1962; 25: 143-148.

Curatolo A, D'Arcangelo P, Lino A, Brancati A. Distribution of N-acetyl-aspartic and N-acetyl-aspartyl-glutamic acids in nervous tissue. *J Neurochem* 1965; 12: 339-342.

D'Adamo AF and Yatsu FM. Acetate metabolism in the nervous system. N-acetyl-L-aspartic acid and the biosynthesis of brain lipids. *J Neurochem* 1966; 13: 961-965.

Davie CA, Hawkins CP, Barker GJ, Brennan A, Tofts PS, Miller DH, et al. Detection of lipid in the brain of healthy subjects by proton NMR spectroscopy [abstract]. In: Proceedings of the eleventh meeting of the Society of Magnetic Resonance in Medicine 1992; Works in

Progress:1724.

Davie CA, Barker GJ, Tofts PS, Quinn N, Miller DH. Proton MRS in Huntington's disease. *Lancet* 1994; 343: 1580.

Davie CA, Hawkins CP, Barker GJ, Brennan A, Tofts PS, Miller DH, et al. Serial proton magnetic resonance spectroscopy in acute multiple sclerosis lesions. *Brain* 1994a; 117: 49-58.

Davie CA, Barker GJ, Brenton D, Miller DH, Thompson AJ. Proton magnetic resonance spectroscopy in adult cases of phenylketonuria [abstract]. *J Neurol Neurosurg Psychiatry* 1994b; 57: 1292.

Davie CA, Wenning GK, Barker GJ, Tofts PS, Quinn N, Marsden CD et al. Differentiation of multiple system atrophy from idiopathic Parkinson's disease using proton magnetic resonance spectroscopy. *Ann Neurol* 1995; 37: 204-210..

Dawson JW. The histology of disseminated sclerosis. *Transac Royal Soc Edinb* 1916; 50: 517-740.

Demaerel P, Faubert F, Wilms G, Casaer P, Piepgras U, Baert AL. MRI findings in leukodystrophy. *Neuroradiology* 1991a; 33: 368-371.

Demaerel P, Johannik K, Van Hecke PV, Van Ongeval C, Verellen S, Marchal G, et al. Localised ^1H NMR spectroscopy in fifty cases of newly diagnosed intracranial tumours. *J Comput Assist Tomogr* 1991b; 15: 67-76.

De Stefano N, Matthews PM, Antel JP, Preul M, Francis G, Arnold DL. Chemical pathology of acute demyelinating lesions and its correlation with disability. *Ann Neurol* 1995; 38: 901-909.

Doddrell DM, Galloway GJ, Brooks WM, et al. Water signal elimination in vivo using "suppression by mistimed echo and repetitive gradient episodes". *J Magn Reson* 1986;70:176-180.

Dousset V, Grossman RI, Ramer KN, et al. Experimental allergic encephalomyelitis and multiple sclerosis lesion characterisation with Gd - DTPA and magnetization transfer imaging. *Radiology* 1992; 182: 483-491.

Fazekas F, Offenbacher H, Fuchs S, Schmidt R, Niederkorn K, Horner S, et al. Criteria for an increased specificity of MRI interpretation in elderly subjects with suspected multiple sclerosis. *Neurology* 1988;38:1822-1825.

Fazekas F. Magnetic resonance signal abnormalities in asymptomatic individuals: Their incidence and functional correlates. *Eur Neurol* 1989; 29: 164-168.

Feinstein A, Ron M, Thompson AJ. A serial study of psychometric and MRI changes in multiple sclerosis. *Brain* 1993; 116: 569-602.

Filippi M, Miller DH, Paty DW, Kappos L, Barkhof F, Compston DAS, et al. Correlation between changes in disability and MRI activity in multiple sclerosis; a follow up study [abstract]. *J Neurol* 1994;241 (suppl): S89.

Fox PT et al. Nonoxidative glucose consumption during focal physiologic neural activity. *Science* 1988; 241: 462-464.

Frahm J, Merboldt KD, Hänicke W. Localised proton spectroscopy using stimulated echoes. *J Magn Reson* 1987; 72: 502-508.

Frahm J, Bruhn H, Gyngell ML, Merboldt KD, Hänicke W, Sauter R. Localised high-resolution proton NMR spectroscopy using stimulated echoes: Initial applications to human brain in vivo. *Magn Reson Med* 1989a; 9: 79-93.

Frahm J, Bruhn H, Gyngell ML, Merboldt KD, Hänicke W, Sauter R. Localised proton NMR spectroscopy in different regions of the human brain in vivo. Relaxation times and concentrations of cerebral metabolites. *Magn Reson Med* 1989b; 11: 47-63.

Frahm J, Michaelis T, Bruhn H, Gyngell ML, Merboldt KD, Hänicke W. Improvements in localised proton NMR spectroscopy of human brain, water suppression, short echo times and 1ml resolution. *J Magn Reson* 1990; 290: 464-473.

Frahm J, Bruhn H, Hänicke W, Merboldt KD, Mursch K, Markakis E. Localised proton NMR spectroscopy of brain tumours using short echo time STEAM sequences. *J Comput Assist Tomogr* 1992; 15: 915-922.

Gadian DG, Connelly A, Cross JH, Iles RA, Leonard JV. ^1H spectroscopy in two children with ornithine transcarbamylase deficiency. In: *The tenth Proceedings of the Society of Magnetic Resonance in Medicine* 1991; 1: 193.

Gass A, Barker GJ, Kidd D, Thorpe JW, MacManus D, Brennan A, et al. Correlation of magnetization transfer ratio with clinical disability in multiple sclerosis. *Ann Neurol* 1994; 36: 62-67.

Gerard G, Weisberg LA. MRI periventricular lesions in adults. *Neurology* 1986; 36: 998-1001.

Gideon P, Henriksen O, Sperling B, Permlle C, Skyhøj Olsen T, Jørgensen HS, et al. Early time course of N acetylaspartate, creatine and phosphocreatine, and compounds containing choline in the brain after acute stroke. A proton magnetic resonance spectroscopy study. *Stroke* 1992; 23: 1566-1572.

Ginsburg KS, Wright EA, Larson MG, et al. A controlled study of the prevalence of cognitive dysfunction in randomly selected patients with SLE. *Arthritis Rheum* 1992 35: 76-82.

Giunti P, Sweeney MG, Spadaro, et al. The trinucleotide repeat expansion on chromosome 6p (SCA 1) in autosomal dominant cerebellar ataxias only in ADCA Type 1. *Brain* 1994;117: 645-649.

Granot J. Selected volume excitation using stimulated echoes (VEST). Applications to spatially localised spectroscopy and imaging. *J Magn Reson* 1986; 70: 488.

Grimaud J, Millar J, Thorpe JW, Moseley IF, McDonald WI, Miller DH. Signal intensity on MRI of basal ganglia in multiple sclerosis. *J Neurol Neurosurg, Psychiatry* 1995; 59: 306-308.

Grossman RI, Lenkinski RE, Ramer KN, Gonzalez-Scarano F, Cohen JA. MR proton spectroscopy in multiple sclerosis. *AJNR* 1992; 13: 1535-1543.

Haase A, Hänicke W, Frahm J, Matthaei D. Surface coil NMR in diagnosis *Lancet* 1983;ii:1082-1083.

Haase A, Frahm J, Hänicke W. ¹H NMR chemical shift selective (CHESS) imaging. *Phys Med Biol* 1985; 30: 341-344.

Halliday AM, McDonald WI, Mushin J. Delayed visual evoked response in optic neuritis. *Lancet* 1972; I: 982-985.

Hanly JG, Fisk JD, Sherwood G, et al . Cognitive impairment in patients with SLE. *J Rheum* 1992; 19: 562-567

Harding AE. The clinical features and classification of the late onset autosomal dominant cerebellar ataxias. A study of 11 families including descendants of "the Drew family of Walworth." *Brain* 1982; 105: 1-28.

Harris EN, Hughes GRV. Cerebral disease in systemic lupus erythematosus. *Semin Immunopathol* 1985; 8: 251-266.

Haseler LJ, Griffey RH, Sibbitt Jr. WL, Sibbitt RR, Griffey BV, Matniyoff NA Evolution of neuropsychiatric systemic lupus erythematosus by volume localised proton nuclear magnetic resonance spectroscopy [abstract]. In: The tenth Proceedings of the Society of Magnetic Resonance in Medicine 1991; 1: 229.

Hawkins CP, Munro PMG, MacKenzie F, Kesselring J, Tofts PS, Du Boulay EPGH, et al. Duration and selectivity of blood-brain barrier breakdown in chronic relapsing experimental allergic encephalomyelitis studied by gadolinium-DTPA and protein markers. *Brain* 1990; 113: 365-378.

Hay EM, Black D, Huddy A, et al. Psychiatric disorder and cognitive impairment in systemic lupus erythematosus. *Arthritis Rheum* 1992; 35: 411-416.

Hayes DJ, Hilton-Jones D, Arnold DL, Galloway G, Styles P, Duncan J, et al. A mitochondrial encephalomyopathy. A combined ^{31}P -magnetic resonance and biochemical investigation. *J Neurol Sci* 1985; 71: 105-118.

Hume Adams J and Duchen LW. 1992 *Greenfield's Neuropathology*. Edward Arnold, Great Britain.

Hoffmann PM, Stuaré WH, Earle KM, Brody JA. Hereditary late onset cerebellar degeneration. *Neurology* 1971; 21: 771-777.

Hume Adams J, Duchen LW. In: *Greenfield's Neuropathology* 1992 Edward Arnold, Great Britain.

Husted CA, Goodin S, Hugg JW, Maudsley A, Tsuruda JS, de Brie SH. Biochemical alterations in multiple sclerosis lesions and normal appearing white matter detected by in vivo ^{31}P and ^1H spectroscopic imaging. *Ann Neurol* 1994; 36: 157-165.

IFBN Multiple Sclerosis Study Group. Interferon beta-1b is effective in relapsing remitting multiple sclerosis. I. Clinical results of a multicenter, randomized, double-blind, placebo-controlled trial [see

comments]. *Neurology* 1993; 43: 655-661. Comment in: *Neurology* 1993; 43: 641-643.

Inglis BA, Brenner RE, Munro PMG, Williams SCR, McDonald WI, Sales KD. Measurement of proton NMR relaxation times for NAA, Cr and Cho in acute EAE. In: *Proceeding of the eleventh Annual Meeting of the SMRM. Book of Abstracts* 1992; Works in progress: 2162.

Jue T, Arias-Mendoza F, Connella NC, Shulman GI, Shulman RG. A ^1H NMR technique for observing metabolite signals in the spectrum of perfused liver. *Proc Natl Acad Sci USA* 1985; 82: 1633-1637.

Johnson RT, Richardson EP The neurological manifestations of systemic lupus erythematosus. *Medicine (Baltimore)* 1968; 47: 337-369.

Katz D, Taubenberger JK, Cannella B, McFarlin DE, Raine CS, McFarland HF, et al. Correlation between MRI and lesion development in chronic active multiple sclerosis. *Ann Neurol* 1993; 34: 661-669.

Kauppinen RA and Williams SR. Nondestructive detection of glutamate by ^1H nuclear magnetic resonance specterosecopy in cortical brain slices from the guinea pig: evidence for change in detectability during severe anoxic insults. *J Neurochem* 1991; 57: 1136-1144.

Kauppinen RA, Nissinen T, Kärkkäinen A, Pirttilä TRM, Palvimo J, Kokko H, et al. Detection of Thymosin β 4 in situ in a guinea pig cerebral cortex preparation using ^1H NMR spectroscopy. *J Biol Chem* 1992; 267: 9905-9910.

Kauppinen RA, Williams SR, Busza AL, van Bruggen N. Applications of magnetic resonance spectroscopy and diffusion-weighted imaging to the study of brain biochemistry and pathology. *TINS* 1993; 16: 88-95.

Kawaguchi Y, Okamoto T, Taniwaki M, Aizawa M, Inoue M, Katayama S., et al. CAG expansions in a novel gene for Machado Joseph disease at chromosome 14q32.1. *Nat Genet* 1994; 8: 213-215.

Kermode AG, Thompson AJ, Tofts P, MacManus DG, Kendall BE, Kingsley DPE, et al. Breakdown of the blood-brain barrier precedes symptoms and other MRI signs of new lesions in multiple sclerosis: pathogenetic and clinical implications. *Brain* 1990;113:1477-1489.

Kesselring J, Miller DH, Robb SA, Kendall BE, Moseley IF, Kingsley D, et al. Acute disseminated encephalomyelitis: MRI findings and the distinction from multiple sclerosis. *Brain* 1990; 113: 291-302.

Kidd D, Thorpe JW, Thompson AJ, Kendall BE, Moseley IF, MacMannus DG, et al. Spinal cord MRI using multi-array coils and fast spin echo. II. Findings in multiple sclerosis. *Neurology* 1993; 43: 2632-2637.

Kidd D, Thompson AJ, Kendall BE, Miller DH, McDonald WI. The benign form of multiple sclerosis: MRI evidence for less frequent and less inflammatory disease activity. *J Neurol Neurosurg Psychiatry* 1994; 57: 1070-1072.

Kish SJ, Currier RD, Schut L, Perry TL, Morito CL. Brain choline acetyltransferase activity in dominantly inherited olivopontocerebellar atrophy. *Ann Neurol* 1987; 22: 272-275.

Koopmans RA, Li DKB, Zhu G, Allen PS, Penn A, Paty DW. Magnetic resonance spectroscopy of multiple sclerosis: in-vivo detection of myelin breakdown product. [letter]. *Lancet* 1993;341:631-632.

Kreiss R, Ross BD, Farrow NA, Ross BD. Metabolic disorders of the brain in chronic hepatic encephalopathy detected with H-1 MR spectroscopy. *Radiology* 1992; 182: 19-27.

Kreiss R. Quantitation in localised proton MR spectroscopy [abstract]. In: *Proceedings of the society of magnetic resonance* 1994; 1: 3.

Kreiss R. Pietz J, Penzien J, Herschkowitz N, Boesch C. Unequivocal identification and quantitation of phenylalanine in the brain of patients with phenylketonuria by means of localised in vivo ¹H MRS [abstract]. In: *Proceedings of the second meeting of the Society of Magnetic Resonance* 1994b; 1: 308.

Kriss A, Francis DA, Cuendet F, Halliday AM, Taylor DSI, Wilson J, et al. Recovery after optic neuritis in childhood. *J Neurol Neurosurg Psychiatry*. 1988; 51: 1253-1258.

Kurtzke JF. Rating neurological impairment in multiple sclerosis: an expanded disability status scale (EDSS). *Neurology* 1983; 33: 1444-52.

Kuwabara T, Watanabe H, Ohkubo M, Sakai K, Tsuji S, Yuasa T. Lactate increase in the basal ganglia accompanying finger movements. -A localized ¹H-MRS study-[abstract]. In *The Proceedings of the Society of Magnetic resonance* 1994; 1: 565.

Larsson HBW, Frederiksen J, Kjaer L, Henriksen O, Oleson J. In vivo determination of T_1 and T_2 in the brain of patients with severe but stable multiple sclerosis. *Magn Reson Med* 1988; 7: 43-55.

Larsson HBW, Christiansen P, Jensen M, Frederiksen J, Heltberg A, Oleson J, et al. Localised in vivo spectroscopy in the brain of patients with multiple sclerosis. *Magn Reson Med* 1991; 22: 23-31.

Lassmann H, Suchanek G, Ozawa K. Histopathology and the blood-cerebrospinal fluid barrier in multiple sclerosis. *Ann Neurol* 1994; 36 (Suppl): S42-S46.

Li DKB, Mayo J, Fache S, Robertson W, Kastrukoff LF, Oger J, et al. Lack of correlation between clinical manifestations and lesions of MS seen by NMR [abstract]. *Neurology* 1984; 34(Suppl 1): S136.

Lim L, Ron MA, Ormerod IEC, David J, Miller DH, Logsdail SJ, et al. Psychiatric and neurological manifestations in systemic lupus erythematosus. *Quart J Med* 1988; 66: 27-38.

Lukes SA, Crooks LE, Aminoff MJ, Kaufman L, Panitch HS, Mills C, et al. Nuclear magnetic resonance imaging in multiple sclerosis. *Ann Neurol* 1983; 13: 592-601.

Lumsden CE. The neuropathology of multiple sclerosis. In: Vincken PJ, Bruyn GW, editors. *Handbook of clinical neurology*. Amsterdam: North Holland, 1970; 9: 217-309.

McAlpine D. The benign form of multiple sclerosis. A study based on 241 cases within three years of onset and followed up until the tenth year or more of the disease. *Brain* 1961; 84: 186-203.

McDonald WI, Miller DH, Barnes D. The pathological evolution of multiple sclerosis. *Neuropathol Appl Neurobiol* 1992; 18: 319-334.

McIlwain H, HS Bachelard. In, *Biochemistry and the central nervous system*. 5th ed. Edinburgh: Churchill Livingstone, 1985: 282-335.

Matthews PM, Andermann F, Arnold DL. A proton magnetic resonance spectroscopy study of focal epilepsy in humans. *Neurology* 1990;40:985-989.

Matthews PM, Francis G, Antel J, Arnold DL. Proton magnetic resonance spectroscopy for metabolic characterisation of plaques in Multiple Sclerosis. *Neurology* 1991a; 41:1251-1256.

Matthews PM, Berkovic SF, Shoubridge EA, Andermann F, Karpati G, Carpenter S, et al. In vivo spectroscopy of brain and muscle in a type of mitochondrial encephalomyopathy (MERRF). *Ann Neurol* 1991b; 29: 435-438.

Matthews PM, Andermann F, Silver K, Karpati G, Arnold DL. Proton MR spectroscopic characterization of differences in regional brain metabolic abnormalities in mitochondrial encephalomyopathies. *Neurology* 1993; 43: 2484-2490.

May GI, Wright LC, Holmes KT, Williams PG, Smith ICP, Wright PE, et al. Assignment of methylene proton resonances in NMR spectra of of embryonic and transformed cells to plasma membrane triglyceride. *J Biol Chem* 1986; 261: 3048-3053.

Merboldt KD, Bruhn H, Hänicke W, Michaelis T, Frahm J. Decrease of glucose in the human visual cortex during photic stimulation. *Magn Reson Med* 1992; 25: 187-194.

Michaelis T, Merboldt KD, Bruhn H, Hänicke W, Frahm J. Absolute concentrations of metabolites in the adult human brain in vivo: quantification of localised proton MR spectra. *Neuroradiology* 1993; 187: 219-227.

Miller BL. A review of chemical issues in ^1H NMR spectroscopy: N-acetyl-L-aspartate, creatine and choline. *NMR Biomed* 1991; 4: 47-52.

Miller BL, Moats RA, Shonk T, Ernst T, Wooley S, Ross BD. Alzheimer disease: depiction of increased myo-inositol with proton MR spectroscopy. *Radiology* 1993; 187: 433-437.

Miller DH, Rudge P, Johnson G, Kendall BE, MacManus DG, Moseley IF, et al. Serial gadolinium enhanced magnetic resonance imaging in multiple sclerosis. *Brain* 1988a; 111: 927-939.

Miller DH, Kendall BE, Barter S, Johnson G, MacManus DG, Logsdail SJ, et al. Magnetic resonance imaging in central nervous system sarcoidosis. *Neurology* 1988b; 38: 378-383.

Miller DH, Johnson G, Tofts PS, MacManus D, McDonald WI. Precise relaxation time measurements of normal appearing white matter in inflammatory central nervous system disease. 1989; 11: 331-336. *Magn Reson Med* 1989;11:331-336.

Miller DH, Austin SJ, Connelly A, Youl BD, Gadian DG, McDonald WI. Proton magnetic resonance spectroscopy of an acute and chronic lesion in Multiple Sclerosis [letter]. *Lancet* 1991; 337: 58-59.

Miller DH, Buchanan N, Barker G, Morrissey SP, Kendall BE, Rudge P, et al. Gadolinium-enhanced magnetic resonance imaging of the central nervous system in systemic lupus erythematosus. *J Neurol* 1992a; 239: 460-464.

Miller DH, Thompson AJ, Morrissey SP, MacManus DG, Moore SG, Kendall BE, et al. High dose steroids in acute relapses of multiple sclerosis. Mri evidence for a possible mechanism of therapeutic effect. *J Neurol Neurosurg Psychiatry* 1992b; 55: 450-453.

Minderhoud JM, Mooyaart EL, Kamman RL, Teelken AW, Hoogstraten MC, Vencken LM, et al. In vivo phosphorus magnetic resonance spectroscopy in multiple sclerosis. *Arch Neurol* 1992; 49: 161-165.

Moon RB and Richards JH. Determination of intracellular pH by ^{31}P magnetic resonance. *J Biol Chem* 1973; 248: 7276-7278.

Morrissey SP, Miller DH, Hermaszewski R, Rudge P, MacManus DG, Kendall BE, et al. Magnetic resonance of the central nervous system in Behçet's disease. *Eur Neurol* 1993; 33: 287-293.

Narayana PA, Wolinsky JS, Jackson EF, McCarthy M. Proton MR spectroscopy of gadolinium-enhanced multiple sclerosis plaques. *J Mag Reson Imag* 1992; 2: 263-270.

Nelson HE. National Adult Reading Test. 1971 NFER-Nelson. Windsor.

Nelson HE. A modified card sorting test sensitive to frontal defects. *Cortex* 1976; 12: 313-324.

Norton WT, Poduslo SE, Suzuki K. Subacute sclerosing leukoencephalitis. II. Chemical studies including abnormal myelin and an abnormal ganglioside pattern. *J Neuropat Exp Neurobiol* 1966; 25: 582-597.

Offenbacher H, Fazekas F, Schmidt R, Freidl W, Flooh E, Payer F., et al. Assessment of MRI criteria for a diagnosis of MS. *Neurology* 1993;43:905-909.

Olsen WL, Longo FM, Mills CM, Norman D. White matter disease in AIDS: findings at MR imaging. *Radiology* 1988; 169: 445-448.

Ordidge RJ, Bendall MR, Gordon RE, Connelly A. Magnetic Resonance in Biology and Medicine. Eds, Govil, Khetrpal and Saran. McGraw-Hill, New Dehli 1985: pp 387.

Ordidge RJ, Connelly A, Lohman JAB. Image-Selected In vivo Spectroscopy (ISIS). A new technique for spatially selective NMR spectroscopy *J Magn Reson* 1986;66:283-294.

Ormerod IEC, Miller DH, McDonald WI, Boulay EPGH du, Rudge P, Kendall BEW, et al. The role of NMR imaging in the assessment of multiple sclerosis and isolated neurological lesions. A quantitative study. *Brain* 1987; 110: 1579-1616.

Papero PH, Bluestein HG, White P, Lipnick RN. Neuropsychologic deficits and anti-neuronal antibodies in paediatric systemic SLE. *Clin Exp Rheum* 1990; 8: 417-424.

Patel TB and Clark JB. Synthesis of N-acetyl-L-aspartate by rat brain mitochondria and its involvement in mitochondrial/cytosolic carbon transport. *J Biochem* 1979; 184: 539-546.

Patel TB and Clark JB. Lipogenesis in the brain of suckling rats. *J Biochem* 1980; 188: 163 -168.

Paty DW, Oger JJF, Kastrukoff LF, Hashimoto SA, Hooge JP, Eisen AA, et al. MRI in the diagnosis of MS: a prospective study and comparison of clinical evaluation, evoked potentials, oligoclonal banding and CT. *Neurology* 1988; 38: 180-184.

Paty DW, Li DKB. Interferon beta-1b is effective in relapsing remitting multiple sclerosis. II. MRI analysis of a multicenter, randomized, double-blind, placebo-controlled trial. UBC MS/MRI Study Group and the IFNB Multiple Sclerosis Study Group [see comments]. *Comment in Neurology* 1993; 3: 641-643. *Neurology* 1993; 43: 662-667.

Perry TL, Hansen S, Berry K, Mok C, Lesk D. Free aminoacids and related compounds in biopsies of human brain. *J Neurochem* 1971; 18: 521-528.

Petroff OAC, Ogino T, Alger JR. High resolution proton magnetic resonance spectroscopy of rabbit brain: regional metabolite levels and postmortem changes. *J Neurochem* 1988; 51: 163-171.

Petroff OAC, Graham GD, Blamire AM, Al Rayess M, Rothman DL, Fayad PB., et al. Spectroscopic imaging of stroke in humans: histopathology correlates of spectral changes. *Neurology* 1992; 42: 1349-1354.

Phadke JG and Best PV. Atypical and clinically silent multiple sclerosis: a report of 12 cases discovered unexpectedly at necropsy. *J Neurol Neurosurg Psychiatry* 1983; 46: 414-420.

Poser CM, van Bogaert L. Neuropathological observations in phenylketonuria. *Brain* 1959; 82: 1-9.

Poser CM, Paty DW, Scheinberg L, McDonald WI, Davis FA, Ebers GC, et al. New diagnostic criteria for multiple sclerosis: guidelines for research protocols. *Ann Neurol* 1983; 13: 227-231.

Poser S, Lürer W, Bruhn H, Frahm J, Brück Y, Felgenhauer K. Acute demyelinating disease. Classification and non-invasive diagnosis. *Acta Neurol Scand* 1992; 86: 579-585.

Preece NE, Williams SR, Jackson G, Duncan JS, Houseman J, Gadian DG. ¹H NMR studies of vigabatrin induced increase in cerebral GABA. In: *Proceedings of the tenth meeting of the Society of Magnetic Resonance in Medicine* 1991; 2; 1000.

Prichard J, Rothman D, Novotny E, Petroff O, Kuwabara T, Avison M., et al. Lactate rise detected by ^1H NMR in human visual cortex during physiological stimulation. *Proc Natl Acad Sci USA* 1991; 88: 5829-5831.

Prineas JW, Barnard RO, Revesz T, Kwon EE, Sharer L, Cho E-S. Multiple sclerosis: pathology of recurrent lesions. *Brain* 1993; 116: 681-693.

Rao SM, Leo GJ, Haughton VM, St Aubin-Faubert P, Bernardin L. Correlation of magnetic resonance imaging with neuropsychological testing in multiple sclerosis. *Neurology* 1989; 39: 161-166.

Rothman DL, Petroff OAC, Behar KL, Matson RH. Localized ^1H NMR measurement of gamma-aminobutyric acid in human brain in vivo. *Proc Natl Acad Sci USA* 1993; 90: 5662-5666.

Rothman DL, Behar KL, Petroff AC. Improved quantitation of short TE ^1H NMR human brain spectra by removal of short T_1 macromolecule resonances. In: *The Proceedings of the Society of Magnetic Resonance* 1994; 1: 47.

Schaefer J, Stejskal EO, Beard CF. Carbon-13 nuclear magnetic resonance analysis of metabolism in soyabeans labelled by $^{13}\text{CO}_2$. *Plant Physiol* 1975; 55: 1048-1053.

Schonell FJ. In: *Backwardness in the basic subjects*. 1942 Oliver and Boyd, Edinburgh.

Schut JW and Haymaker W. Hereditary ataxia. A pathologic study of five cases of common ancestry. *J Neuropath Clin Neurol* 1951; 1: 183-213.

Scolding NJ, Sussman J, Compston DAS. In vitro studies of oligodendrocytes derived from adult human white matter. *J Neurol* 1994;241(suppl 1):S27.

Shiino A, Matsuda M, Morikawa S, Inubushi T, Akiguchi I, Handa J. Proton magnetic resonance spectroscopy with dementia. *Surg Neurol* 1993; 39: 143-147.

Simmons ML, Frondoza CG, Coyle JT. Immunocytochemical localization of N-acetyl-aspartate with monoclonal antibodies. *Neuroscience* 1991; 45: 37-45.

Smith I, Beasley MG, Ades AE. Intelligence and quality of dietary treatment in phenylketonuria. *Arch Dis Child* 1990; 65: 472-478.

Stehbens WE, Pathology of the cerebral blood vessels. St Louis: Mosby. 1972.

Tallan HH, Moore S, Stein WH. N-acetyl-L-aspartic acid in brain. *J Biol Chem* 1956; 219: 257-264.

Tallan HH. Studies on the distribution of N-acetyl-L-aspartic acid in brain. *J Biol Chem* 1957; 224: 41-45.

Tan EM, Cohen ES, Fries JF, Masi AT, McShane DJ Rothfield NF, et al. The 1982 revised criteria for the classification of systemic lupus erythematosus. *Arth Rheum* 1982; 25: 1271.

Taylor-Robinson SD, Weeks RA, Sargentoni J, Marcus CD, Bryant DJ, Harding AE, et al. Evidence for glutamate excitotoxicity in Huntington's disease with proton magnetic resonance spectroscopy [letter]. *Lancet* 1994; 343: 1170.

Thompson AJ, Hutchinson M, Brazil J, Martin EA. A clinical and laboratort study of multiple sclerosis. *Q J Med* 1986; 58: 69-80.

Thompson AJ, Kermode AG, MacManus DG, Kendall BE, Kingsley DPE, Moseley IF, et al. Patterns of disease activity in multiple sclerosis: clinical and magnetic resonance imaging study. *BMJ* 1990a; 300: 631-634.

Thompson AJ, Smith I, Brenton D, Youl BD, Rylance G, Davidson DC, Kendall B., et al. Neurological deterioration in young adults with phenylketonuria. *Lancet* 1990b; 336: 602-05.

Thompson AJ, Kermode AG, Wicks D, MacManus Dg, KendAll BE, Kingsley DPE et al. Major differences in the dynamics of primary and secondary progressive multiple sclerosis. *Ann Neurol* 1991; 29: 53-62.

Thompson AJ, Miller D, Youl B, MacManus D, Moore S, Kingsley D, et al. Serial gadolinium-enhanced MRI in relapsing-remitting multiple sclerosis of varying disease duration. *Neurology* 1992; 42: 60-63.

Thompson AJ, Tillotson S, Smith I, Kendall BE, Moore SG, Brenton DP. Brain MRI changes in phenylketonuria. Associations with dietary status. *Brain* 1993; 116: 811-821.

Thorpe JW and Miller DH. MRI: its application and impact. *International MS Journal* 1994; 1: 7-16.

Tofts PS and Wray S. A critical assessment of methods of measuring metabolite concentrations by NMR spectroscopy. *NMR Biomed* 1988; 1: 1-9.

Twieg DB, Meyerhoff DJ, Hubesch B, Roth K, Sappey-Marnier D, Boska MD, et al. Phosphorus-31 magnetic resonance spectroscopy in humans by spectroscopic imaging: localised spectroscopy and metabolite imaging. *Magn Reson Med* 1989; 12: 291-305.

Urenjak J, Williams SR, Gadian DG, Noble M. Specific expression of N-acetylaspartate in neurons, Oligodendrocyte-type-2 astrocyte progenitors, and immature oligodendrocytes in vitro. *J Neurochem* 1992; 59: 55-61.

Urenjak J, Williams SR, Gadian DG, Noble M. Proton nuclear magnetic resonance spectroscopy unambiguously identifies different neural cell types. *J Neurosci* 1993; 13(3): 981-989.

Van der Knaap MS, Van der Grond J, Luyten PR, Hollander JA, Nauta JJP, Valk J. ¹H and ³¹P magnetic resonance spectroscopy of brain degenerative cerebral disorders. *Ann Neurol* 1992; 31: 202-211.

Van Hecke P, Marchal G, Johannik K, Demaerel P, Wilms G, Carton H, et al. Human brain proton localized NMR spectroscopy in multiple sclerosis. *Magn Reson Med* 1991; 18: 199-206.

Van Rijen PC, Luyten PR, van der Sprenkel JWB, et al. ^1H and ^{31}P NMR measurement of cerebral lactate, high energy phosphate levels, and pH in humans during voluntary hyperventilation: associated EEG, capnographic, and Doppler findings. *Magn Reson Med* 1989;10:182-

Vion-Dury J, Meyerhoff DJ, Cozzone PJ, Weiner MW. What might be the impact on neurology of the analysis of brain metabolism by in vivo magnetic resonance spectroscopy. *J Neurol* 1994; 241:354-371.

Wing JK, Cooper JE, Sartorius N. In: The measurement and classification of psychiatric symptoms. An instruction manual for the Present State Examination and CATEGO program. 1974 Cambridge University Press: Cambridge.

Wolinsky JS, Narayana PA, Fenstermacher MJ. Proton magnetic resonance spectroscopy in multiple sclerosis. *Neurology* 1990; 40: 1764-69.

Young IR, Hall AS, Pallis CA, Legg NJ, Bydder GM, Steiner RE. Nuclear magnetic resonance imaging of the brain in multiple sclerosis. *Lancet* 1981; ii: 1063-1066.

Appendix A

MRS quantification: practical implementation

1. The concentration of a metabolite can be estimated from the peak area

$$[\text{metabolite}] = k * \text{peak_area} * 2 (R2(0) - R2) * 2 (R1(0) - R1) * 10(TG - TG(0))/200 \\ \text{over vol_VOI} * N_{\text{protons}}$$

where **k** is the calibration constant of the scanner (in fact =1/sensitivity). This can be determined using the spectrum from a compound of known concentration (see below section 2). It may vary with time, and should be measured periodically (ideally before and after each exam, until its stability has been established). Data must be collected in a consistent way (ie keeping spectral width fixed, from same part of coil).

NB **k** for all metabolites, and for water, should be identical.

peak_area must be measured in a consistent way. Ultimately this will be by curve fitting, to reduce intra- and inter-observer variability, and the time needed for analysis.

R1 gain must be recorded for each spectrum; **R1(0)** is a standard value, which can be chosen for convenience (eg. 7).

R2 gain must be recorded for each spectrum; **R2(0)** is a standard value, which can be chosen for convenience (eg. 20).

TG is the transmitter gain (in units of 1/10dB); **TG(0)** is a standard value

(e.g. 70). Note that if spectra are collected at several echo times (see comments on T_1 and T_2 below) TG will change by 60 units between short and long TEs, even if everything else (including the patient/phantom) remains constant. In this case a different value of TG(0) should be used for long and short echo spectra, eg 130 for short TEs and 70 for long TEs.

vol_VOI is the size of the volume of interest in ml.

N_protons is the number of protons that contribute to the peak. (See section 6).

At each acquisition the following parameters must be recorded: **R1, R2, TG, vol_VOI**.

2. The calibration constant k can be determined in 2 ways:

2.1 This can be achieved most accurately, from a phantom of water or metabolites of known high concentration (eg 100mM for good signal to noise ratio (SNR) and short acquisition time). A long TR (to avoid T_1 relaxation) and short TE (to avoid T_2 losses) should be used; however there may be extra underlying peaks at short TE, and a plot of signal vs TE may be useful. To avoid standing wave effects, the phantom should be small (e.g. <10 cm in diameter), or made of oil.

2.2 This is most conveniently, from a water spectrum of the same VOI in the head; water spectra have been collected for nearly all metabolite spectra collected recently and can be used to retrospectively calculate the k

values for the scanner, and hence approximate concentrations. Water concentration taken from control data (Norton et al., 1966) has been taken as 45.5M in grey matter and 39.75 M in white matter) and is likely to vary in lesions, but it should be possible to use a PD weighted image to relate the unknown concentration to that in normal appearing white matter or grey matter, which is less likely to change.

For either calibration method R1, R2, TG and vol_VOI must be noted, as for the metabolite spectra.

3. Accuracy and assumptions

3.1 The dependence of peak area on TG, R1 and R2 is as expected. This can be checked by varying the coil loading over the range of TG's normally found, and ensuring k does not alter. (This is true at least over the TG range 45-150). Altering NEX has no effect on peak area .

3.2 The spectra have no T_1 or T_2 losses. T_1 and T_2 determined in a phantom will, in general, be quite different from those *in vivo*. (See section 5, below).

3.3 Sensitivity k is independent of position in the coil (i.e. the non-uniformity in the head coil can be ignored). This can be checked over the normal range of VOI positions, and if necessary a different value of k used for each position.

3.4 There are no standing wave effects in the head or phantom

3.5 The VOI dimension are accurate. This can be checked by measuring k at several VOI sizes.

3.6 Water suppression does not affect metabolite peak area. If it does reduce some peaks (e.g.Cr) in a consistent way, then k can be determined for this particular peak.

4. Water content of the brain

In 2.2 we assumed it is 39.75M and 45.5M for white and grey matter respectively. However it can be measured using 1 and 2.1 (to determine k for water); this more accurate value would have 2 uses:

4.1 it could be used in place of the control values to calculate retrospective k values and metabolite concentrations. It may vary significantly between VOI's in NAWM and VOI's containing mostly lesion.

4.2 Proton Density (PD) might be interesting in its own right, as a further characteriser of lesions.

5. T₁ and T₂:

Unless very long TRs and very short TEs were used to collect the spectra corrections must be made for T₁ and T₂ relaxation. Assuming that the mixing time, T_M, is negligible (which it should be for all our spectra), [metabolite] calculated from equation†1 must be multiplied by:

$$1 / \exp(\text{TE} / T_2) * (1 - \exp(\text{TR} / T_1))$$

For water spectra (TE=10ms, TR=6000ms) this factor will be very close to 1.0 for most tissue, and can be neglected. For phantom studies, however, it may be necessary to allow for T₁ saturation in the water signal. For metabolites Frahm (1989b) gives the following relaxation times:

Compound	Group	chem/ shift		Insula r grey matter		Occip ital white matter		Thala mus		Cereb ellum
			T ₁	T ₂	T ₁	T ₂	T ₁	T ₂	T ₁	T ₂
Lac	CH ₃	1.3			1550	1200				
NAA	CH ₃	2.0	1650	330	1450	450	1400	340	1700	300
Cr/PCr	N-CH ₃	3.0	1750	250	1550	240	1750	200	1500	190
	N-CH ₂	3.9	1750	160	1050	190				120
Cho	N-(CH ₃) ₃	3.2	1100	380	1150	330	1200	320	1500	410
Tau	N-CH ₂ , S-CH ₂	3.3			1700	270				
Ins	- 4H	3.5	1350	130	900	110	1100	150	1850	130
	- 1H	4.0								
Lipid		0.9 1.3								

Note that we don't know how T₁ and T₂ change with pathology; it is possible to measure T₁ and T₂ in every patient, but the measurements are very time consuming and are not normally made. Any concentrations calculated using the 'standard' values above should therefore probably be referred to as '**apparent concentrations**'.

6. Examples

Note 1) that the term $(TG > 30)$ is zero if $TG \leq 30$ and one if $TG > 30$, so that an extra 60 is added to $TG_{\text{metabolite}}$ for long echo spectra, to match the 'extra' 60 in the short TE water spectrum.

2) that if an external standard other than water is used, the factor of 111M (the concentration of the standard) should be changed appropriately.

where **Intensity** is the intensity measured from a proton density image.

PD weighted spin echo (SE) or (FSE) images can be used for the intensity measurement, but if for any reason measurements on lesion are to be made from one sequence and NAWM from the other, it should be noted that PD measured on FSE images must be multiplied by a calibration factor of 0.952 to be comparable with the SE values. No calibration factor is required if both measurements are made on images from the same sequence.

Note that if an area other than NAWM is used to calibrate the lesion PD, the factor of 39.75M (the water concentration of white matter) should be changed appropriately.

6.3 If T_1 and T_2 are assumed not to change with pathology, then **A, B, C, and D** are constants for a particular metabolite and pulse sequence. For the 'standard' sequences we typically use ($TE=10, 135, 270$, $TR = 2000$ (pre-upgrade, 4.7 software), 2200 (4.8 software)) the relevant values of **A, B, C and D** for white matter are given below.

When using either calibration method it is important to include all the water signal in the **area_{water}** measurement; even when well shimmed the base of the water peak may be very wide so an integration range of 3.0 - 8.0 ppm is suggested. It is also vital to correct both the metabolite and the water spectrum for DC offsets before integration; a baseline correction may also be necessary for the metabolite spectrum.

Compound	Group		N_protons	A	C (TE = ...)			D (TR = ...)	
					10	135	270	2000	2200
Lac	CH ₃	1.3	3	0.666					
NAA	CH ₃	2.0	3	0.666	1.03	1.51	2.26	1.42	1.36
Cr/PCr	N-CH ₃	3.0	3	0.666	1.04	1.72	2.94	1.47	1.40
	N-CH ₂	3.9	2	1.000	1.06	2.32	5.41	1.47	1.40
Cho	N-(CH ₃) ₃	3.2	9	0.222	1.03	1.43	2.04	1.19	1.16
Tau	N-CH ₂ , S-CH ₂	3.3	2 2	1.000					
Ins	?? - 4H	3.5	4	0.500	1.08	2.83	7.98	1.29	1.24
	?? - 1H	4.0	1	2.000					
Lipid		0.9							
		1.3							

R1 _{metabolite} - R1 _{water}	R2 _{metabolite} - R2 _{water}	B	R1 _{metabolite} - R1 _{water}	R2 _{metabolite} - R2 _{water}	B
0	0	1	1	0	2
0	1	2	1	1	4
0	2	4	1	2	8
0	3	8	1	3	16
0	4	16	1	4	32
0	5	32	1	5	64
0	6	64	1	6	128
0	7	128	1	7	256

A = 2/proton index

B = 1/ (R1 - R 2)

C = T₂ correction factor

D = T₁ correction factor